1-89

[redacted]
Copy No. 34

NASA CR-179642

NASA

National Aeronautics and
Space Administration

REVOLUTIONARY OPPORTUNITIES FOR MATERIALS AND STRUCTURES STUDY

By

F.A. Schweiger
General Electric Company
Aircraft Engine Business Group
Cincinnati, Ohio 45215

Prepared for
National Aeronautics and Space Administration

NASA Lewis Research Center
Cleveland, Ohio 44135

Contract NAS3-24622

1. Report No.	2. Government Accession No.	3. Recipient's Catalog No
NASA CR-179642		

4. Title and Subtitle	5. Report Date
Revolutionary Opportunities for Materials and Structures Study	February 1987
	6. Performing Organization Code

7. Author(s)	8. Performing Organization Report No.
F.A. Schweiger	
	10. Work Unit No.

9. Performing Organization Name and Address	11. Contract or Grant No.
General Electric Company Aircraft Engine Business Group Advanced Technology Programs Department Cincinnati, Ohio 45215	NAS3-24622
	13. Type of Report and Period Covered

12. Sponsoring Agency Name and Address	14. Sponsoring Agency Code
National Aeronautics and Space Administration Washington D.C. 20546	

15. Supplementary Notes

Project Manager, Gerald Knip, NASA Lewis Research Center, Cleveland, Ohio

16. Abstract

The revolutionary opportunities for materials and structures study was performed to provide Government and Industry focus for advanced materials Technology.

This study covers both subsonic and supersonic engine studies and aircraft fuel burn and DOC evaluation.

Year 2010 goal materials were used in the advanced engine studies. These goal materials and improved component aero yielded subsonic fuel burn and DOC improvements of 13.4% and 5%, respectively and supersonic fuel burn and DOC improvements of 21.5% and 18%, respectively.

Conclusions are that the supersonic study engine yielded fuel burn and DOC improvements well beyond the program goals; therefore, it is appropriate that advanced material programs be considered.

17. Key Words (Suggested by Author(s))	18. Distribution Statement
Advanced Supersonic Transport Engine, Unducted Fan Engine, Subsonic, Supersonic, Fuel Burn, Direct Operating Costs, Advanced Engines, Advanced Materials, Aero Improvements, and Year 2010 Technology	

19. Security Classif. (of this report)	20. Security Classif. (of this page)	21. No. of Pages	22. Price
		163	

FOREWORD

The propulsion system definition study reported herein was performed under the technical direction of Gerald Knip, NASA Lewis Research Center. The Advanced Technology Programs Department of General Electric Company conducted the study.

The Conceptual Preliminary Design Staff established referee aircraft simulations, established baseline and advanced cycles, developed preliminary engine designs with advanced materials, performed mission analyses to evaluate potential fuel burned and direct operating cost (DOC) savings, established material payoff, and completed flowpath and engine drawings. The study was performed with inputs from Engineering Materials Technology Laboratories.

The principal General Electric Engineering personnel performing this study were as follows:

- Task I: P. Feig
- Task II: V. Sprunger, R Steinmetz, L. Dunbar and J. Ciokajlo.
- Task III: P. Feig
- Task IV: D. Carlson
- Task V: P. Feig, V. Sprunger, R. Steinmetz, L. Dunbar, J. Ciokajlo and D. Carlson.

NASA Langley and The Boeing Aircraft Company provided assistance through the review of Task I reference airplanes.

TABLE OF CONTENTS

TABLE OF CONTENTS (Concluded)

LIST OF ILLUSTRATIONS

LIST OF ILLUSTRATIONS (Concluded)

LIST OF TABLES

LIST OF TABLES (Continued)

LIST OF TABLES (Concluded)

I. SUMMARY

The Revolutionary Opportunities for Materials and Structures (ROMS) study was performed to provide focus for Government and industry gas turbine programs by identifying subsonic transport and supersonic transport payoffs with year 2010 technology readiness materials and innovative structural approaches. The study scope is as follows:

- Baseline Aircraft and Engine Definitions
- Advanced Engine Cycle, Configuration, and Material Selections
- Mission, Fuel Burn, and DOC Analysis
- Propulsion Evaluation and Technology Ranking
- Technology Recommendations and Material Program Plans.

The study was divided into the following tasks:

- Task I Definition of Baseline Aircraft and Missions
- Task II Engine Cycle, Configuration, and Materials Selection
- Task III Propulsion Evaluation and Technology Ranking
- Task IV Recommended Technology Programs
- Task V Reporting.

The following baseline and engine technology improvement targets were established at the outset of the ROMS study:

- Year 1984 - Technology Readiness Base
- Year 2010 - Technology Improvements to Provide:
  - Subsonic - 15% Fuel Burn - 7% Direct Operating Cost (DOC)
  - Supersonic - 15% Fuel Burn - 5% DOC.

The mutually selected study engines were as follows:

- Subsonic - Unducted Fan (UDF) study engine, 22,000 lb thrust size
- Supersonic - Mach 2.7 Advanced Supersonic Transport (AST) study engine, 47,500 lb thrust size.

In the performance of this study, various advanced subsonic and supersonic engines were evaluated. The advanced engine cycles were mutually selected. The subsonic and supersonic fuel burn goals included payoff from both material improvements and aero improvements. The subsonic DOC improvement goal was reduced from 7% to 5%. The subsonic advanced material goal costs were also established at the same level as the baseline engine in order to achieve the reduced DOC goals.

The advanced study engine fuel burn and DOC improvements were identified as follows:

	Δ Fuel Burn	Δ DOC
Subsonic		
• 1984 Baseline UDF	Base	Base
• Target	-15%	-5%
• Advanced UDF (with Aero)	-13.4%	-5%
Supersonic		
• 1984 Baseline AST	Base	Base
• Target	-15%	-5%
• Advanced AST (with Aero)	-21%	-18%

From the above comparison, one can conclude that the subsonic payoffs did not quite meet the goals, but the supersonic payoffs significantly exceeded the goals.

The supersonic study engine material and aero rankings based on DOC improvement are as follows:

Material	Payoff, % of Total
Intermetallics	60
Carbon-Carbon	31
Advanced Aero	7
Fiber-Reinforced Metal Matrix	3

The conclusions are that both subsonic and supersonic engines will benefit from Year 2010 material and aero technology. The aircraft mission and aircraft utilization impact the magnitude of the payoff.

II. NOMENCLATURE

Symbol	Definition
AST	Advanced Supersonic Transport
ASP	Aircraft Synthesis Program software (NASA LaRC)
ATA	Air Transport Association
A17	Area, aft variable area bypass injector (VABI)
A8	Area, core nozzle
A14B	Area, forward VABI
AR	Aspect Ratio
BPR	Bypass Ratio
KCAS	Calibrated Air Speed in nautical miles
CMC	Ceramic Matrix Composite
CVD	Chemical Vapor Deposition
CAMAL	Commercial Aircraft Mission Analysis software (General Electric)
CAE	Computer Aided Engineering
W2R	Corrected Air Flow, engine inlet
δ	Corrected Pressure, ambient over standard day ambient
θ	Corrected Temperature, ambient over standard day ambient
dBA	A weighted sound level in decibels (dB)
ρ	Density
DOC	Direct Operating Cost
EPNdB	Effective Perceived Noise Level in decibels
ηc	Efficiency, compressor
ΔH	Energy, turbine extraction
EBU	Engine Buildup Unit
STP205	Engine core fan inlet guide vane (IGV) angle
EFH	Engine Flight Hour
FAR	Federal Aviation Requirements
fps	Feet per second
W	Flow
Wc	Flow, cold exhaust
W36	Flow, combustor air

Symbol	Definition
$W\sqrt{T}/P$	Flow function
WH	Flow, hot core exhaust
gal	Gallon
HPC	High Pressure Compressor
HIP	Hot Isostatic Pressure
IGV	Inlet Guide Vane
kNt	Kilonewtons
L/D	Lift over Drag
ψ	Loading, turbine pitch
LPC	Low Pressure Compressor
M_0	Mach Number, free stream
MH	Maintenance Hour
m	Meters
E	Modulus of Elasticity
E^3	NASA Energy Efficient Engine
NASA	National Aeronautics and Space Administration
nmi	Nautical Mile
NDE	Nondestructive Evaluation
OEW	Operating Empty Weight
OPR	Overall Pressure Ratio
PAX	Passengers
lb	Pounds
P0	Pressure, ambient
P8	Pressure, core exhaust nozzle
HP	Pressure, high
LP	Pressure, low
PR	Pressure Ratio
J	Propeller Advance Ratio
SHP/A	Propeller Disk Loading
P/A	Propeller Pressure Coefficient
T/A	Propeller Thrust Coefficient
R/r	Radius Ratio
ROC	Rate of Climb

Symbol	Definition
ROMS	Revolutionary Opportunities for Materials and Structures Study
rpm	Revolutions per minute
SL	Sea Level
SLS	Sea Level Static
DN	Shaft Diameter (mm) × Shaft Speed (rpm)
sfc	Specific Fuel Consumption
σ	Stress
Msi	millions of pounds per square inch
ksi	thousands of pounds per square inch
Γ	Swirl, turbine exit
TOFL	Takeoff Field Length
MTOGW	Takeoff Gross Weight, maximum
T3	Temperature, compressor discharge
T8	Temperature, core exhaust
ΔTamb	Temperature Difference (ambient minus standard day ambient)
T41	Temperature, turbine inlet
TBC	Thermal Barrier Coating
FN	Thrust, engine net
T/W	Thrust to weight ratio
AN^2	Turbine exit area times shaft speed squared
UDF	Unducted Fan
VABI	Variable Area Bypass Injector
VCE	Variable Cycle Engine
Vt	Velocity, blade tip
Vc	Velocity, cold exhaust
Vr	Velocity, compressor rim
VH	Velocity, hot core exhaust
Sw	Wing Area
W/S	Wing Loading
$\Lambda c/4$	Wing Quarter Chord Sweep Angle

III. INTRODUCTION

Over the years, both subsonic and supersonic propulsion systems have been improved significantly through improved cycles (higher overall pressure ratios, higher bypass ratios, and hotter turbine inlet temperatures). However, material properties have limited improvement due to loss in material properties at increased operating temperatures. Challenging material goals have been developed for future materials, which would permit another significant propulsion system improvement. This program was established to rank the goal materials and identify the fuel burn and DOC payoffs for each material, so that the limited development funding could be effectively utilized.

IV. EXECUTIVE SUMMARY

The mutually selected study engines for the ROMS program are as follows:

- Subsonic - Unducted Fan Study Engine, 22,000 lb thrust size
- Supersonic - Mach 2.7 Advanced Supersonic Transport Study Engine, 47,500 lb thrust size.

A comparison of the subsonic baseline and advanced UDF study engine flowpaths is shown on Figure 1. The baseline engine is a 1984 technology version of the General Electric proposed production UDF. The advanced subsonic engine incorporates improved aerodynamics and materials. This comparison illustrates the effect of the higher overall pressure ratio and higher bypass ratio of the advanced study engine. Table I compares the advanced versus baseline engine cross sections. The advanced engine weight reduction is due to reduced core size and lower density materials. The advanced engine centrifugal compressor stage is required to minimize the effect of the small compressor exit flow area. The small compressor exit flow area results from low compressor flow at high bypass ratio and the selected overall pressure ratio of 110. The advanced engine high bypass ratio contributes to the greater number of power turbine stages.

Table I. UDF Advanced Versus Baseline Engine Cross Section Comparisons.

- Engine Envelope Unchanged
- Advanced Engine 14% Lighter
- Advanced Engine has Centrifugal Compressor Stage
- Advanced Engine Core Significantly Smaller
- Advanced Engine Power Turbine has 12×12 Stages Versus 8×8

The supersonic baseline and the advanced study engines are compared on Figure 2. The baseline engine is considered 1984 technology level and is identical to the earlier AST study engines. This comparison illustrates the

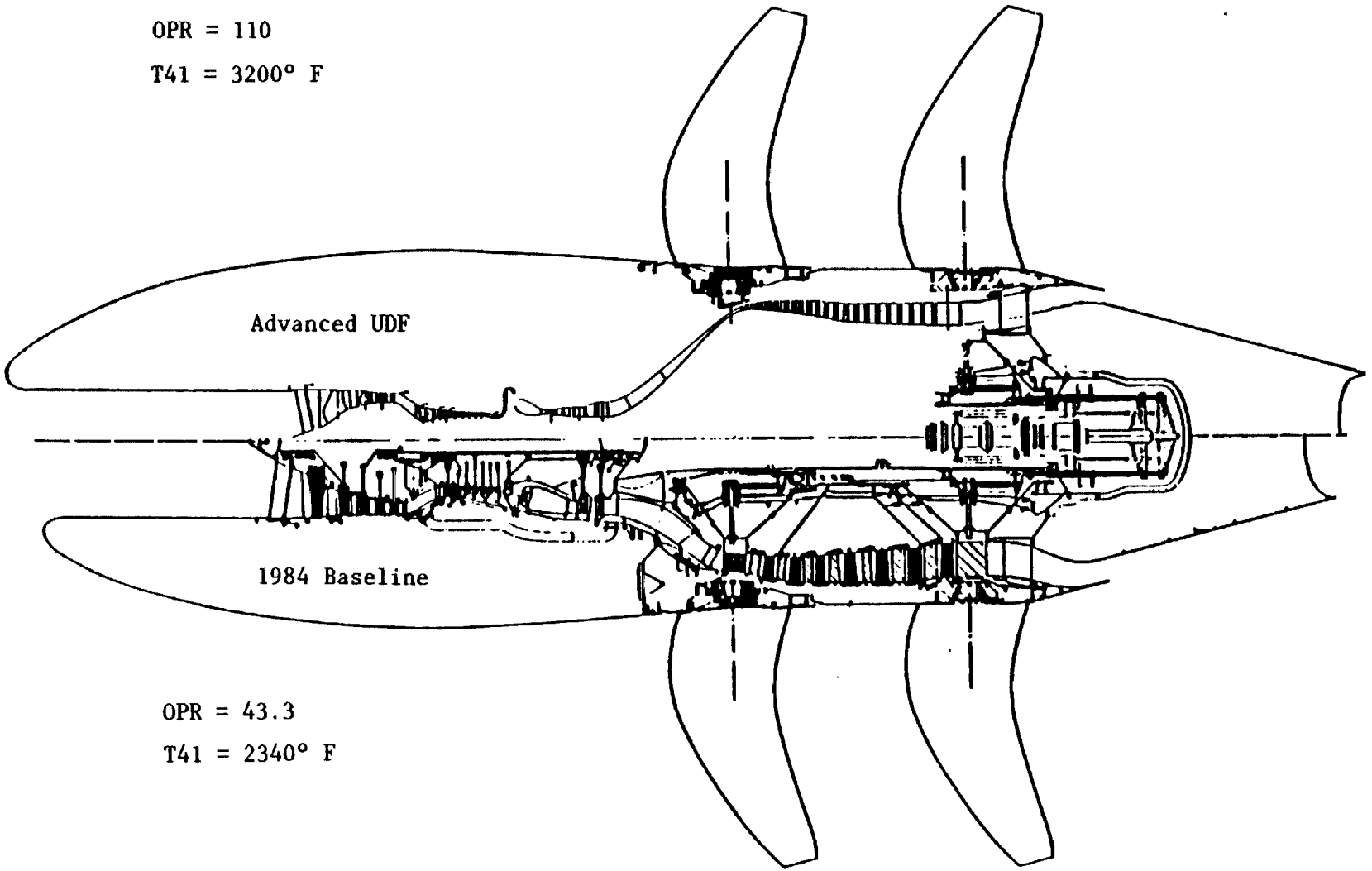

Figure 1. Advanced and Baseline UDF Flowpath Comparison.

OPR = 16
T41 = 4100° F
BPR = 2.44

Advanced AST

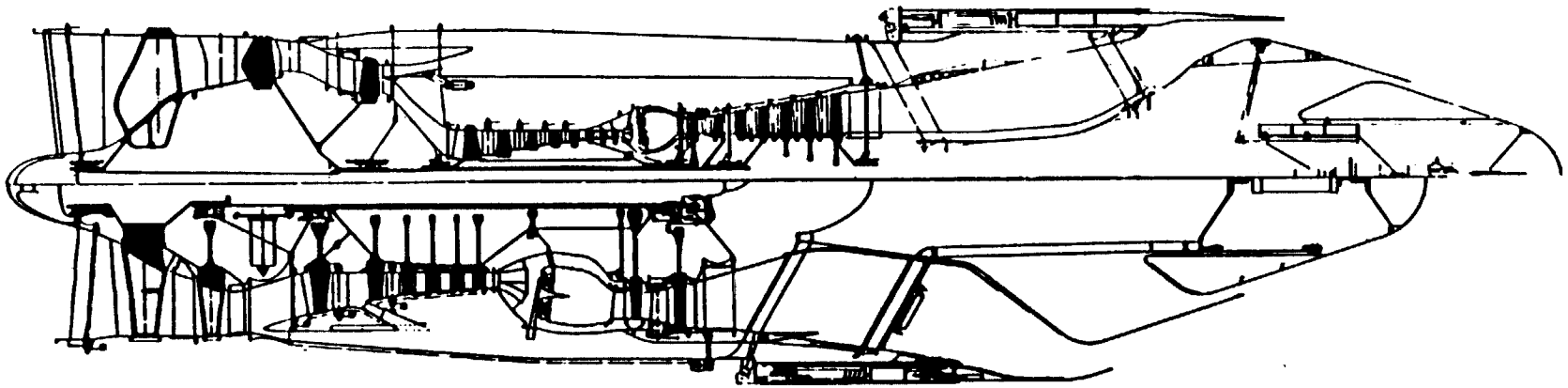

OPR = 5.4
T41 = 2700° F
BPR = 0.58

1984 Baseline

Figure 2. Advanced Versus AST Engine Comparison.

effect of the advanced engine's higher bypass ratio, higher overall pressure ratio, and advanced structural components.

Table II is a comparison of the advanced versus baseline study engines. Again this comparison illustrates the effects of the higher bypass ratio and the lower density material. The supersonic study engine is the GE supersonic variable cycle engine (VCE), which was evaluated as a supersonic transport study engine power plant. This baseline engine incorporated a core-driven third stage fan. Since the advanced study engine operates at a considerably higher bypass, the fan-driven third stage fan would operate at a lower tip speed than the core-driven stage, thereby increasing component efficiency and improving sfc. The high turbine inlet temperatures of the advanced engine provided adequate thrust without the augmentor, thereby reducing weight and eliminating a component from the advanced study engine.

Table II. AST Advanced Versus Baseline Engine Cross Section Comparisons.

- Advanced AST is Longer, with Smaller Maximum Diameter
- Advanced Engine is 44% Lighter
- Advanced Engine has Fan-Driven 3rd Stage Versus Core-Driven
- Augmentor Eliminated from Advanced Engine
- Advanced Engine Core Significantly Smaller
- Six LP Turbine Stages Versus One LP Turbine Stage

Table III is a brief list of advanced materials (compared to baseline materials) used on both the subsonic and the supersonic study engines.

Table III. Advanced Versus Baseline Materials Comparisons.

	Baseline	Advanced
Cold Parts	Current Metals (Iron, Nickel, and Titanium Alloys)	Fiber-Reinforced Metal Matrix
Hot Parts	Nickel-Based Alloys	Nonmetallic Composites
	Cobalt-Based Alloys	Intermetallics

Table IV is a list of some of the key structures which can be adopted because of the availability of the advanced materials.

Table IV. Advanced Versus Baseline Structures Comparisons.

Uncooled Turbine Blades and Vanes
Uncooled Combustor Liners
Rod Frames Versus Strut Frames
Blisk Versus Dovetail Design
Dry Bearings Versus Lube Bearings

Advanced study engine production costs were determined as an input to the DOC evaluation. The subsonic advanced study engine costs increased more than the supersonic advanced study engine costs. Table V shows the high stage and blade count of the subsonic engine which contributes to this increased cost.

Table V. Advanced Study Engine Stage Count and Airfoil Count Comparison.

	UDF		AST	
	No. of Stages	No. of Airfoils	No. of Stages	No. of Airfoils
Prop	2	20	-	-
Fan	3	306	3	314
Compressor	7+1	885	8	740
HP Turbine	2	148	1	82
IP Turbine	2	92	-	-
LP Turbine	12x12	4230	6	972
Totals	29	4796	18	2108

Two baseline aircraft (one subsonic and one supersonic) were used to determine fuel burn and DOC improvements. The subsonic study aircraft is defined in Figure 3 and the supersonic study aircraft is defined in Figure 4.

The baseline and advanced subsonic and supersonic study engine fuel burn and DOC improvements are compared on Table VI. Note the significant supersonic improvements, which far exceed the target values. Figure 5 illustrates the impact of engine acquisition cost and maintenance cost on DOC improvement. Figure 6 illustrates the impact of sfc improvement and weight improvement on subsonic and supersonic engine size. This size reduction favorably impacts supersonic DOC improvement due to reduction in fuel burn and engine costs. Higher engine and maintenance costs had a greater impact on subsonic Δ DOC than on supersonic Δ DOC.

Table VI. Fuel Burn and DOC Improvement.

	Δ Fuel Burn	Δ DOC
Subsonic		
1984 Baseline UDF	Base	Base
Revised Target	-15%	-5%
Advanced UDF (w/Aero)	-13.4%	-5.0%[1]
Supersonic		
1984 Baseline AST	Base	Base
Target	-15%	-5%
Advanced AST (w/Aero)	-21.5%	-18%[2]

[1] Assumes no increase in advanced engine costs and 0% interest rate

[2] Includes advanced material costs

- Fuel cost is $1.50/gal
- Subsonic mission was 500 nmi
- Supersonic mission was 5000 nmi

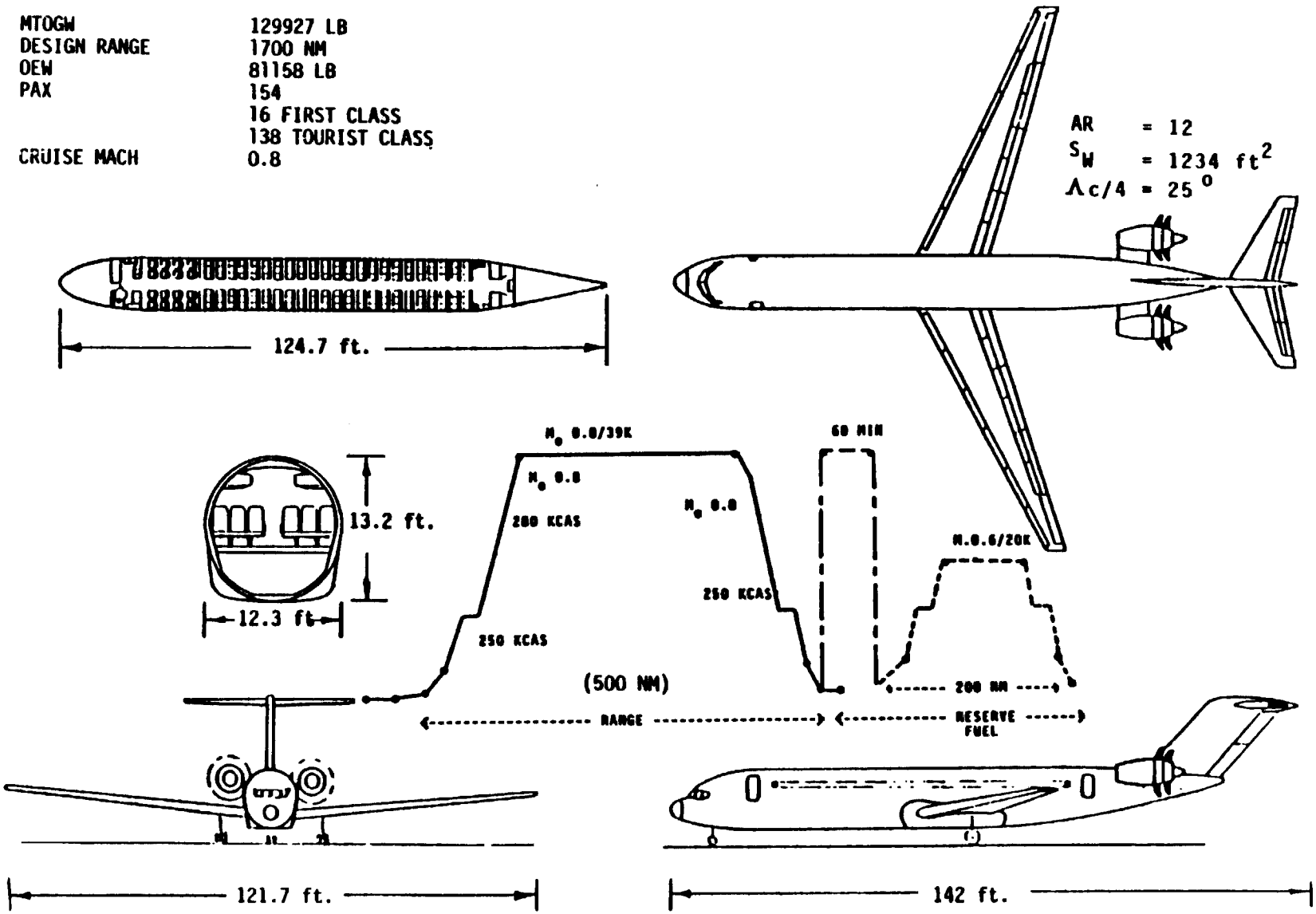

Figure 3. Subsonic Study Aircraft and Mission Definition.

AR = 1.9
S_W = 7938 ft
$\Lambda_{c/4}$ = 47.4°

MTOGW	601,435 lb
Design Range	5000 nmi
OEW	233,810 lb
Passengers	290
Cruise Mach	2.62

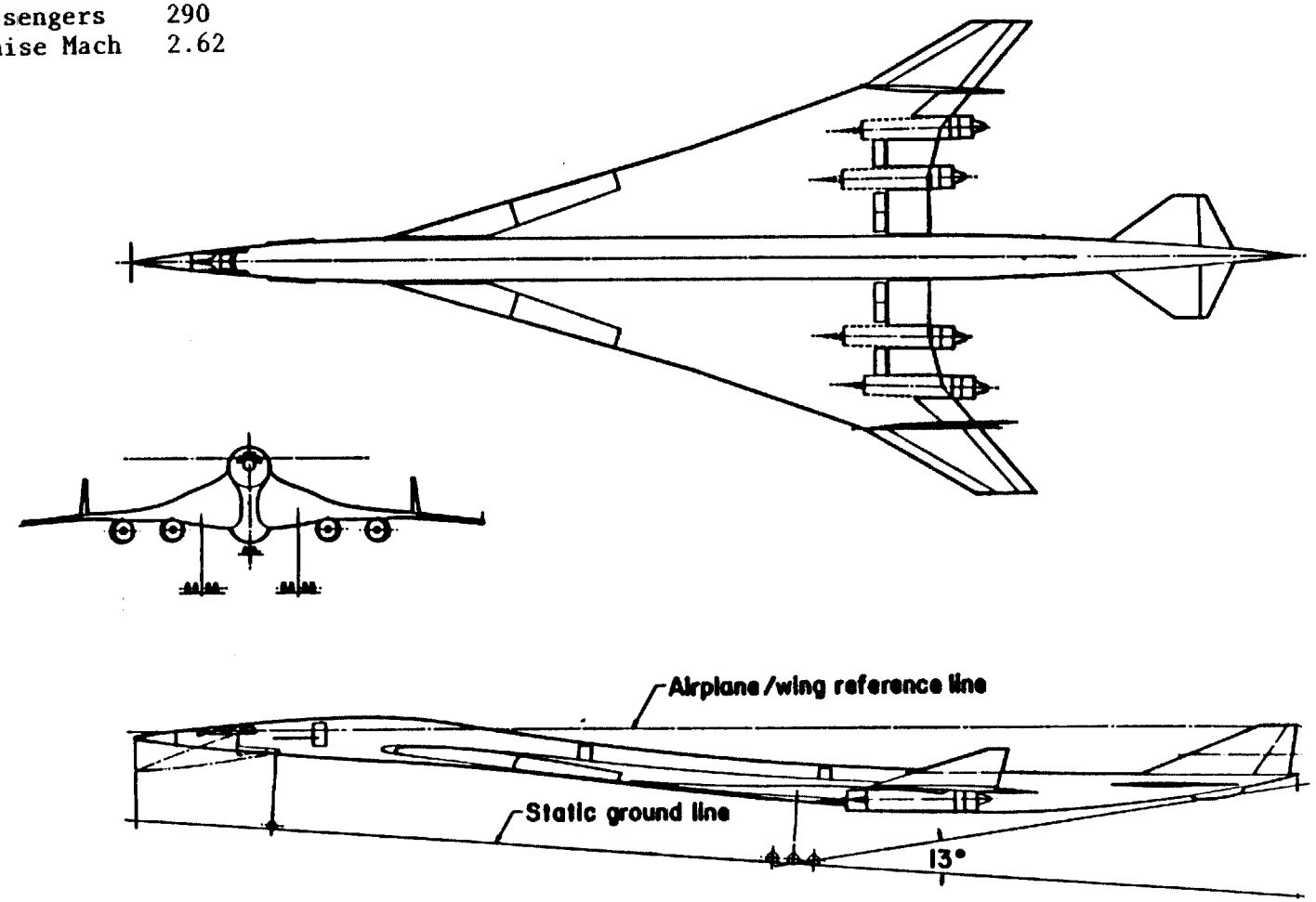

Figure 4. Supersonic Study Aircraft and Mission Definition.

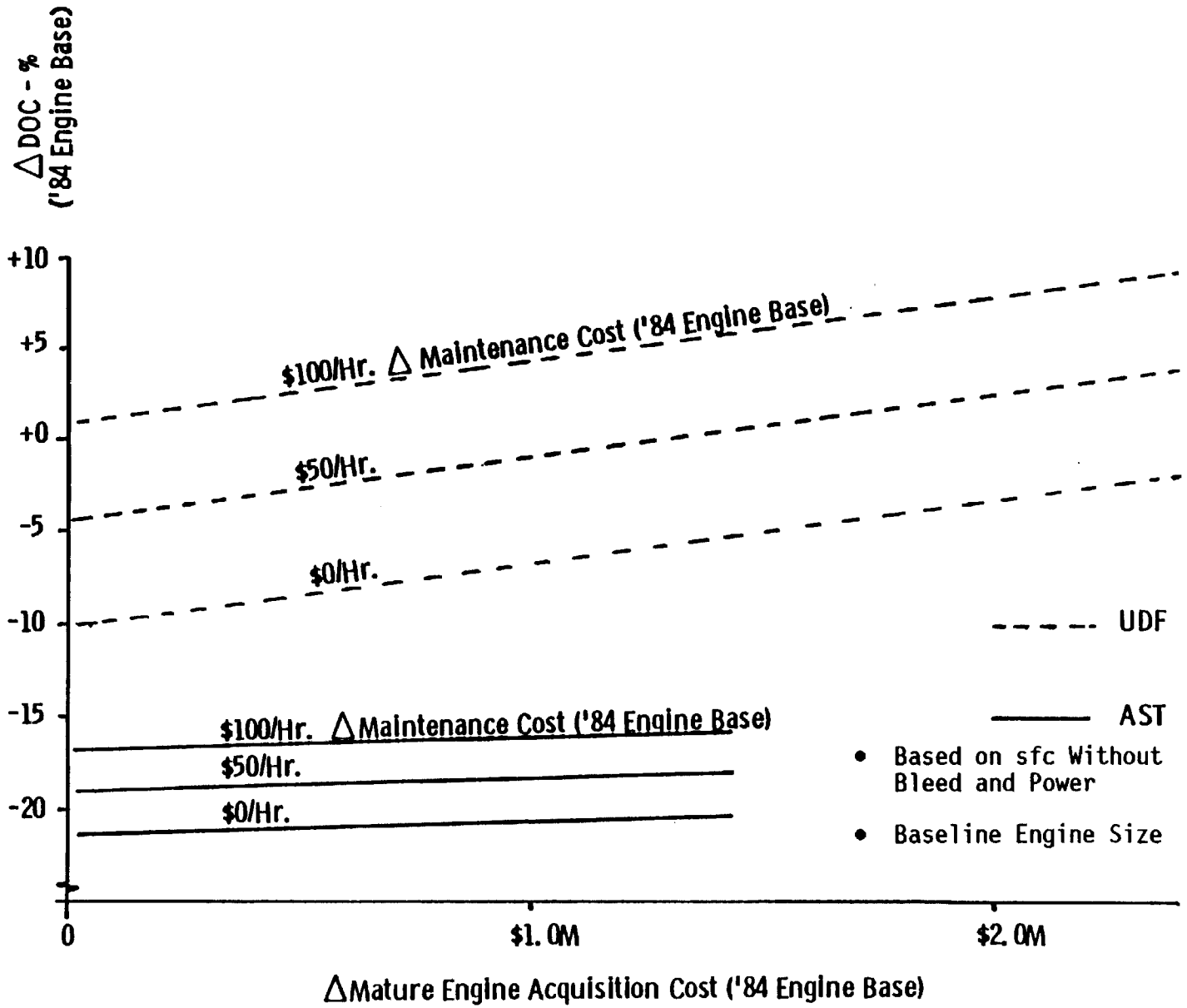

Figure 5. Advanced Study Engine DOC Payoff Versus Δ Acquisition and Maintenance Cost.

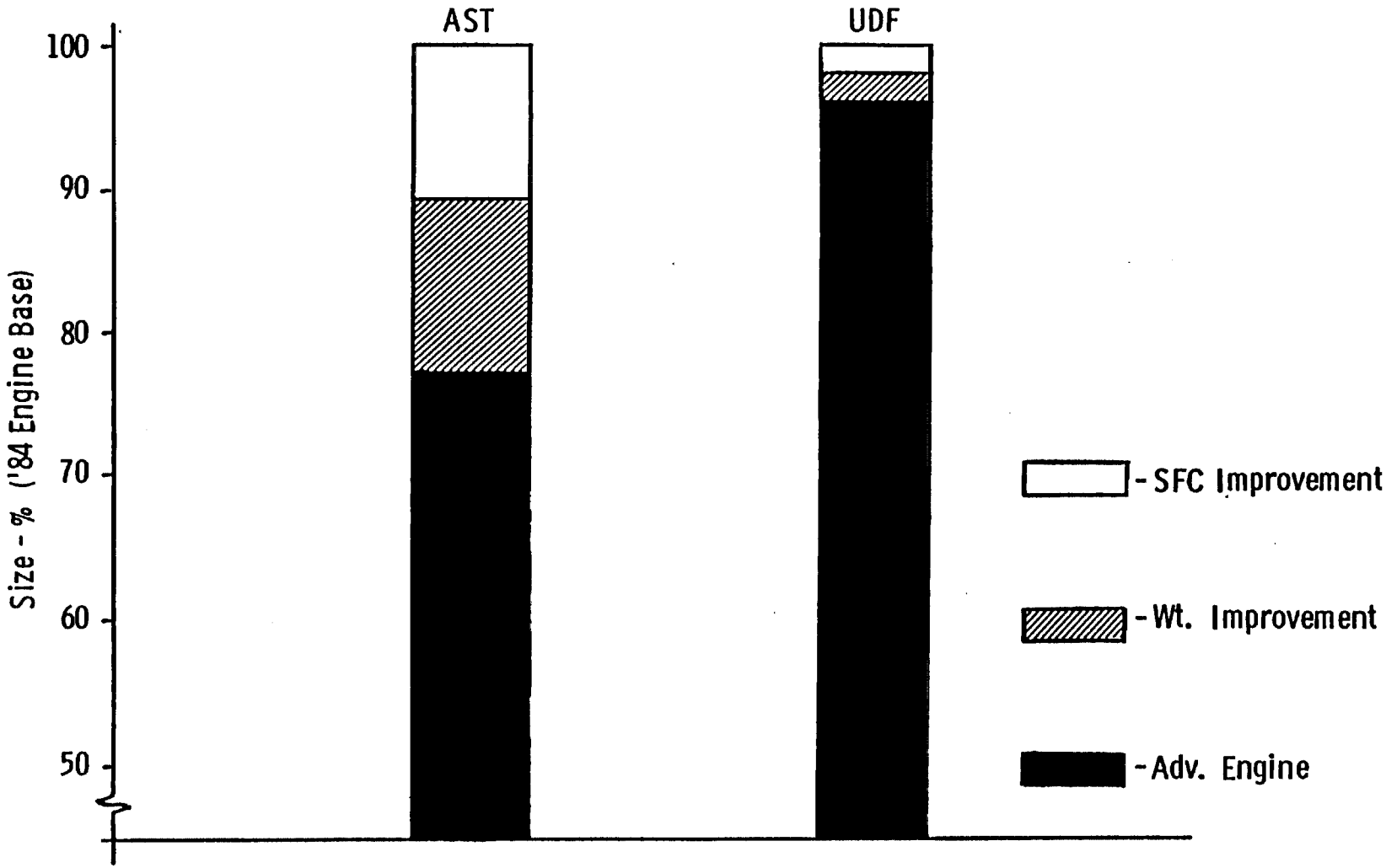

Figure 6. Influence of SFC and Weight Reduction on Engine/Aircraft Size.

DOC and fuel burn payoffs were determined for each of the advanced materials and for improved aerodynamics. The advanced materials were then ranked for both the subsonic study and the supersonic study. The subsonic material rankings are shown on Table VII, and the supersonic material rankings are shown on Table VIII. Carbon-carbon and intermetallics show the greatest material payoffs on both study engines.

The study conclusions are that both subsonic and supersonic study engines show significant fuel burn payoff, but the supersonic DOC material payoff far exceeds that of the subsonic study because of the longer range supersonic mission.

Table VII. ROMS Subsonic Study, Advanced Material and Aero Rankings.

	DOC Payoff, %	Material or Aero	Fuel Burn Payoff, %
	-2.34	Adv. Aero	-6.5
	-1.55	Carbon/Carbon	-3.9
	-1.08	Intermetallics	-3.0
Totals	-4.97		-13.4

Notes:
- 0% Interest
- $1.50/gal fuel cost
- No increase in advanced material costs
- No increase in engine maintenance cost

Table VIII. ROMS Supersonic Study, Advanced Material and Aero Rankings.

	DOC Payoff, %	Material or Aero	Fuel Burn Payoff, %
	-10.79	Intermetallics	-11.4
	- 5.57	Carbon-Carbon	-6.7
	- 1.25	Advanced Aero	-1.5
	- 0.48	Fiber Reinforced Metal Matrix	-1.1
	+ 0.03	Advanced Titanium	-0.05
	+ 0.03	Ceramic Composites	-0.05
Totals	-18.03		-21.5

Notes:
- 0% Interest
- $1.50/gal fuel cost
- 100% of estimted advanced materials costs
- Material content of maintenance costs proportional to acquisition costs.

V. DISCUSSION

1.0 TASK I - BASELINE AIRCRAFT AND MISSION SELECTIONS

Two study aircraft were selected (one subsonic and one supersonic) and representative mission scenarios were formulated to provide realistic appraisals of the influences of the engine technology advancements on fuel burn and DOC between the 1984 baseline and the year 2010 technology readiness subsonic and supersonic study engines. The aircraft and mission selections were based primarily on the Statement of Work ground rules as defined in Table IX.

To provide study results that reflect only engine technology influences on fuel burn and DOC, General Electric chose to use the same configuration for both the 1984 and 2010 year aircraft, except that the aircraft and engines were "rubberized" (scalable). This approach permitted the inclusion of aircraft resizing benefits due to changes in engine technology advancements from fuel burn and DOC results desired in a propulsion study.

1.1 SUBSONIC AIRCRAFT AND MISSION

The candidate subsonic aircraft and mission were based on typical 150-passenger study configurations being used to evaluate General Electric's aft-mounted Unducted Fan Engine (UDF™). This initial candidate configuration was reviewed on August 28, 1985 with engineering personnel of the Boeing Commercial Aircraft Company and the NASA LeRC program manager. Comments and recommended modifications to the selected High-Tech initial configuration for a 1700 nmi design range at MTOGW with maximum passengers were as follows:

- Reduce the vertical tail approximately 10%
- For an aircraft with negative stability, the horizontal tail could be reduced approximately 25%
- Pylon weight should be increased so that installed engine, nacelle and pylon should weigh between 13,000 and 13,500 pounds.
- The high speed drag polars and cruise L/D are representative of a proposed 154-passenger aircraft.

Table IX. Statement of Work Rules.

1. Propfan-powered Subsonic Transport

- 154 passenger (design)
- Twin engine
- Mach 0.72 - 0.8 at cruise
- 1700 nmi design range with 154 passengers
- 400 nmi typical range with 65% load factor
- Engine size

  FAR 36 community noise and 82dBA cabin noise; takeoff field length 7,000 ft at 85° F SL; initial cruise altitude 35,000 ft

- No drag penalty for propeller slipstream swirl effect for wing-mounted engines
- Reference propeller - 8 to 10 blades for single rotation or 5 × 5 to 8 × 8 for counterrotation

2. Supersonic Transport

- 300 passenger (design)
- Four engine
- Mach 2.7 at cruise
- 5000 nmi design range with 300 passengers
- 3600 nmi typical range with 80% load factor
- Engine size

  FAR 36 traded noise levels; takeoff field length 12,400 ft; initial cruise altitude 50,000 ft

- The associated wing and fuselage weights plus the overall OEW are reasonable for a High-Tech aircraft.

- Change the TOFL objective for MTOGW sea level from 6000 to 7000 feet to represent a more reasonable challenge.

The recommended modifications to the High-Tech were incorporated into the three view, and geometry and weight definitions as shown in Figure 7 and Table X.

The mission leg definition, as shown in Figure 8, was employed in the 1700 nmi, standard day, still air design sizing mission shown in Figure 9. The mission and speed schedules shown Figure 9 were also used to evaluate the fuel burns and DOC baseline values, and to calculate the weight and nacelle drag sensitivities at 500 nmi.

1.2 SUPERSONIC AIRCRAFT AND MISSION

The supersonic aircraft studies previously conducted by airframers were directed at Mach 2.2 to 2.4 cruise speed range. The Mach 2.7 cruise suggested in the Statement of Work (Table IX) was basically centered on studies conducted by NASA LaRC. In particular, a 1981 supersonic aircraft configuration designated the AST 205-1, References 1 and 2, represented an up-to-date effort on a Mach 2.7 cruise supersonic aircraft. The AST 205-1 is a 290 passenger aircraft powered by four General Electric GE21/J11-B14a variable cycle engines. Basically, the structure is a superplastic formed/diffusion bonded titanium construction, which resulted in a 640,000 pound takeoff gross weight for a 5000 nmi design range.

The AST 205-1 configuration and weights plus the mission scenario, as shown in References 1 and 2, were reviewed. Since documenting the AST 205-1 configuration, NASA LaRC had perturbed the design while maintaining the original wing loading and thrust-to-weight ratio. These perturbations were intended to represent potential improvements in weight technology for such items as structural materials, carbon brakes, and lighter interior fixtures. Based on these studies, NASA LaRC recommended the following changes to the baseline study configuration:

MTOGW	129927 LB
DESIGN RANGE	1700 NM
OEW	81158 LB
PAX	154
	16 FIRST CLASS
	138 TOURIST CLASS
CRUISE MACH	0.8

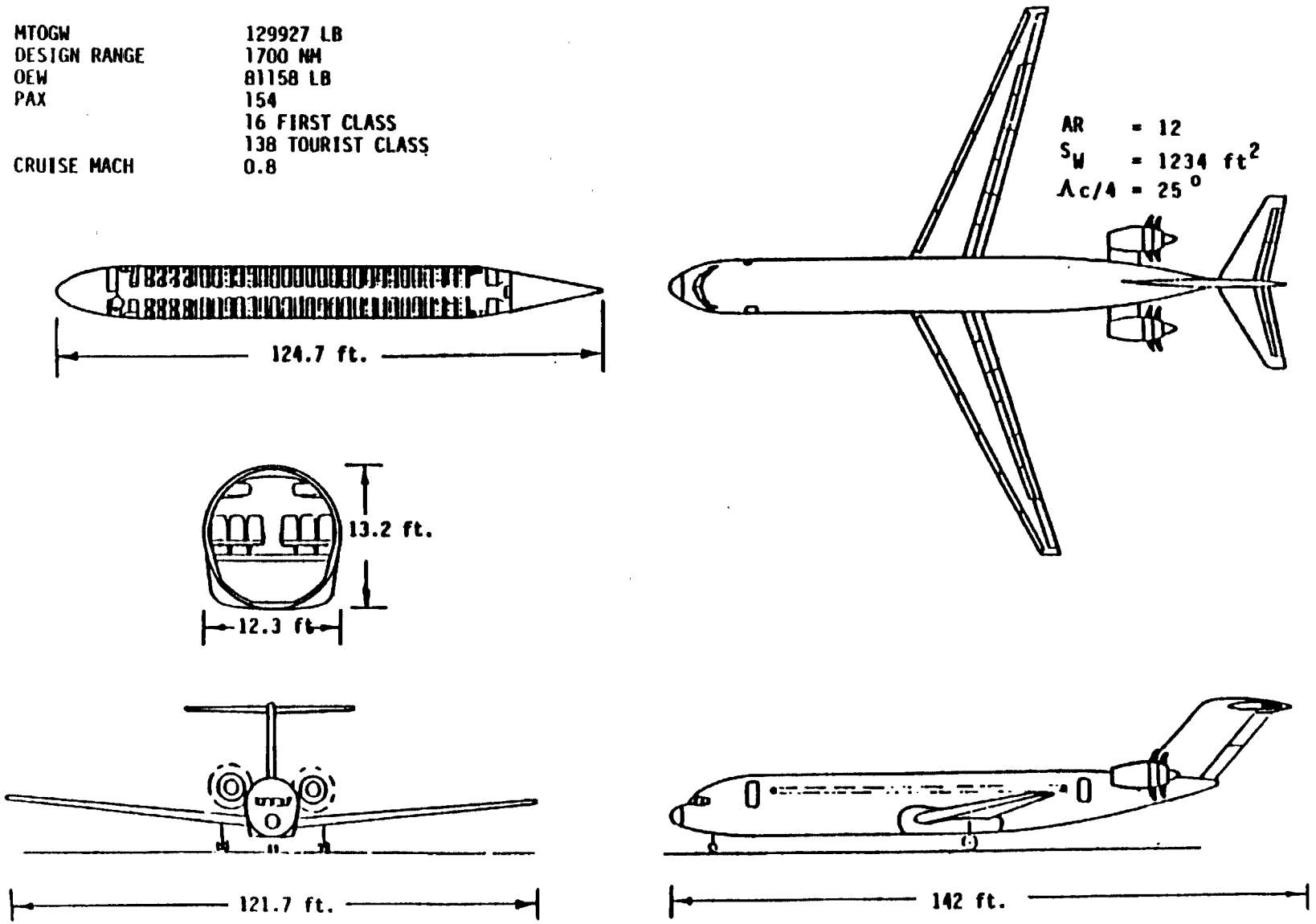

Figure 7. Subsonic Baseline Aircraft.

Table X. Subsonic Aircraft Weight and Geometry.

- Design Criteria: 1700 NMi, Maximum Passengers
  Year 1984

Wing Loading, Nt/m^2 (lb/ft^2)	5043 (105.3)
Passengers	154
Effective Body Diameter, m (ft)	3.91 (12.84)
SLS Thrust, kNt (lb)	90.04 (20,243)
MTOGW, kNt (lb)	577.9 (129,927)
OEW, kNt (lb)	358.6 (80,618)

	Wing	Horizontal Tail	Vertical Tail
Quarter-Chord Angle	25.00	30.00	40.00
Aspect Ratio	12.00	4.93	0.95
Thick/Chord	0.105	0.105	0.110
Taper Ratio	0.305	0.395	0.650
Camber	0.0125		
Reference Area, m^2 (ft^2)	114.64 (1234)	42.4 (456)	27.78 (299)
Span, m (ft)	37.18 (122)	14.3 (47)	
Mean Aero, Chord, m (ft)	3.38 (11.1)	3.11 (10.2)	5.49 (18.0)
Wetted Area, m^2 (ft^2)	199.6 (2148)	83.0 (893)	57.1 (615)
Volume Coefficient		2.4	0.13

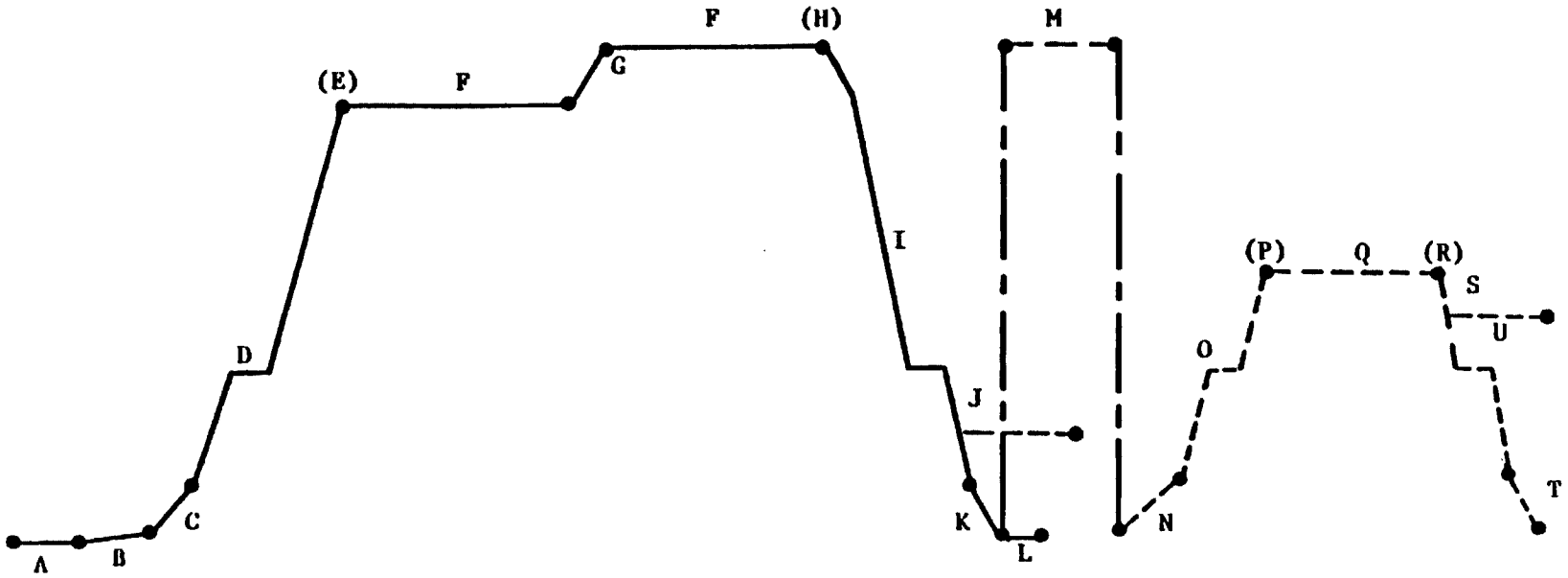

A - Taxi Out
B - Takeoff 35 ft
C - Climb Out 1500 ft
D - Climb
(E)- Acceleration
F - Cruise

G - Step Climb
(H)- Decel
I - Descent
J - Hold (Bookkeep in Reserves)
K - Approach and Landing
L - Taxi In
M - Extended Cruise

N - Missed Approach
O - Climb
(P)- Accel
Q - Cruise
(R)- Decel
S - Descent
T - Approach and Landing
U - Hold

Figure 8. Subsonic Mission Leg Definition.

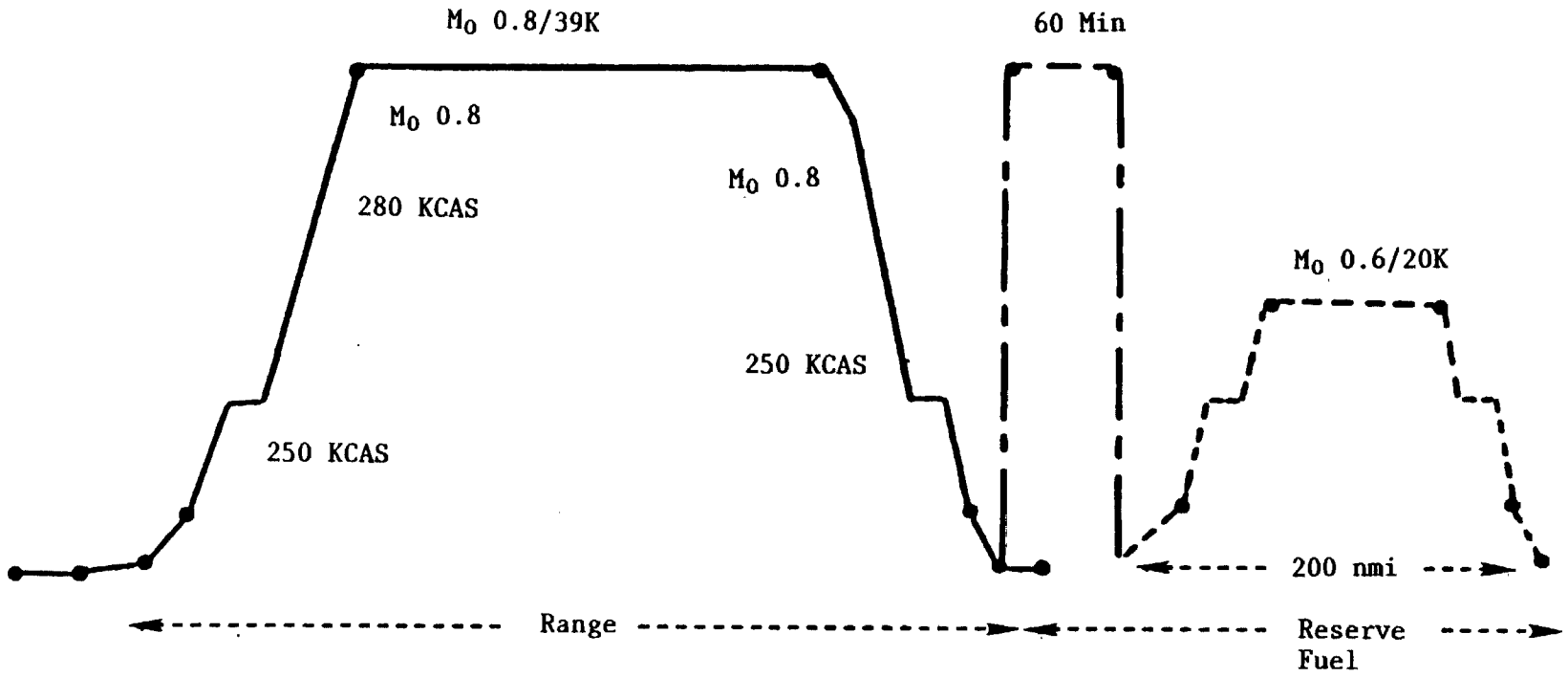

Figure 9. Subsonic Design Mission.

- Structures -15%
- Landing Gear -25%
- Furnishings -30%

These improvements in the aircraft's OEW downsized the original 640,000 pound MTOGW of the baseline aircraft; however, the NASA Program Manager requested that the design range be increased from 4500 to 5000 nmi (Figure 10). The change in the design range was accomplished by rubberizing the aircraft to the longer range and not by reoptimizing the configuration. A three view of the AST 205-1 is shown in Figure 11, and the baseline geometry and weights, after incorporation of the weight and range changes, are shown in Table XI.

1.3 DIRECT OPERATING COST METHODOLGY

The direct operating cost (DOC) measure of merit for the ROMS baseline and technology study engines was based on a computerized version of the formulas published by the Air Transport Association (ATA) in 1967 and modified in 1978 by a major commercial airframe manufacturer. The ATA method is the standard generic method generally used to calculate DOC; it includes the major cost elements and is consistent with the data reported by the airlines on Form 41.

The element of the DOC methodology and the interactions of these elements is shown in Figure 12.

The DOC ground rules, major elements, and baseline values for the subsonic and supersonic aircraft are shown in Tables XII and XIII.

1.4 NASA APPROVALS

In accordance with the ROMS Statement of Work, the NASA LeRC Program Manager's approval was required for the baseline subsonic and supersonic transport configurations and the Direct Operating Cost methodology.

PRIMARY
MISSION

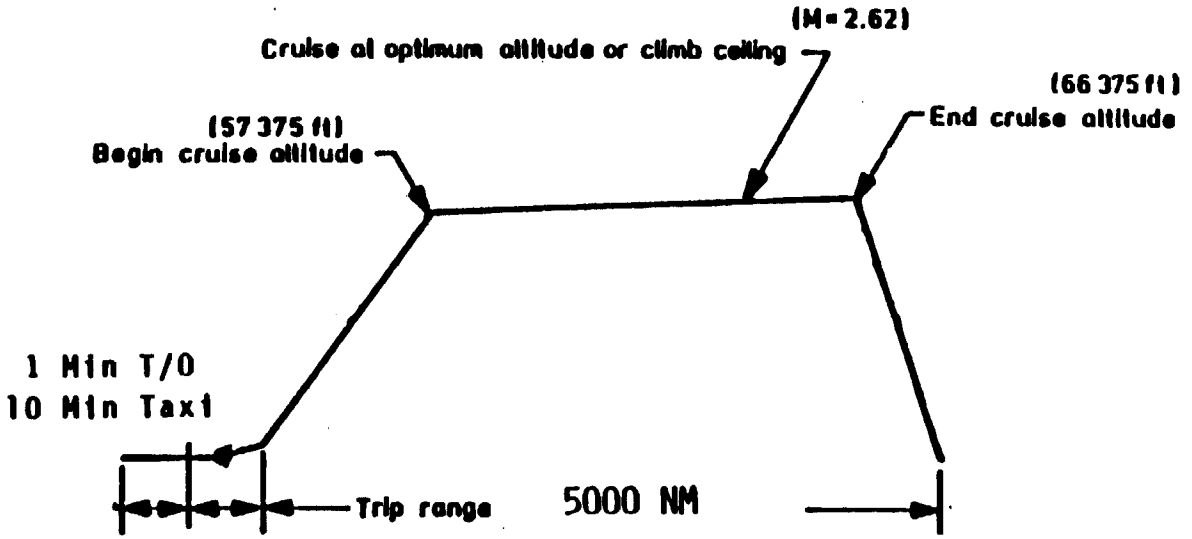

RESERVE
ALLOWANCE
MISSION

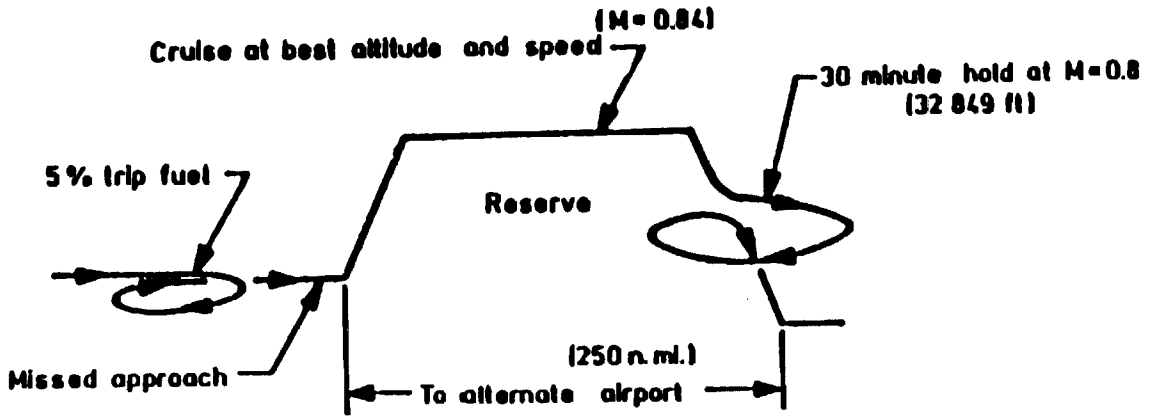

Figure 10. Supersonic Design Mission.

MTOGW	601435 lb
DESIGN RANGE	5000 NMi
OEW	233810 lb
PAX	290
CRUISE MACH	2.62

AR	1.9
S_W	7938 ft^2
$\Lambda_{c/4}$	47.4°

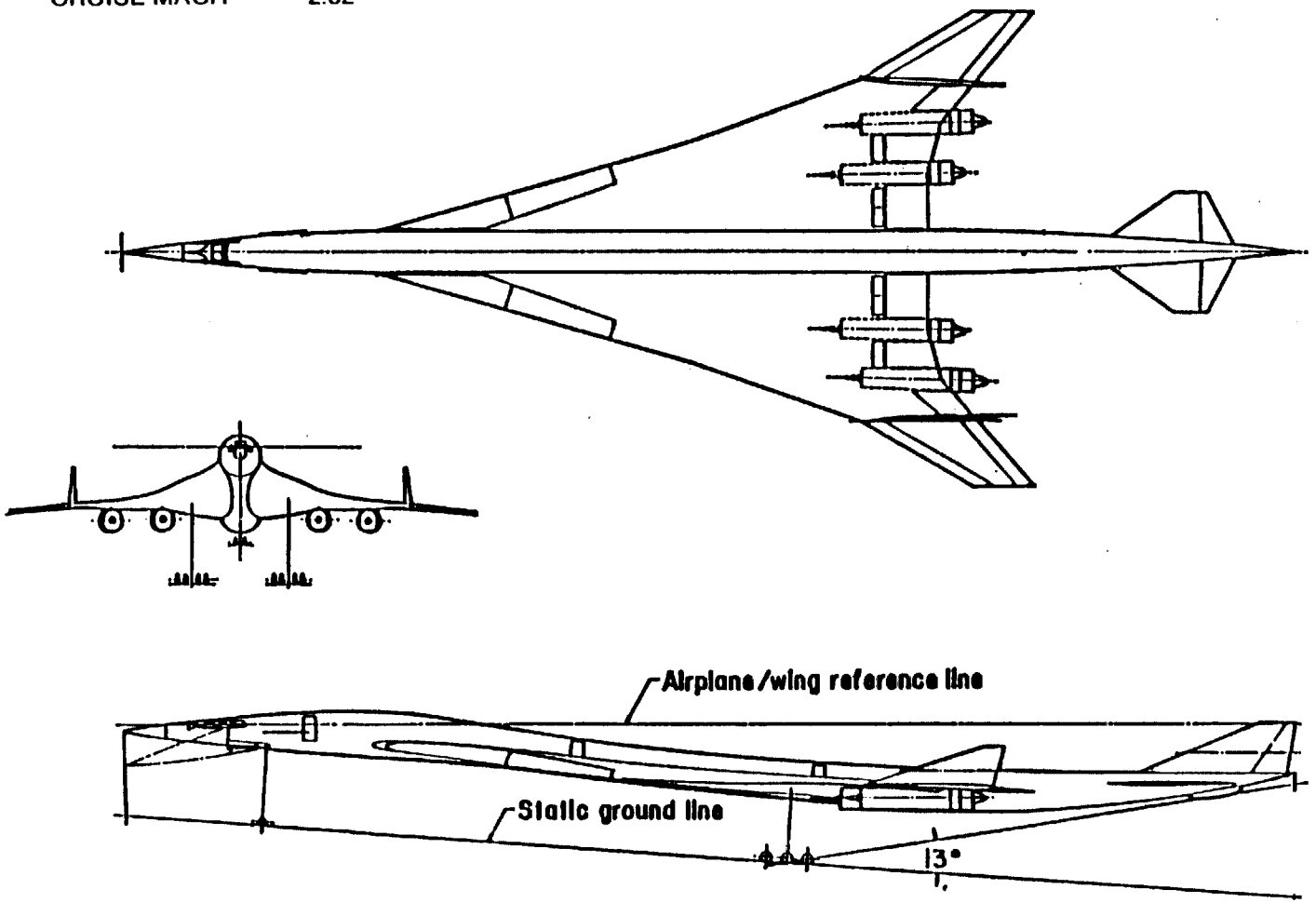

Figure 11. Supersonic Baseline Aircraft.

Table XI. Supersonic Aircraft Weight and Geometry.

- ROMS AST-205 Baseline Geometry Comparison 1984 Versus 2010
- Design Criteria: 5000 nmi with Maximum Passengers

Wing Loading, Nt/m^2 (lb/ft^2)	3629 (75.77)
Passengers	290
Maximum Fuselage Diameter, m (ft)	3.25 (10.66)
Quarter-Chord Angle	47.42
Aspect Ratio	1.90
Thick/Chord	0.03062
Total Wetted Area, m^2 (ft^2)	2451 (26384)
SLS Thrust, kNt (lb)	200.6 (45107)
MTOGW, kNt (lb)	2675.2 (601435)
OEW, kNt (lb)	1040.0 (233811)

	Wing	Horizontal Tail	Vertical Tail
Reference Area, m^2 (ft^2)	737.41 (7937.6)		
Wetted Areas, m^2 (ft^2)	1401.2 (15083)	92.07 (991)	68.93 (742)
Span, m (ft)	37.47 (122.9)		
Volume Coefficient		0.075	

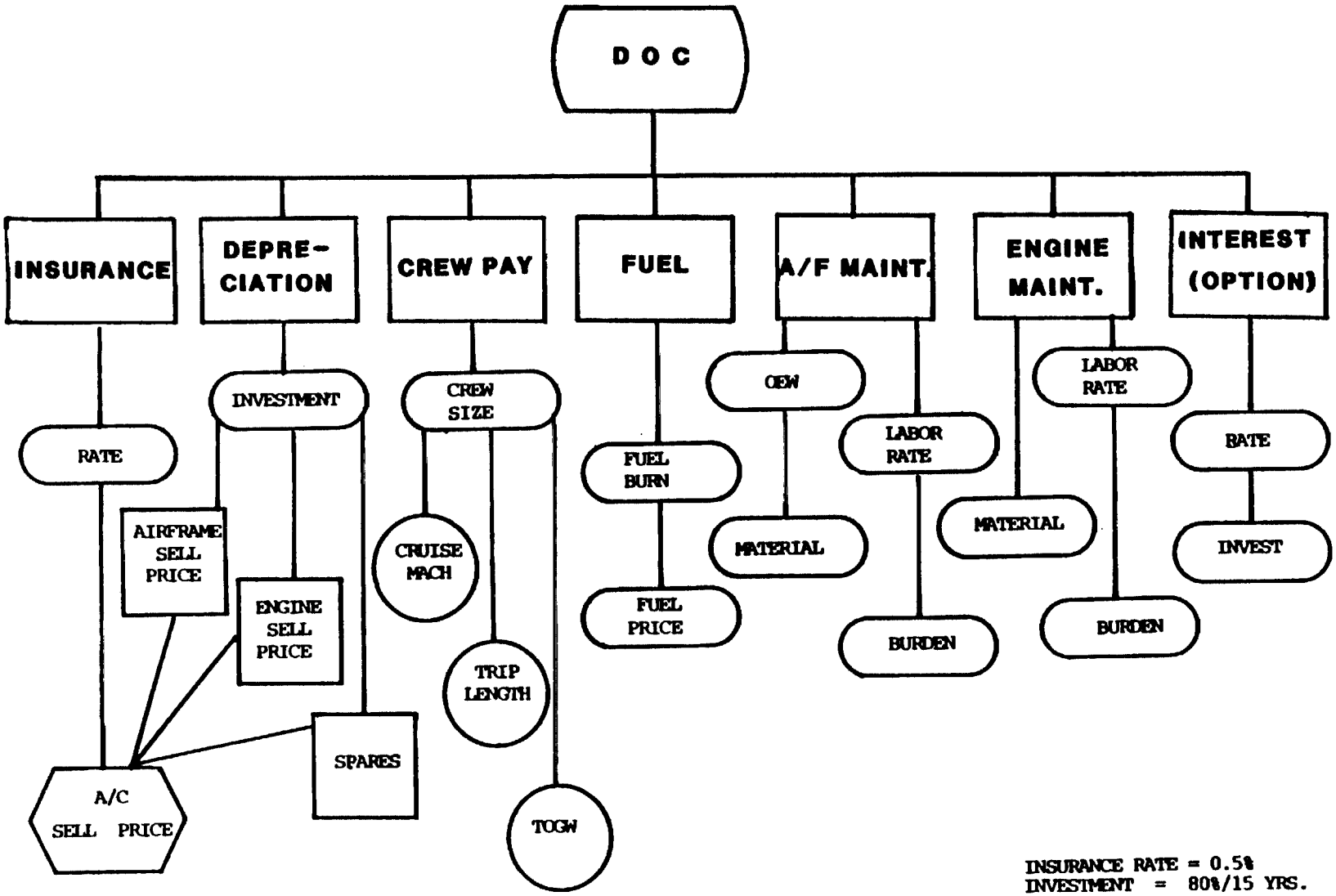

Figure 12. DOC Elements.

Table XII. DOC Ground Rules.

Subsonic High-Tech, 1984 UDF Baseline Inputs

Year Dollars	1985
Block Time, hr	1.56
Stage Length, nmi	500
Flight Profile	Domestic
Aircraft Economic Life, years	15
Aircraft Residual Value %	10
Utilization, trips/year	2200
Insurance Price, Percent of Initial Aircraft Price/year	0.5
Interest Rate, %/year	0.0, 3.0
Period of Loan, years	15
Propulsion System[(1)] Labor Price (fully burdened), $/MH	15.00
Labor Index, MH/EFH	0.737
Propulsion System Materials Cost, $/EFH	45.00
Ground Maneuver Time, min/flight	14
Passengers	160
TOGW, lb	121470
Configuration Layout	Mixed
Fuel Price, $/gal	1.00-2.50 in 0.50 Increments
Crew	2
Airframe Spares, Percent of Airframe Price	6
Propulsion System Spares, Percent of Propulsion System Price	30
Airframe Price, $/lb of Airframe Weight	250.53
Propulsion System Price, $/lb	985.31
Down Payment, Percent of Aircraft Price	10
SLS Thrust	20244
OEW, lb	80618
Propulsion System Weight, lb	4384
Average Airframe Parts Price, $/lb	250.53
Additional Propulsion System Weight Price, $/lb	985.31
Cruise Mach	0.8

[(1)]Propulsion System Includes Nacelle and Engine Buildup Unit (EBU).

Table XIII. AST DOC Ground Rules.

SST-DOC Baseline Inputs

Year Dollars	1985
Block Time, hr	3.8
Stage Length, nmi	5000
Flight Profile	International w/o Subsonic Cruise Leg
Aircraft Economic Life, years	15
Aircraft Residual Value, %	10
Utilization, Trips/year	1302
Insurance Price, % of Initial Aircraft Price/yr	0.5
Interest Rate, %/year	0.0, 3.0
Period of Loan, years	15
Engine Labor Price (fully burdened), $/MH*	0.00
Labor Index, MH/EFH*	0.000
Engine Materials Price, $/EFH*	0.000
Ground Maneuver Time, min/flight	10
Passengers	290
TOGW, lb	599617
Configuration Layout	All Tourist
Fuel Price, $/gal	1.00-2.50 in 0.50 increments
Crew	3.0
Airframe Spares, Percent of Airframe Price	6.0
Engine Spares, Percent of Engine Price	30.0
Airframe Price, $/lb of Airframe Weight	494
Engine Price, $/lb	592
Down Payment, Percent Aircraft Price	10.0
SLS Thrust	45107
OEW, lbs	233811
Engine Weight, lb	10193
Average Airframe Parts Price, $/lb	494
Additional Engine Weight Price, $/lb	592
Cruise Mach	2.62

*Baseline data not available - 2010 IOC advanced engine changes included deltas.

2.0 TASK II - ENGINE CYCLE, CONFIGURATION, AND MATERIAL SELECTION

Task II dealt with establishing subsonic and supersonic baseline and advanced engine cycles, configuration, and materials.

2.1 SUBSONIC ENGINE CYCLE

The ROMS subsonic engine cycle design and performance effort was based on the unducted fan engine configuration (Figure 13). Its features include:

- Two-spool core with bleed between the spools for cooling the power turbine mixer frame
- Counterrotating LP/HP spools
- Counterrotating power turbine driving a two-stage counterrotating UDF.

The reference or baseline engine was established as representative of technology available in 1984. With this cycle design established, cycle design parametric studies were conducted to guide the selection of the advanced (year 2010) ROMS engine.

The parametric studies covered a wide range of turbine inlet temperatures and compression pressure ratios. Component technology advances were attributed to aerodynamic improvements, and to materials and structures. The payoffs in the engine cycle design and performance for these advances were kept separate.

2.2 1984 BASELINE STUDY ENGINE

The cycle design selected for the ROMS baseline engine was established at the end of climb (Altitude = 35,000 ft, Mach No. = 0.80, ΔTamb = 18° F) for a maximum climb engine rating. The cycle design constraints included:

Thrust, lb	5510
Overall Compression Pressure Ratio	43.3
Bleed Bypass Ratio (LPC Discharge)	0.088

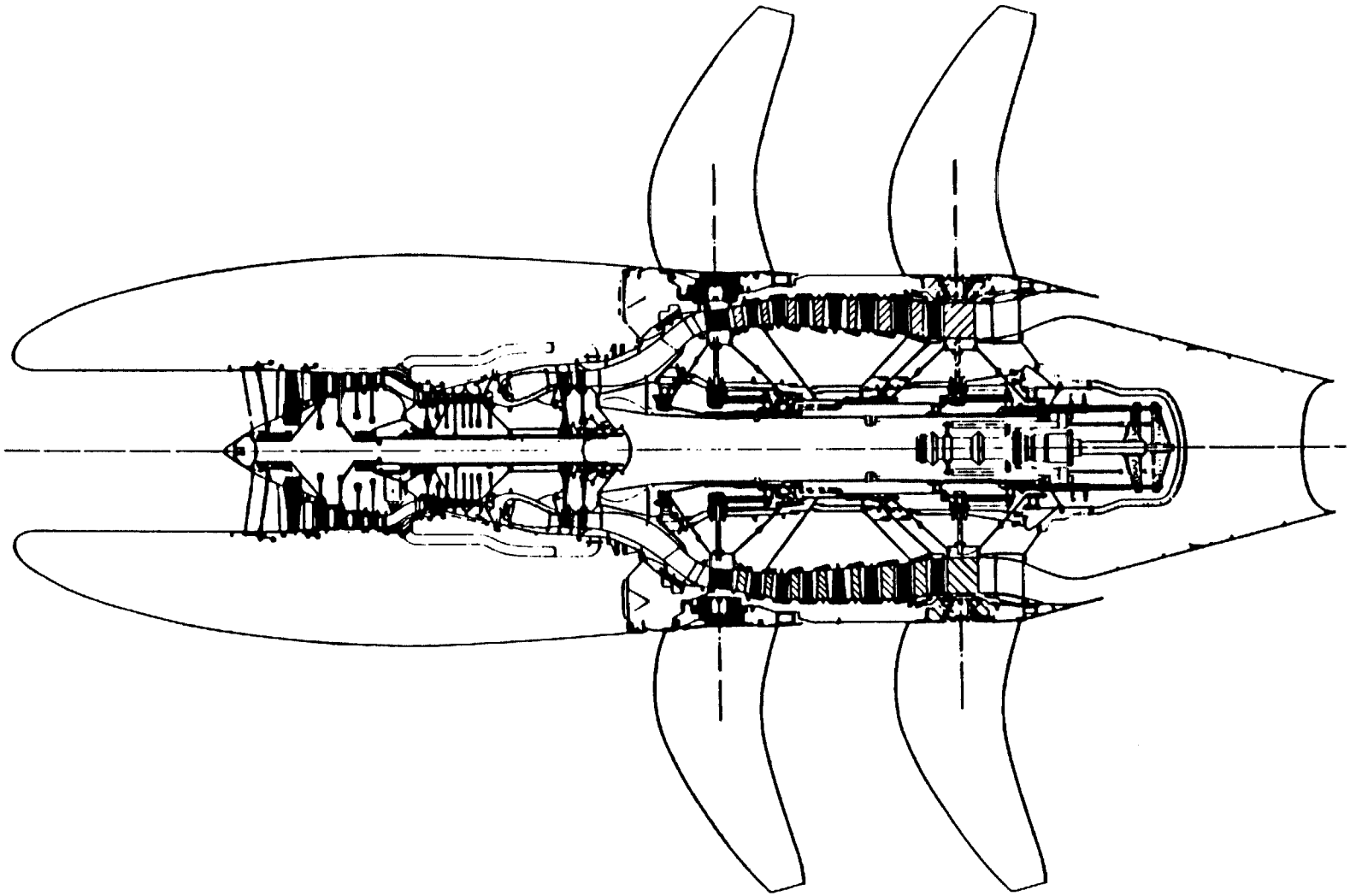

Figure 13. 1984 Baseline Subsonic Study Engine.

Exhaust Velocity, fps	1480
HPT Inlet Temperature, ° F	2340
UDF Diameter, ft	11.3

Table XIV is a tabulation of baseline engine performance at takeoff and end of climb flight conditions.

Performance at SLS and Denver takeoff, along with maximum climb, are shown in Table XV. The thrust includes engine-operation-related aft cowl and core plug scrubbing drags. The end of climb sfc is ~ 10.6% better than the GE/NASA Energy Efficient Engine (E^3) FPS-9 performance at its M_0 0.80/35,000 ft/standard day cruise bucket.

2.3 ADVANCED STUDY ENGINE CYCLE

Cycle parametric (T41, OPR) studies to identify the advanced engine were chosen initially to cover the range of:

OPR: 43-60

T41: 2340°-3800° F

The cycle design was specified at the end of climb (M_0 0.80/35,000/ΔTamb = 18° F) for a thrust of 5510 lb. Study guidelines included:

- Constant LP compressor/HP compressor stage efficiency
- Exhaust velocity = 1480 fps
- Uncooled turbines

The most promising of these engines in terms of uninstalled sfc were further refined for component technology levels, size/Reynolds No. effects, and configuration options.

The sfc trends as a function of OPR and T41, shown in Figure 14, indicate that sfc continues to improve beyond OPR = 60 at increased T41 levels. However, HPC minimum blade height restrictions for an all-axial-flow compressor precluded cycle design selection above ~OPR = 60. After flowpath analysis of these engine cycle designs,

Table XIV. ROMS 1984 Baseline UDF Cycle Performance.

No Customer Offtakes, Uninstalled Engine

Mach No./Alt/ΔTamb	0/0/+27° F	0.80/35000/+18° F
Thrust[1]	23830	5510
SFC	0.235	0.481
$w\sqrt{\theta}/\delta$ - LP Compressor	89.2	107.0
PR - LP Compressor	5.77	6.86
LPC Bleed, % W_{HPC}	8.8	8.8
PR - HP Compressor	5.9	6.39
PR - Overall	34.1	43.8
T3, ° F	1158	1065
T41, ° F	2400	2340
UDF HP/Annulus Area	179.4	94.9
UDF - Tip Speed, fps	798	800

[1] Performance does not include aft cowl and core plug scrubbing drag.

Table XV. ROMS 1984 Baseline UDF Performance Comparison.

No Customer Offtakes

Flight Condition	MP 0.8/35K/0° F	SLS/+27° F	MP 0.2/5330/+52° F
Power Setting	Maximum Climb	Takeoff	Takeoff
Thrust	5460	23800	18025
SFC	0.472	0.235	0.254
T3° F	1002	1158	1170
T41° F	2234	2400	2415

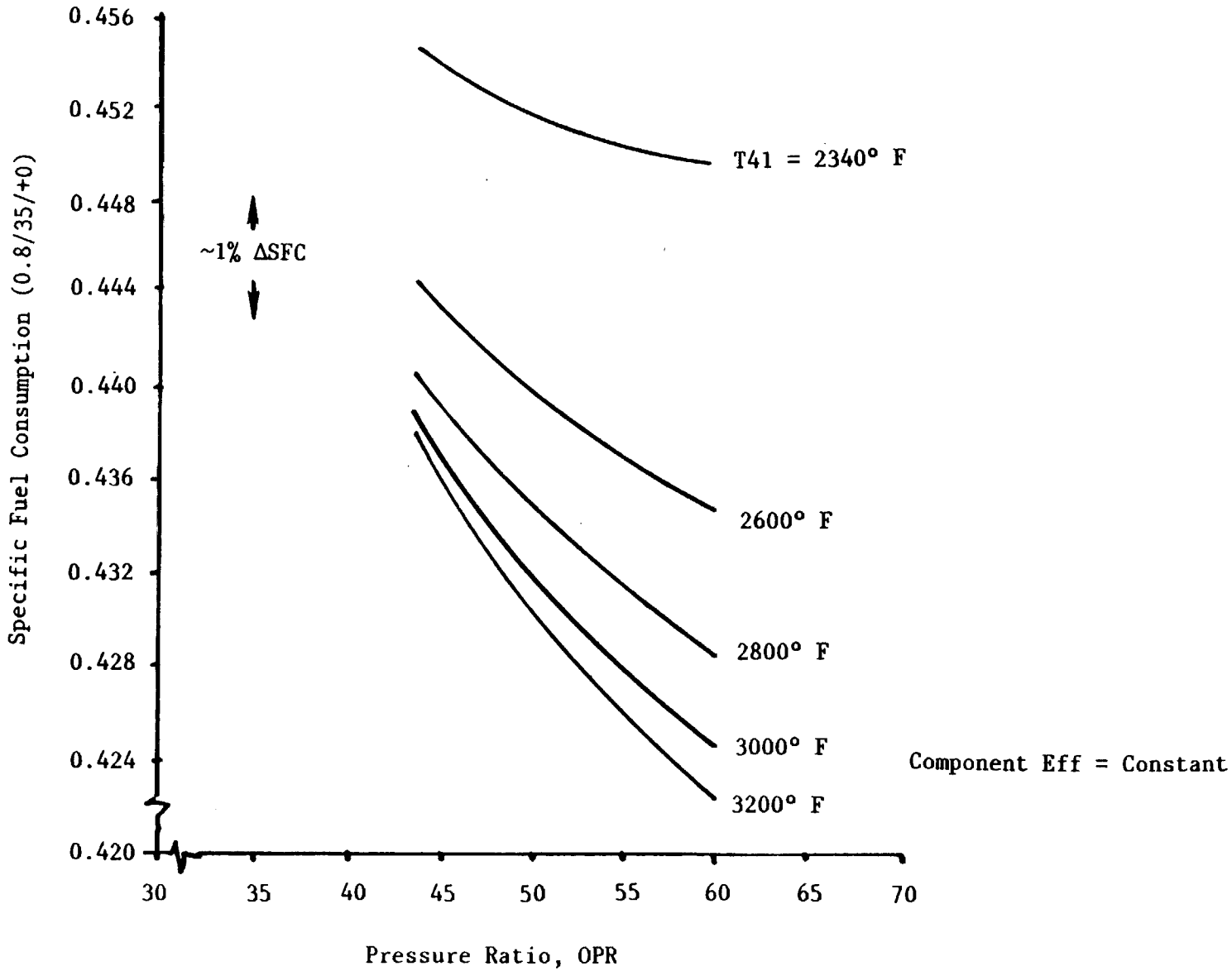

Figure 14. Advanced Subsonic Study Engines.

OPR	T41 (° F)
50	2900
60	2800
70	2600

the parametric study was broadened to include cycle designs of OPR up to 200 and T41 levels of 3800° F.

Figure 15 shows the sfc results for extending the T41/OPR range. SFC continues to improve out to OPR = 200, but when HPC and HPT size/Reynolds effects are factored in the cycle design, the best engine cycle design occurs at reduced OPR and T41 levels. This is illustrated in Figure 16.

In addition, minimum HPT flow function (blade height) and LPC bore/bearing requirements preclude increasing T41/OPR to give the best sfc levels. Because of these considerations, the advanced engine cycle design was specified as:

OPR	110
$(w\sqrt{\theta}/\delta)_{LPC}$	60.9
T_{41}, ° F	3200
LP-HP Bleed, % W_2	3.07
PR-HP Compressor	23.0

An over-and-under comparison of the 1984 baseline and advanced study engine is shown in Figure 1. The advanced engine has an axicentrifugal high pressure compressor configuration to achieve the high overall cycle pressure ratio. The ROMS baseline and advanced engine cycles and performance are compared at their cycle setup (M_0 0.80/35,000 ft/ΔTamb = 18° F) in Table XVI. The advanced engine cycle performance is demonstrated for component performance with and without improved aero performance, so that the cycle benefits due to materials and structural advances can be examined separately from the aerodynamic technology advances.

The sfc improvement for the advanced engine with aero improvements is on the order of 16% relative to the 1984 baseline and ~23% compared to the GE/NASA E^3 FPS-9 turbofan.

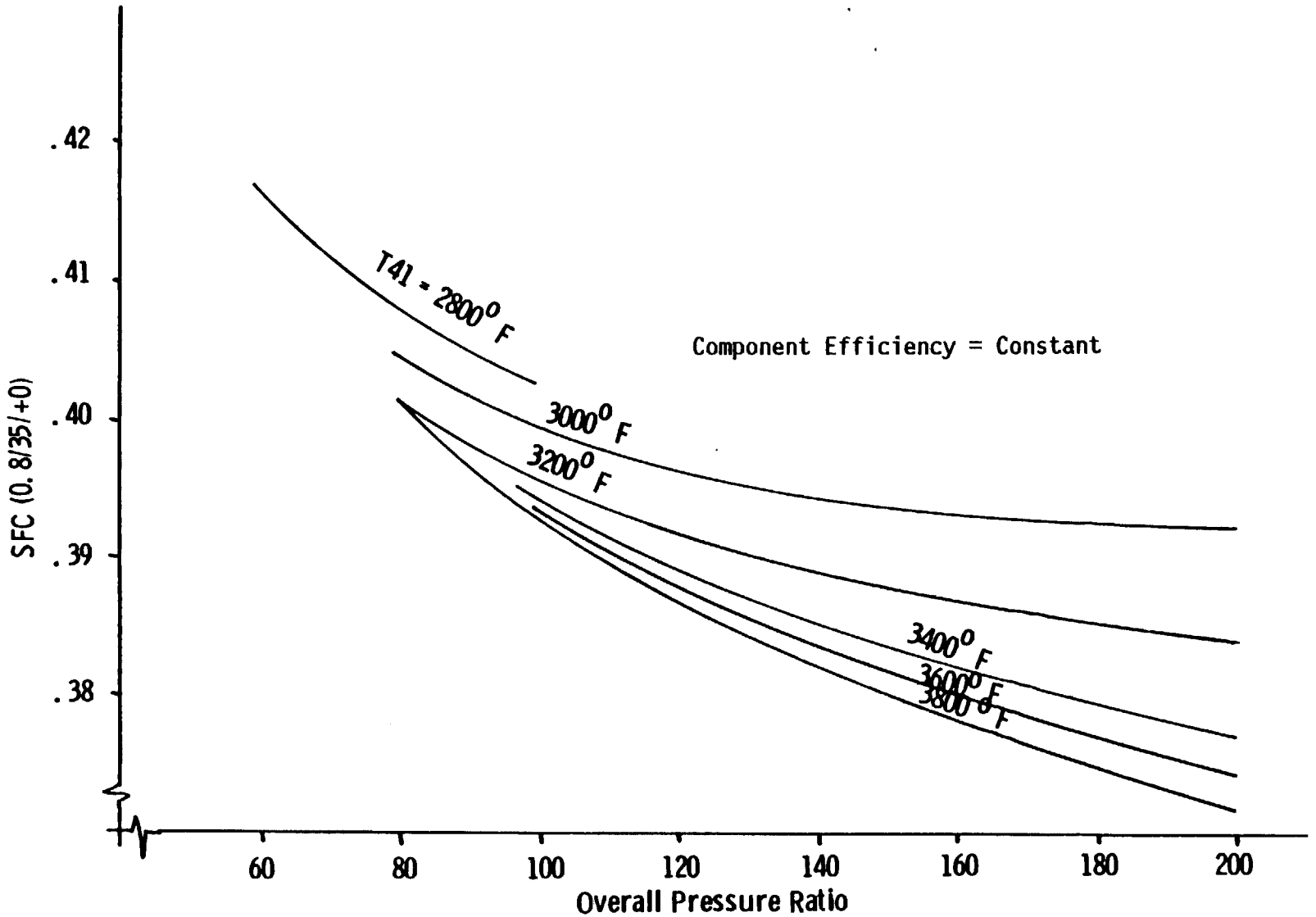

Figure 15. Advanced Subsonic Study Engines, SFC Versus T41 and OPR.

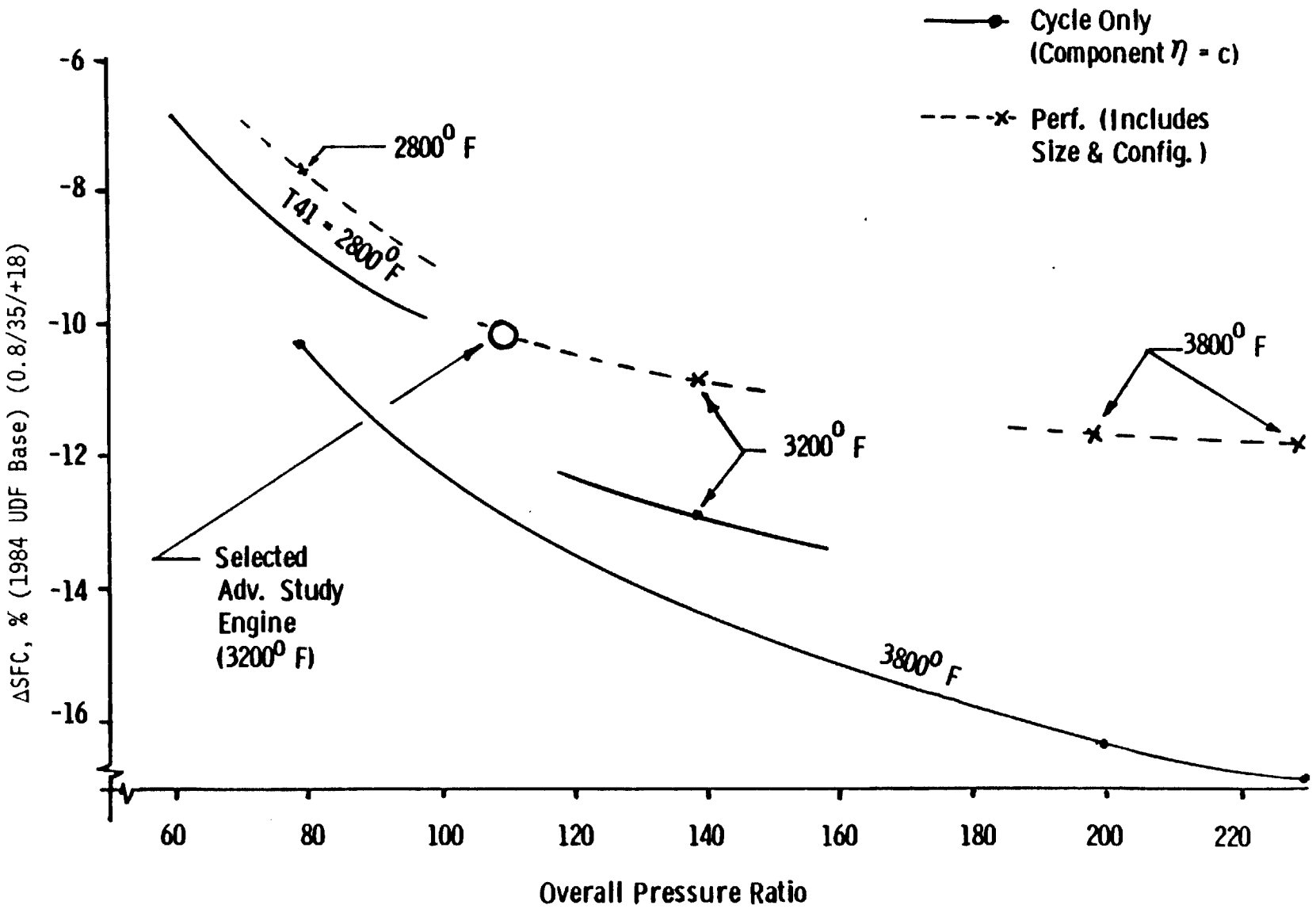

Figure 16. Advanced Subsonic Study Engines (Efficiency Adjusted).

Table XVI. Baseline and Advanced Subsonic Engine Cycle Comparisons at Maximum Climb.

	1984 Baseline	Advanced Cycle Material/Structure and Improved Aero	Advanced Cycle Material/Structure and No Aero
Altitude	35K	35K	35K
MP	0.8	0.8	0.8
ΔTamb	+18	+18	+18
FN	5510	5510	5510
T41, ° F	2340	3200	3200
OPR	43.3	110	110
W2R	107.0	54.34	60.95
P23/P2	6.86	4.78	4.78
P25	35.6	24.838	24.839
T25, ° R	865	759.2	773.75
W25R	19.8	14.264	16.149
P3/P25	6.39	23.005	23.005
W3	36.4	19.73	22.12
P3	227.7	571.3	571.3
T3, ° R	1525	1945.2	2024.9
W41R	8.549	2.228	2.496
W45R	25.162	8.942	11.322
W48R	57.839	13.553	17.795
PT ΔH - Btu/lb	143.0	307.4	276.2
P8	6.078	4.839	4.839
T8, ° R	1218.0	1384.5	1414.7
A8, in^2	453.5	345.9	391.8
UDF Diameter, ft	11.3(1)	10.56	10.59
UDF R/R	0.3858	0.436	0.3858
SFC(2)	0.485	0.4073	0.4370
	(Base)	(-16.1%)	(-10.0%)

(1) 11.58 feet diameter at 0.436 R/R

(2) Includes aft cowl and core plug scrubbing drags

2.4 SUPERSONIC BASELINE AST CYCLE

A baseline AST cycle was reestablished. The performance of this baseline cycle was used as the reference for comparison in studying advanced cycles with constraints relaxed arising from materials limitations. In order to minimize cycle-to-cycle installation effects, airflow schedules, ram recovery, engine thrust, and exhaust nozzle performance of each of the cycles were maintained at the baseline cycle levels. Several key flight conditions were examined in cycle comparisons. Table XVII lists three flight conditions along with airflow and thrust to which the baseline engine cycle along with all advanced cycles were run.

Table XVII. Supersonic Engine Sizing Requirements.

M_0	0	2.62	0.90
Altitude, ft	0	60000	50000
ΔTamb ° F	+27	+14.4	0
W2R, lb/sec	843	843	843
FN, lb	47230	17460	10300

The baseline engine configuration is a two-spool, variable cycle turbofan with an acoustic nozzle featuring coannular exhaust streams. A sketch of this engine is shown in Figure 17. The fan component of this engine is made up of two blocks. The front block consists of two stages and is driven by a single stage, low pressure turbine. The fan rear block consists of a single stage which, along with the five-stage high pressure compressor, is driven by a single-stage high pressure turbine. The design corrected airflow, design pressure ratio, and design adiabatic efficiencies of the compression components are shown in Table XVIII. However, the manner in which the engine is operated is such that the operating conditions of the components listed in Table XVIII never occur simultaneously.

The baseline engine configuration is referred to as a variable cycle engine because of the flexibility offered in the operation of the engine because of variable geometry features that are included. These variable geometry features are indicated in Figure 18. Engine performance at key

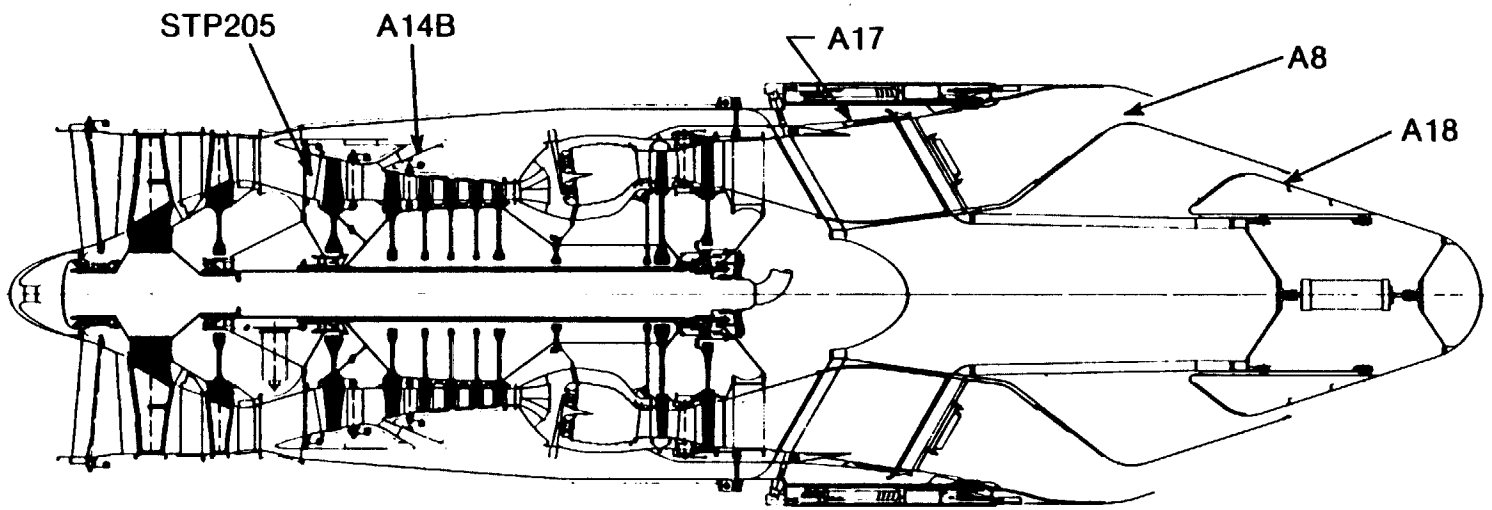

STP205	—	Core Fan IGV	—	Modulates Core Fan Airflow - Increasing or Decreasing Bypass Ratio
A14B	—	Fwd VABI	—	Controls Flow from Discharge of 3rd Stage Fan into Bypass Duct with a Sliding Valve
A17	—	Aft VABI	—	Controls Flow from Bypass Duct into Core Discharge
A8	—	Core Nozzle	—	Controls Mixed Flow Core Nozzle Discharge Area by Translating Nozzle Shroud
A18	—	Bypass Nozzle	—	Controls Flow from Bypass Duct Via Path Through Turbine Frame Struts by Translating Inner Nozzle Plug

Figure 17. 1984 Baseline Supersonic Study Engine Variable Geometry Features.

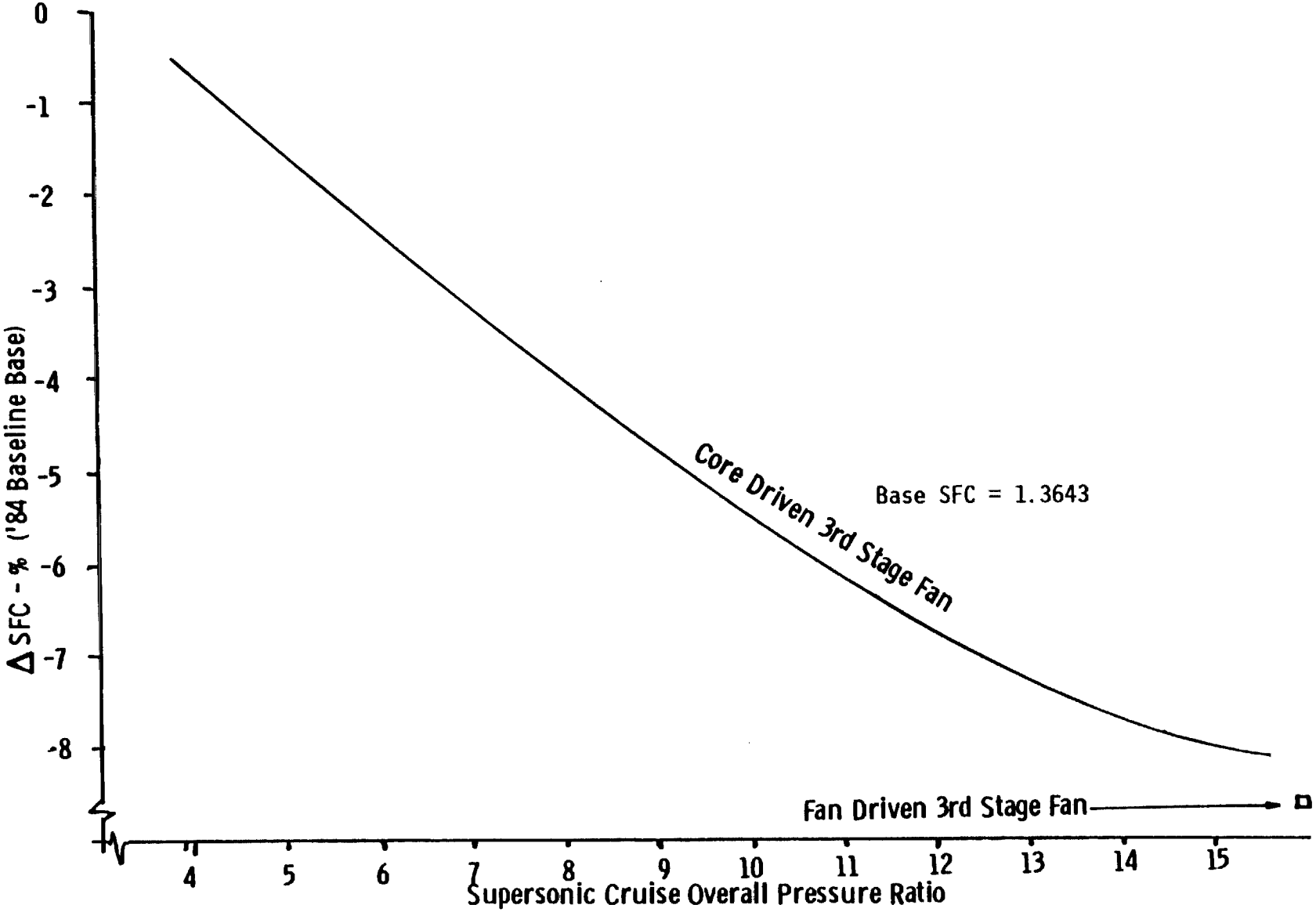

Figure 18. Advanced AST Cycle Studies.

Table XVIII. Baseline VCE Component Design Conditions.

- Mach 2.62/60,000 ft/+14.4° F

	Corrected Flow, lb/sec	P/P	η_{ad}
Block I Fan (Stages 1 & 2)	813.9	2.8	0.8637
Block II Fan (Stage 3)	340.7	1.368	0.8769
HP Compressor	208.7	4.14	0.8811

flight conditions can be enhanced or takeoff noise minimized by proper setting of these variable geometry components. Although these components are adjusted simultaneously, the major impact of each of these is discussed below.

STP205 - Core-Fan Inlet Guide Vane Setting - Varying the core-fan inlet guide vane setting angle allows modulating the corrected airflow of this stage. This variable is employed to increase the operating bypass ratio and reduce the overall fan pressure ratio to minimize takeoff noise and to reduce fuel consumption at subsonic cruise. Minimum bypass ratios are obtained for maximum thrust during climb and acceleration with open settings of this guide vane.

A14B - Front VABI Area - This variable essentially controls the core fan operating line relative to the front fan operating line. The engine operates in modes where either all of the front fan airflow passes through the core fan or where some of this airflow is bypassed around the core fan through the outer bypass duct. In the latter case A14B must be set such that the static pressure in both bypass streams are equal at their point of entry into the main bypass duct for the desired fan operating lines.

A17 - Aft VABI Area - This variable sets the static pressure and Mach number in the bypass stream at the point where it is injected into the hot stream aft of the low pressure turbine. The baseline engine cycle operates on both the mixed flow and separated flow turbofan concepts. For takeoff noise reduction, a substantial portion of the bypass air is passed through the rear

frame struts and exhausted through a secondary nozzle (A18) on the nozzle plug surface downstream of the main exhaust nozzle throat (A8). The requirement for a static pressure balance between the bypass air and hot stream of the aft VABI for a mixed flow cycle remains since there is always some bypass air involved in the mixing process. The turbomachinery speed and operating temperatures must be such that the static pressure in the hot stream in the aft VABI mixing plane is equal to that of the bypass stream.

A8 and A18 - Main Exhaust Nozzle and Bypass Nozzle Throat Areas - These areas together set the back pressure environments for both the low pressure turbine and the fan system. Operating lines on the two fan blocks are thus set as well as turbomachinery speed and operating temperature. Flow may be interchanged between hot and cold exhaust streams by relative variation between A8 and A18 for minimization of noise. Shown in Table XIX are values of the above variable cycle parameters for three important flight conditions for the baseline cycle. Table XX shows values of key cycle parameters of the baseline engine cycle at supersonic cruise.

Table XIX. 1984 Baseline AST VABI and Nozzle Operation.

	Supersonic Cruise	Takeoff	Subsonic Cruise
M_0	2.62	0	0.9
Altitude, ft	60K	0	50K
Fn, lb	17461	47468	7118
Inlet Corrected Flow	438	700	843
Overall Bypass*	0.56	0.45	0.504
Fwd. VABI Area, in^2	290	38	125.7
Aft VABI Area, in^2	783	71	383
Core Nozzle Area, in^2	1336	1306	1892
Bypass Nozzle Area, in^2	1.1	309	3.7
STP205, Degrees	0	38.3	25

*Overall bypass is determined by bypass engine flow divided by core flow

Table XX. 1984 Baseline AST Study Engine Cycle.

MP	2.62
Altitude, ft	60K
ΔTamb, ° F	+14.4
Inlet P, psia	19.471
Inlet T, ° R	955.78
Fn, lb	17461
sfc	1.3643
BPR	0.56
W2R	437.60
2 Stage Fan P/P	1.504
2 Stage Fan Eff.	0.872
Core Fan Cor. Flow	283.8
Core Fan Stg. P/P	1.258
Core Fan Stg. Eff.	0.873
HPC W25R	165
HPC P/P	2.86
HPC ηad	0.879
T3, ° F	1133
HPT FF	143.18
T41, ° F	2703.4
HPT Eff.	0.905
LPT FF	333.93
LPT Eff.	0.897
P8/P0	27.05
A8, in^2	1336.2

2.5 ADVANCED AST STUDY ENGINE CYCLES

The basic engine configurations for the baseline AST cycle was maintained in the advanced study cycles. Cycle parameters of fan pressure ratio, overall bypass ratio, overall cycle pressure ratio, and high pressure turbine inlet temperature (T41) were studied in a parametric manner to establish performance levels. Component efficiencies were adjusted to account for advanced aerodynamic technology levels, operating differences due to relaxed material limitations, and reduced cooling air requirements of advanced materials. In all cases, the airflow and thrust values of Table XVII were maintained. In the AST mission, the cruise sfc at supersonic cruise is of utmost importance when comparing engine cycles. Since at this cruise point the airflow and thrust remained constant, the manner in which the study variables affect average

nozzle exhaust gas pressure and temperature determine the specific fuel consumption of the cycle.

The initial range of cycle variables covered were:

$3.2 \leqq$ P/P Fan $\leqq 5.3$

$13.5 \leqq$ Cycle P/P (SLS) $\leqq 26$

$2800°$ F $\leqq$ T41 $\lesssim$ Stoichiometric.

Overall bypass ratio was a dependent variable which was established by combination of the above variables. In cases where the dry Mach 2.6 thrust fell short of the requirement of Table XVII, modest tailpipe augmentation was used to make up the thrust deficiency. These cases resulted in unattractive cycles because the sfc increased to values considerably above that of the baseline engine cycle.

It became obvious that overall engine cycle pressure ratio impacted supersonic cruise sfc more than any other variable. Cycle studies were then extended out of the range of the initial parametric field. Several bypass ratios were examined at a number of overall cycle pressure ratios. Fan pressure ratio and turbine inlet temperatures were adjusted to maintain constant Mach numbers in the cold and hot streams in the aft VABI mixing plane. As overall cycle pressure ratios were increased, significant reductions in supersonic cruise sfc were noted. A curve showing the effect of overall cycle pressure ratio on relative sfc at supersonic cruise is shown in Figure 18. Overall bypass ratio produced a minimal effect on sfc.

Table XXI presents some of the parameters of these study cycles which showed improvement over the baseline values of sfc at supersonic cruise. Engine cycle numbers below and including 33 were part of the initial parametric investigation, while subsequent numbers were done in the expanded study.

Engine cycle 37A resulted from a preliminary mechanical study of cycle 37 which showed advantage for relocating the second fan block from the core shaft to the low pressure fan shaft. Engine cycle 37A was selected as the cycle for more detailed mechanical design studies and for evaluation in the AST mission.

Table XXI. Advanced AST Study Engine Cycles.

Cycle	Fan P/P	Supersonic Cruise			
		OPR	T_{41}, ° F	BPR	ΔSFC
Baseline	3.27	5.39	2703	0.56	Base
13	4.25	4.42	3556	2.06	-0.7
11	4.25	4.73	2596	0.69	-0.8
12	4.25	4.57	3038	1.29	-0.9
23	5.3	5.33	2799	0.90	-1.9
24	5.3	5.50	3194	1.44	-2.0
25	5.3	5.44	3750	2.34	-2.0
30	5.3	5.54	3704	2.25	-2.1
29	6.5	7.06	3283	1.48	-3.3
33	4.5	7.43	3994	2.78	-4.7
28	5.3	7.62	4047	2.88	-4.8
31	5.3	7.45	4064	2.96	-5.1
35	6.58	10.66	3701	1.98	-5.1
34	5.3	9.00	3600	1.95	-6.1
36	6.58	12.59	4027	2.53	-6.8
37	6.58	15.74	4111	2.57	-8.1
37A	6.58	16.21	4079	2.48	-8.5

The improvement in cruise sfc for the advanced AST cycle was realized by greatly increasing cycle pressure ratio, by reducing cooling flow with uncooled HPT blades, and by anticipated improvements in aerodynamic performance of the rotating components. In order to access the improvement in cruise sfc attributable to each of these factors, the baseline cycle was rerun with the improved levels of component performance. Table XXII shows a comparison of cycle parameters of supersonic cruise of the baseline cycle, the baseline cycle with improved components, and the selected advanced AST cycle. The improvements in sfc resulting from the improved aerodynamic component performance was slightly less than 1%. The improved efficiencies are manifested in slightly higher nozzle pressure ratio and a slight reduction in exhaust gas temperature. Since thrust and airflow remain constant in the comparison, increases in nozzle pressure ratio are automatically accompanied by decreases in exhaust gas temperature (which reduces fuel flow) and thus reduces sfc.

Table XXII. 1984 Baseline, Improved Aero and Advanced AST Cycles.
(Cruise 2.62/60,000 ft/+14.4° F)

	1984 Baseline	Improved Aero Configuration	Study Engine
Mach No.	2.62	2.62	2.62
Altitude, ft	60K	60K	60K
Fn, lb	17461	17461	17461
ΔTamb, ° F	+14.4	+14.4	+14.4
T41, ° F	2703.4	2686.3	4079.4
Overall Pressure Ratio	5.4	5.43	16.21
Front Fan Corrected Flow	437.66	437.66	438.00
Front Fan P/P	1.504	1.504	2.157
Rear Fan Corrected Flow	283.8	285.2	193.1
Rear Fan P/P	1.258	1.260	1.271
HP Compressor Corrected Flow	165.0	164.5	54.5
HP Compressor P/P	2.86	2.88	6.01
HP Turbine Flow Function	143.18	141.55	28.64
LP Turbine Flow Function	333.93	325.41	62.17
Chargeable Turbine Cooling Flow, %	5.1	2.8	2.8
A8, in^2	1336.2	1235.6	990.0
Nozzle Pressure Ratio, P8/Po	27.05	27.72	35.6
T8, ° F	1524.0	1517.0	1316.0
ΔSFC	Base	-0.8%	-8.5%

The improved component aerodynamic performance resulted in a minor increase in exhaust nozzle pressure ratio while increasing the cycle operating pressure ratio resulted in a much greater increase in nozzle pressure ratio and decrease in exhaust gas temperature.

Performance points were run to compare the acoustic characteristics of the baseline and advanced AST cycles for sideline and community evaluation. Tables XXIII and XXIV show comparisons of engine cycle parameters of these two conditions. From the velocity and air flow ratios it is concluded that the two cycles have essentially equal noise characteristics.

2.6 COMPONENT FLOWPATH CONFIGURATIONS AND PERFORMANCE

The NASA ROMS study required an extensive cycle and flowpath configuration parametric examination to determine possibilities for engine improvement. For both engine classes, the supersonic AST and the subsonic UDF, baseline engines were described using engine technologies that could be committed to a production engine in 1984. These baseline engines then served as the anchor point in the parametric matrix for both engine classes.

The AST baseline engine was built on the work performed for NASA in 1978 through 1980 on the Supersonic Cruise Research contract NAS3-22000. For ROMS, the baseline engine mission was increased from Mach 2.4 to Mach 2.7. The engine size was increased to achieve this mission. The components defined for this engine are built on the technologies which are being produced into the current F110 and F404 GE fighter engines. The critical oversized fan and exhaust nozzle technologies were retained for all the AST studies in this work. These concepts were defined in the earlier studies to solve the engine acoustic problems at takeoff and approach. The cross section of this engine is presented in Figure 2.

The UDF baseline engine was built on the work performed for NASA in the 1983 through 1986 UDF demonstrator engine contract. The engine configuration was modified to be representative of what was visualized as a 1984 product configuration. The items affected by this restriction were as follows:

Table XXIII. Community Acoustic Comparison.

Study Advanced AST Cycle Versus 1984 Baseline Cycle (0.326/1.2K/+27° F)

	1984 Baseline AST	Advanced AST
Mo	0.326	0.326
Altitude, ft	1200	1200
ΔTamb	+27	+27
Fn, lb	34500	34500
T_{41}, ° F	2095	3318
Overall Pressure Ratio	15.2	30.7
Front Fan Corrected Flow	714.7	714.7
Front Fan P/P	2.46	3.22
Rear Fan Corrected Flow	284.6	194.2
Rear Fan P/P	1.180	1.226
HP Compressor Corrected Flow	200.4	66.2
HP Compressor P/P	4.07	8.01
Total Exhaust Flow, lb/sec	702.3	700.1
Avg. Exhaust Temp., ° F	1235	1412
Avg. Exhaust Velocity, fps	2024	2026
Velocity Ratio (VC/VH)	0.633	0.648
W_C/W_H	161/533	366/328

Conclusion: Same acoustic characteristic

Table XXIV. Sideline Acoustic Comparison.

Study Advanced AST Cycle Versus 1984 Baseline Cycle (Takeoff 0.3/0/+27° F)

	1984 Baseline AST	Advanced AST
Mo	0.3	0.3
Altitude, ft	0	0
ΔTamb	+27	+27
Fn, lb	51336	51336
T41, ° F	2436	3889
Overall Pressure Ratio	15.16	40.8
Front Fan Corrected Flow	843.2	843.2
Front Fan P/P	3.021	4.151
Rear Fan Corrected Flow	270.4	177.2
Rear Fan P/P	1.254	1.129
HP Compressor Corrected Flow	199.95	71.2
HP Compressor P/P	4.07	8.90
Total Exhaust Flow, lb/sec	855.9	854.5
Avg. Exhaust Temp., ° F	1428	1768
Avg. Exhaust Velocity, fps	2356	2360
Velocity Ratio (VC/VH)	0.638	0.629
W_C/W_H	147/696	434/409

Conclusion: Same acoustic characteristic

- The intermediate pressure (IP) compressor inlet radius ratio was increased to allow a bladed Stage 1 blade design. The technology of the GE F110 fan was applied to this component, and a radius ratio of 0.45 was selected for this baseline engine.

- Counterrotating vaneless HP and IP turbines were thought to be beyond a 1984 product. This resulted in a reduction in the HP turbine loading and an extra stage on the HP compressor. The loading reduction is needed to maintain a turning limit on the nozzle between the two turbines. The extra compressor stage was needed to slow the spool down to meet the turbine maximum tip speed requirement for a current product.

- The UDF fan configuration is based on the results of the NASA-sponsored UDF blade simulator testing. The F7A7 configuration was chosen as the most appropriate of the blades tested for a 1984 product. The same NASA-sponsored work has led to definition of design considerations to achieve sideline and cabin acoustics levels required by FAR 36, Stage 3. The important considerations can be reduced to fan blade aspect ratio or activity factor, total number of fan blades, and the spacing between blades at critical operating points. These considerations and the assumption of a maximum number of fan blades for a 1984 product of 18 in a 10×8 combination established the fan tip diameter, radius ratio, and rotational speed. The F7A7 configuration was scaled appropriately to conform to these requirements. The performance of this fan was determined by applying this scale factor to the F7A7 simulator data.

The cross section of this UDF baseline engine is presented in Figure 19.

The cycle matrix for the advanced AST engine encompassed 38 different engines. The major cycle parameters varied in the study (see Table XXI) were the overall compression pressure ratio (5.4 to 16.2), T41 (2700° to 4120° F), and the pressure ratio of the front block fan (2.8 to 4.3). Of these cycle engines, 20 were deemed worthy of flowpath configuration definition. The preliminary weight and cycle fuel burn results were used to screen the configurations to select engines to be developed further. Because of the results of the flowpath iterations, the rear block fan was studied as both fan driven and core driven in the later parts of the matrix.

The cycle studies performed on the advanced UDF engines varied overall compression pressure ratio and T41. The pressure ratio variations ranged from the baseline level of 43.3 to ultrahigh values approaching 200. T41 was

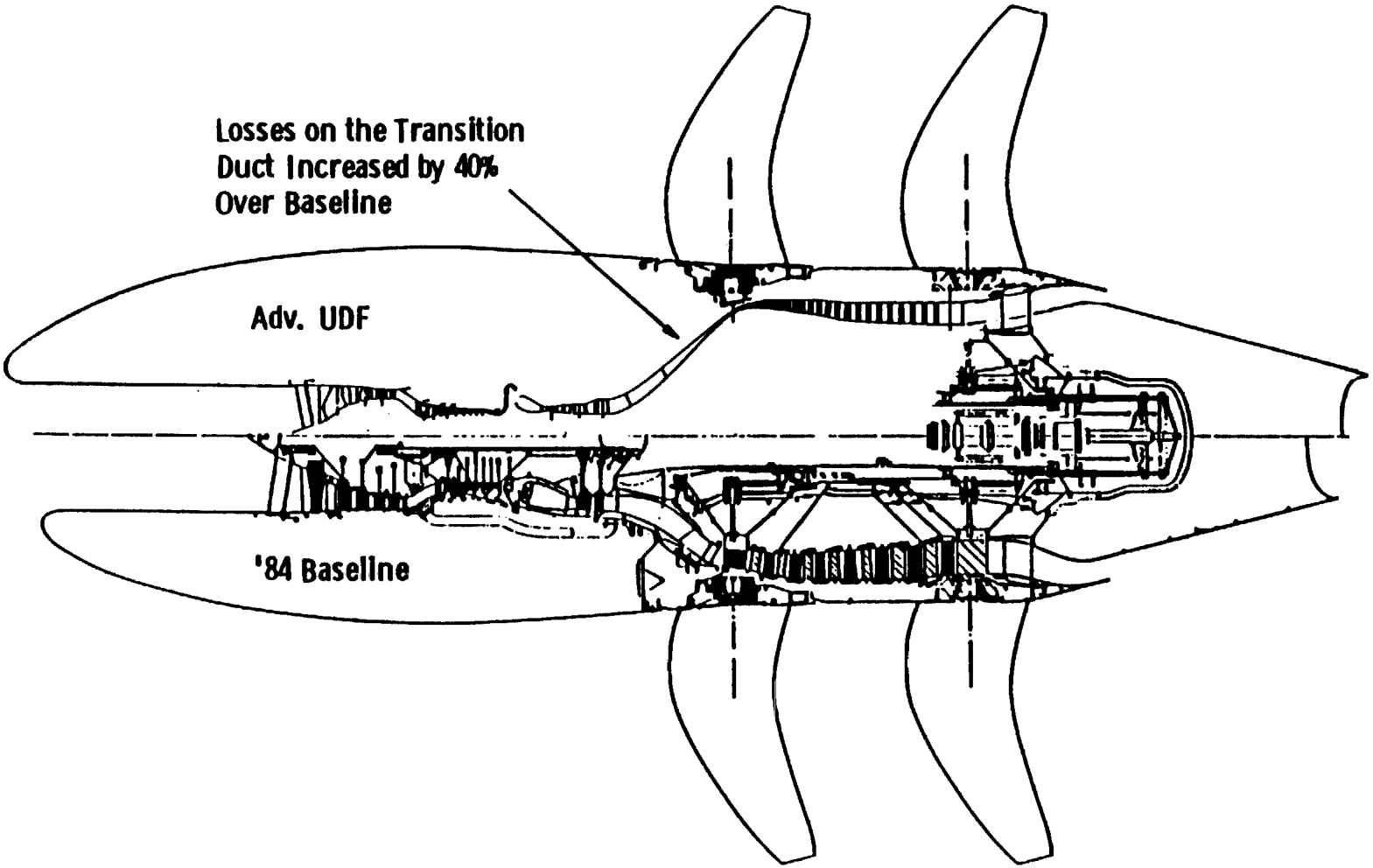

Figure 19. Advanced UDF Flowpath Comparison.

varied from 2400° to 4100° F. Because of power turbine temperature limitations and HP compressor exit annulus height restrictions (≧ 0.5 inch), T41 for the initial flowpath studies was limited to 2900° F. During this initial round, three complete flowpaths were developed to establish the engine benefits of each. Because the program objectives for fuel burn and DOC for this class engine were not met with these initial configurations, the limits were changed to allow engine configurations with substantially higher pressure ratio and turbine temperature. The compressor blade height limit was usurped by utilizing an advanced technology centrifugal compressor stage in the rear of the HP compressor. The cycle parameters used for the final engine configuration were 110 OPR and 3800° F T41.

2.7 ENGINE DESIGN TECHNOLOGY GROUND RULES

The advanced configuration studies for both classes of engines were performed after establishing the mechanical design limits that are projected to be consistent with the properties of the improved materials. These design ground rules were established to maintain consistency in the development of the advanced configuration flowpaths to achieve reasonable weight and size trends for the screening process. It was not intended to imply that these parameters were adequate to normalize the impact of the material stress-to-density or other property changes. These parameters are compared in Table XXV. The values listed for the baseline engines are the limiting values used in the baseline components. In every case, these levels are currently being built in GE aircraft engine products. The advanced configuration values were the targets that were strived for in the components. It was impractical to set all the limits for all the configurations; however, a consistent logic path was applied in determining the limits which were dominant from flowpath to flowpath.

2.8 YEAR 2010 COMPONENT PERFORMANCE IMPROVEMENTS

The effect of dramatic material property improvements on a given engine configuration can be determined without assuming component performance influence. However, there are many instances where the component improvements have been directly tied to material property improvements. The component

performance levels were forecast and included in this study to achieve the most meaningful configuration results.

Table XXV. Engine Design Technology Ground Rules.

The Engine Studies for Both the Subsonic UDF and the Supersonic AST were Performed Using the Following Ground Rules:

	Baseline	Advanced
Turbine Blade Stress Parameter, AN^2	32×10^9	65×10^9
Fan or Compressor Maximum Tip Speed	1612	2000 fps
Compressor Maximum Rim Speed	1300	1500 fps
Minimum Compressor Radius Ratio	0.40	0.33
Minimum Turbine Radius Ratio	0.71	0.55
Maximum Turbine Tip Speed	1869	2000 fps

The process of this forecast requires engineering assumptions which are based on past experience and the directions and influence that the advances in modeling technologies are expected to have on the component performance potentials. The foundation for the forecast is a GE commitment to reduce the basic loss sources by 10% by the early 1990's. In addition, the computing power and software technologies have been advancing at a very fast pace. The near Navier-Stokes flow model solutions which will be available will allow further reduction of the basic losses. For this study, an additional reduction of 10% was used in the performance forecasts.

The process used in making these performance estimates was to determine the component performance using current technology. This performance was then modified by making the appropriate assumptions of loss reductions. In this process, the efficiency of the advanced component can be lower than the baseline component because of size, loading, and Mach number effects. In these cases the engine system is better served by the selected advanced configuration than by striving for the maximum efficiency in the component. This is particularly true for the AST class of engines. In this class engine, weight has a major impact on fuel burn and DOC. For the UDF class of engines this

was not as clear cut. In the UDF, the level of performance was emphasized ahead of weight savings.

The detailed considerations used in these performance forecasts are as follows:

Fans and Compressors

- Conventional airfoils include a 20% three-dimensional (3D) loss improvement
- Swept airfoil configurations include the improvement of the swept airfoils and a 10% reduction in 3D losses.

Turbines

- Basic stage loading, $\Delta h/(2 \times U_p^2)$, improved by an 11% loss reduction
- Secondary or 3D associated loss characteristics improved by 10%
- Profile losses associated with low Reynolds number due to size and high altitude improved by 25%.

These improvements will be brought about by improvements in flow field modeling and the improved material properties. The advanced material will allow increased airfoil chords to reduce the Reynolds number losses without the cooling flow penalties that would be encountered with current material properties.

2.9 MATERIAL AND TIP SPEED IMPACT ON AERODYNAMIC IMPROVEMENTS

The improvements in material properties envisioned in this study will have a very significant impact on the engine configurations. The strength-to-density change will allow higher blade speeds, which will reduce the number of turbomachinery stages required for a given configuration. This will also lead to significant diameter reductions in the turbomachinery, which will further improve the engine weight. Greater strength will allow extended use of swept fans. If the concept is to be achieved using current materials, the tip speed of the airfoil will either be maintained or reduced slightly as shown in Figure 20. The improved material properties will allow an additional trade between component performance and blade speed also shown in Figure 20.

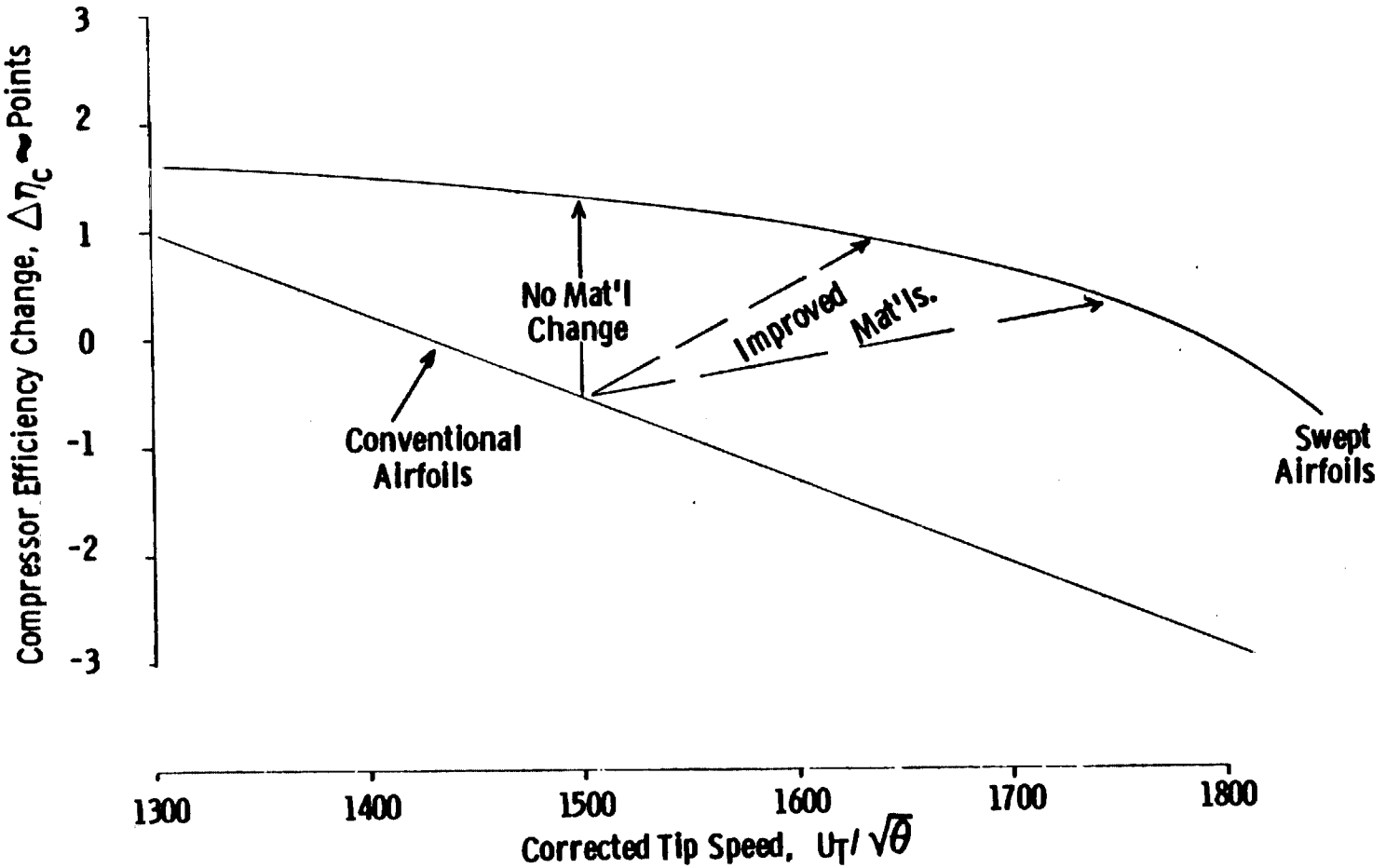

Figure 20. Swept Compressor Blade Advantage.

In the case of the AST class of engines, the blade speed increase has reduced the component diameters dramatically.

The strength characteristic will increase the flexibility in employing 3D design concepts. This will allow concepts such as the end bends used in the NASA Energy Efficient Engine compressor to be expanded to other components and emphasized according to the advanced three dimensional model design desires.

The higher temperature capabilities will permit hotter compressor discharge temperatures associated with ultrahigh compression pressure ratios. This is due to the improved compressor materials and the elimination or reduction of the required turbine cooling flows that use compressor discharge air as the cooling source. The expected reduction for the AST engine HPT chargeable cooling flows is shown in Figure 21. The flow remaining in the advanced material configurations is thought to be used to purge the resulting cavities in the real engine flowpath. This purge flow is a very weak variable with turbine inlet temperature. Thus, the advantage of the advanced materials is emphasized as T41 is increased.

The elimination of the cooling requirement in the turbines in conjunction with the strength-to-density improvements allow greater geometric flexibility in the airfoil designs. This will allow utilization of low loss supersonic discharge Mach number vector diagrams. The result will be substantial increases in average turbine stage loadings. In addition, as mentioned previously, the removal of the cooling flow penalties will allow a different solidity optimization which will reduce the low Reynolds number associated losses because of engine size and high altitude missions.

2.10 ADVANCED UDF ENGINE CONFIGURATION

The advanced UDF engine configuration is characterized by substantial increases in T41 and OPR. A comparison of the advanced UDF engine flowpath and the baseline engine cross section is shown in Figure 19. These cycle parameter increases lead to substantial reductions in the component corrected flow sizes in the engine. For example, the intermediate pressure compressor inlet flow size has been reduced by a factor of two. The HPT inlet flow

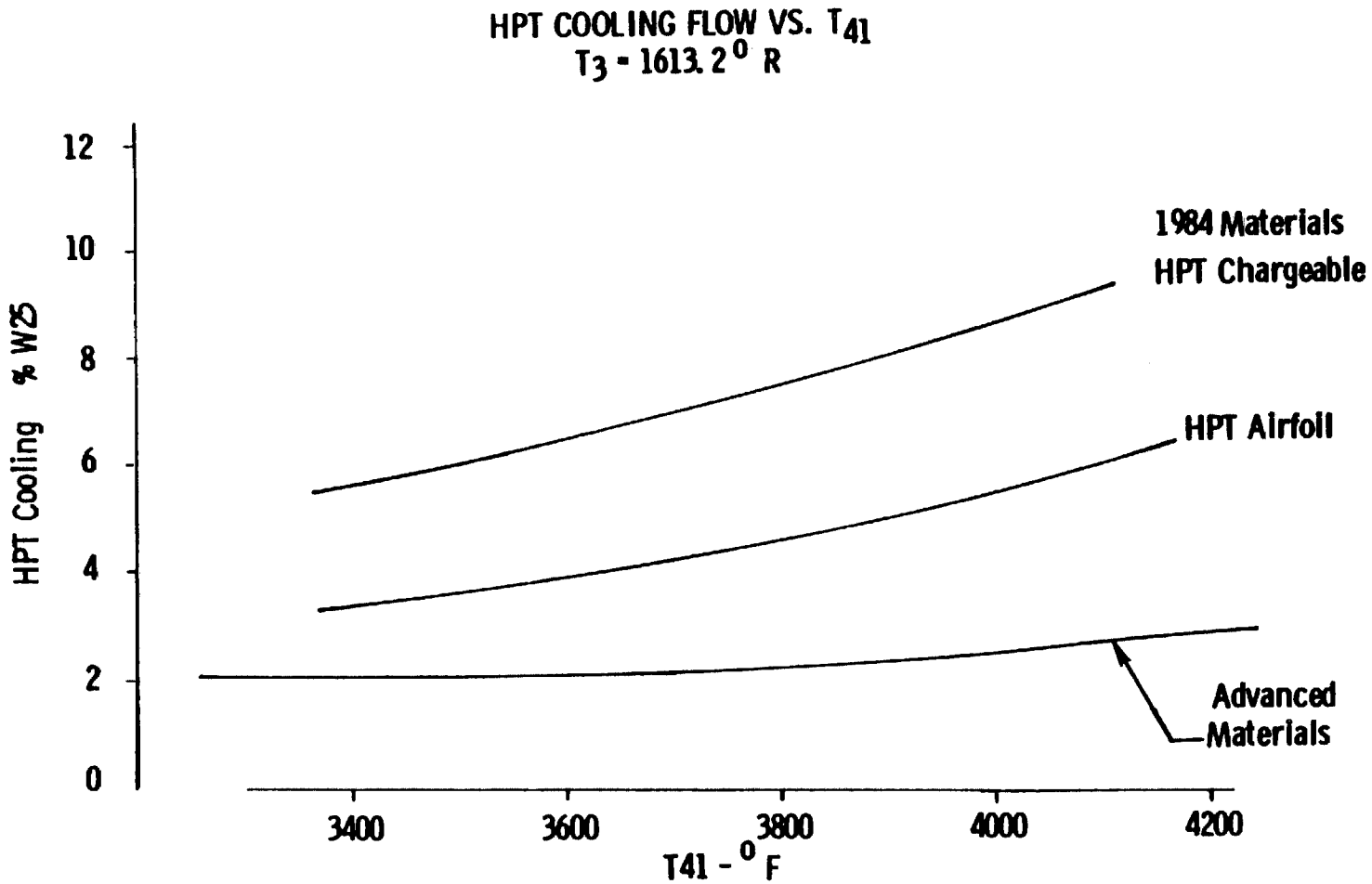

Figure 21. ROMS AST Baseline.

function has been reduced by a factor of four. These size reductions, coupled with the requirement to achieve the best possible component performance for the cycle fuel burn and DOC benefit, result in component tip speed and stage counts which are more conservative than the advanced materials would allow in a larger size. A dramatic increase in stage count is seen in the propulsor turbine. Because of the temperature increase and the flow reduction that was discussed earlier, the Reynolds number and blade height associated losses become dominant in this turbine problem. The resulting configuration to maintain the required performance goal is a 12×12 counterrotating turbine with an average stage loading that is lower than the baseline levels (see the propulsor turbine discussion later in this section).

Direct comparisons of the baseline and advanced UDF engine components are shown in Figures 22 through 27. In these figures, the component details are shown in the same scale in a size that highlights the salient differences in the two engine concepts.

The IP compressors are compared in Figure 23. As previously discussed, the corrected flow size has been reduced by more than 2X in the component parameter comparisons included in this table. The data in these tables for the UDF and the AST engines (which will be discussed later) are the early design iteration data which specified the flowpath configuration details. Since this flowpath specification, the engines have been rubberized and scaled for thrust size mission changes due to the actual fuel burn and DOC derivatives of the particular engine system. The flowpath details were not updated for all these resulting engine size changes. Thus, component design cycle data presented in these figures could be different than those presented elsewhere in this report.

The advanced materials are used in the advanced UDF IP compressor to achieve the swept blade planform at a radius ratio of 0.34. In this configuration, a blisk type design has been required in current materials and current airfoil planforms at similar inlet radius ratios. The advanced materials will allow these two features to be used in combination with an increase in the characteristic blade tip speeds. These speeds were not pushed to the maximum limits. The 2.5 point improvement in polytropic efficiency has been determined to be of more value in this engine configuration than the turbine

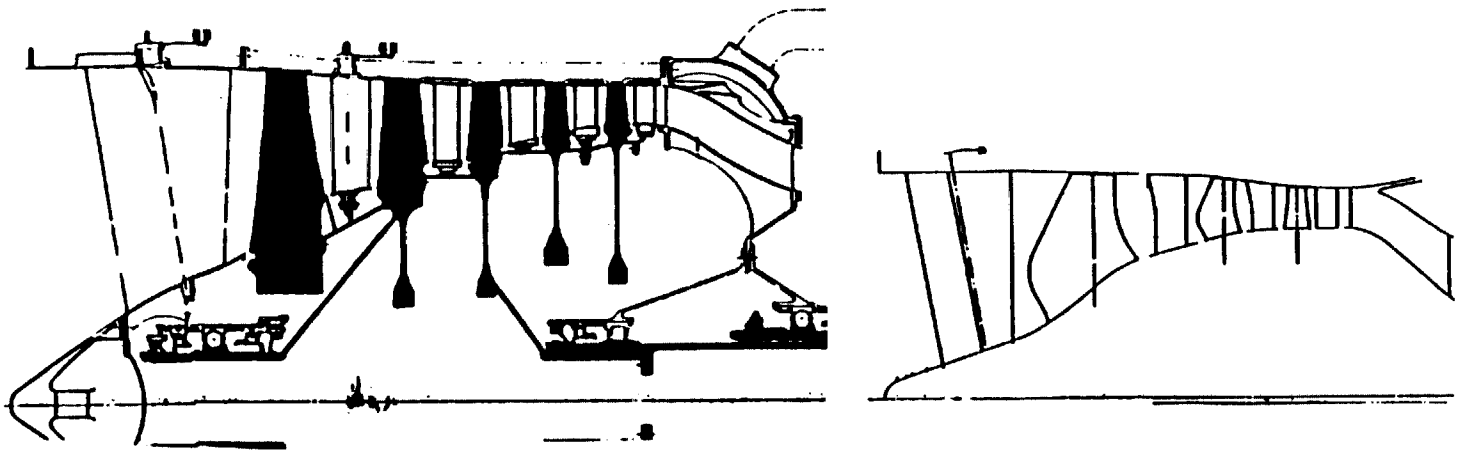

Baseline		Advanced
105.1	Corrected Flow, $W\sqrt{\theta}/\delta$ ~lb/sec.	51.6
40.0	Inlet Specific Flow $W\sqrt{\theta}/\delta_A$ - lb/sec-ft^2	40.0
6.78	Design Pressure Ratio, P/P	4.78
1437	Corrected Inlet Tip Speed, $U_T/\sqrt{\theta}$ ~fps	1584
5	Number of Stages	3
.45	Inlet Radius Ratio, r_H/r_T	.34
1373	Maximum Tip Speed, U_T ~FPS	1514.1
0.8863	Polytropic Efficiency	0.9117
0.8525	Adiabatic Efficiency	0.8907

Figure 22. UDF Engine Component Comparison, Intermediate Pressure Compressor.

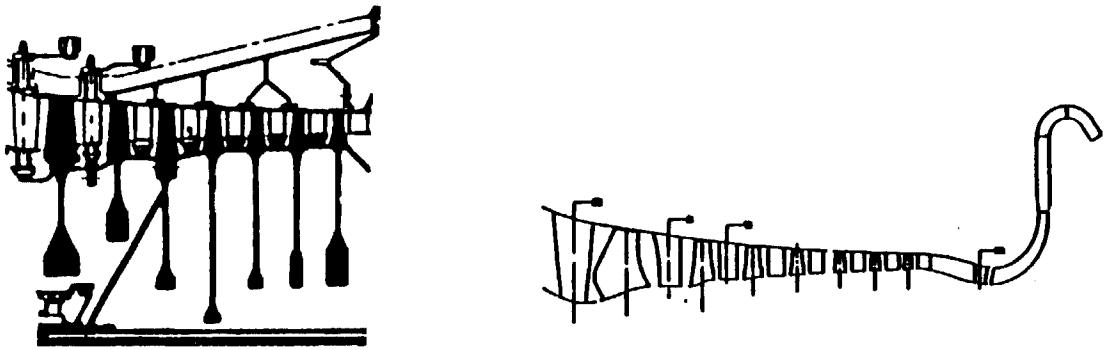

Baseline		Advanced		
		Axial	Centrifugal	Overall
19.6	Corrected Inlet Flow, $W\sqrt{\theta}/\delta$ ~ lb/sec.	13.56	1.75	
36.5	Inlet Specific Flow, $W\sqrt{\theta}/\delta_A$ ~ lb sec.	36.5	23.7	
6.13	Design Pressure Ratio, P/P	10.88	2.113	23.0
1091	Corrected Inlet Tip Speed, $U_T/\sqrt{\theta}$ ~ fps	1556.3	1113.8	
7	Number of Stages	7	1	
0.837	Inlet Radius Ratio, r_H/r_T	0.600	0.882	
1455	Maximum Tip Speed, U_T ~ fps	1892.4	1915.1	
1293	Maximum Rim Speed, U_H ~ fps	1447.9	-	
0.8948	Polytropic Efficiency	0.8998	-	0.8947
0.8655	Adiabatic Efficiency	0.8622	0.8598	0.8418

Figure 23. UDF High Pressure Compressor.

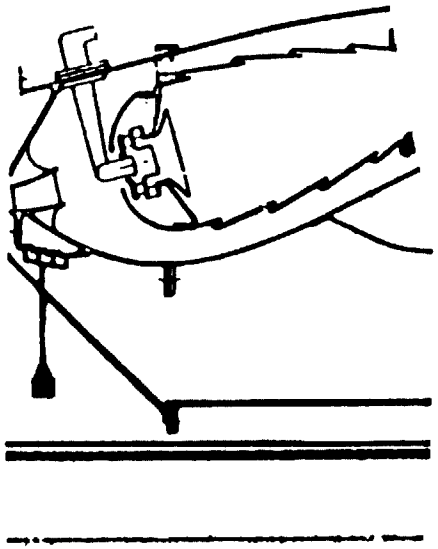

	Baseline	Advanced
Dome Velocity, fps	28	25
Pattern Factor	1.2	1.2
Profile Factor	1.03	1.03
Maximum ΔT, ° F	1353	1686
Length/Dome Height	2.3	2.0
Fuel/Air Ratio	0.0231	0.0311
$\Delta P/P$, %	4.3	4.3

Figure 24. UDF Combustor.

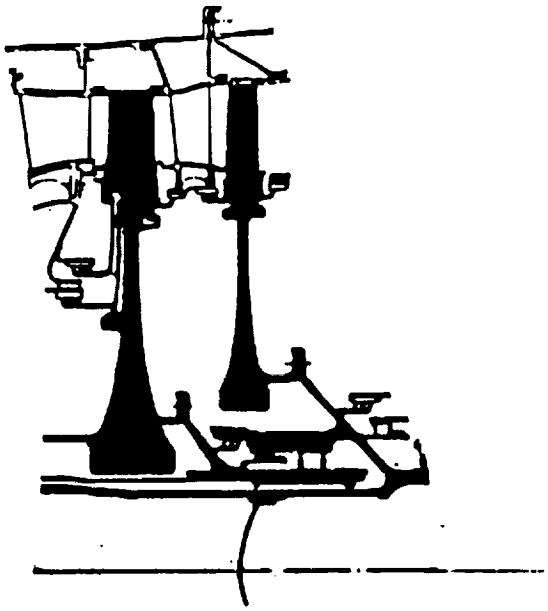

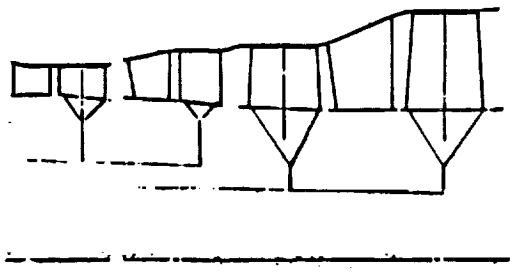

Baseline			Advanced	
HP	IP		HP	IP
8.5	24.5	Inlet Flow Function, $W\sqrt{T}/P$ ~ lb/sec.	2.1	9.7
3.12	2.77	Pressure Ratio, P/P	1.96	1.26
336.1	269.6	Corrected Speed, $N\sqrt{T}$ ~ rpm	689.0	411.0
166.2	106	Energy Extraction, Δh ~ BTU/lbm	142.0	36.2
2696	2253	Inlet Temperature, ^{0}R	3526.0	2526
0.75	0.89	Design Pitch Loading, ψ	0.71	0.75
32.0	22.0	Bucket Root Stress Parameter, $AN^2 \times 10^{-9}$	46.1	18.1
0.882	0.836	Radius Ratio, r_h/r_T	0.833	0.703
1	1	Number of Stages	2	2
1869	1330	Maximum Tip Speed, U_T ~ fps	1754	930.0
32.0	22.0	Exit Swirl, Γ ~ deg.	28.0	13.0
0.9070	0.9250	Turbine Efficiency	0.9273	0.9475

Figure 25. High Pressure and Intermediate Pressure Turbines.

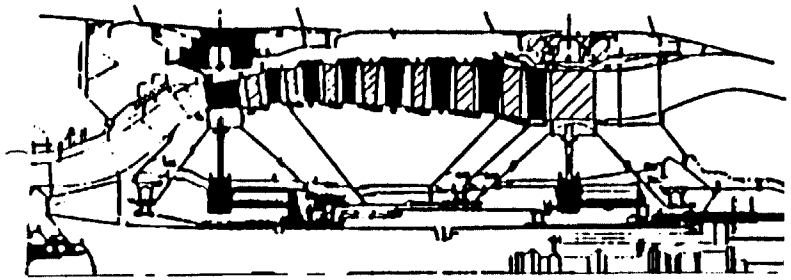

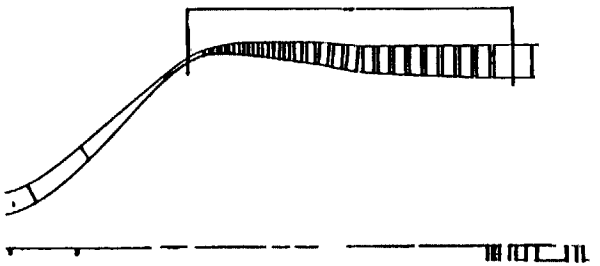

Baseline		Advanced
55.7	Inet Flow Function, $W\sqrt{T}/P \sim$ lb/sec.	12.2
4.87	Pressure Ratio, P/P	16.4
32.7	Corrected Speed, $N/\sqrt{T} \sim$ RPM	28.8
129.9	Energy Extraction, $\Delta h \sim$ BTU/lb	311.8
1626	Inlet Temperature, $T_{41} \sim {}^{0}R$	2385
0.908	Design Pitch Loading, ψ	1.29
1.2	Bucket Root Stress Parameter, $AN^2 \times 10^{-9}$	0.9
0.747	Radius Ratio, r_H/r_T	0.835
8x8	Number of Stages	12x12
255	Maximum Tip Speed, $U_T \sim$ fps	264
21	Exit Swirl, $\Gamma \sim$ deg.	30.0
0.9240	Turbine Efficiency	0.9032

Figure 26. UDF Propulsor Turbine.

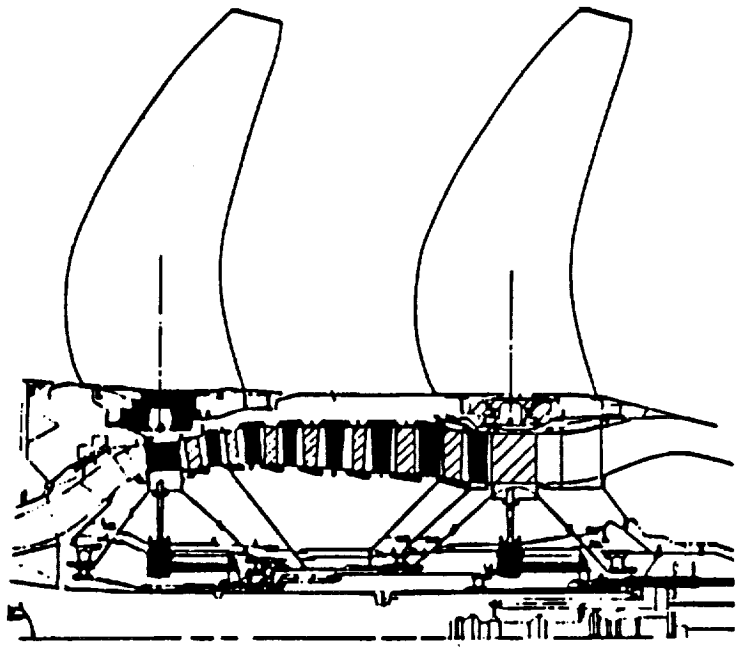

Baseline		Advanced
4281	Thrust, F_N ~ lb_f	5510
35K	Altitude, ft.	35K
0.80	Mach Number	0.80
10x8	Number of Blades	11x9
3.13	Advance Ratio, J	3.06
4.20	Pressure Coefficient, P/A	6.05
1.11	Thrust Coefficient, T/A	1.62
85.7	Disk Loading, Sh p/A ~ hp/A	131.6
780	Tip Speed, U_T ~ fps	798
0.386	Radius Ratio, r_H/r_T	.436
0.8285	Net Efficiency	0.8410

Figure 27. UDF Fan Blades.

diameter reduction that could result from further increases in blade tip speeds. The aerodynamic technologies that are designed into these compressor components have been selected to achieve the same level of component stall margin. Engine system operational integrity requirements were assumed to be constants in the studies. The parameters which influence this stall margin potential were selected to achieve the required design levels of operational margin. These parameters are blade speed, airfoil cascade solidity and aspect ratio, and stage static pressure rise requirement. Of these, the first two items are directly influenced by the use of the advanced materials assumed in these studies.

The high pressure compressor components for the two UDF engines are compared in Figure 23. In this case, the increased wheel speeds made available with the materials have significantly affected the number of stages required to do the compression job. In the axial part of the advanced component, the pressure rise is increased by 4.75 atmospheres in the same number of compressor stages. This is accomplished by increasing both the tip and rim speed limits on the compressor. In spite of the blade speed increases, the polytropic efficiency of the axial compressor has been improved by sweeping the first stage and by reducing the inlet radius ratio. This last change improves the blade height associated loss conditions in the compressor. Because the overall pressure ratio is so large and the flow size is so small, the compressor blade height at Stage 7 drops to 0.45 inch. This is a lower limit to maintain reasonable discharge clearance-to-blade height levels in an axial compressor.

Because of this, the final 2.1 atmospheres of pressure rise were achieved with an advanced technology centrifugal compressor stage. The blade speed limits for this stage were established to achieve a tip speed of less than 2000 fps. The study material advantages are required to keep the weight of this compressor stage at a reasonable level.

The combustor flowpaths are compared in Figure 24. The aerodynamic and mechanical design considerations for these combustors are discussed in another section.

The high pressure and intermediate pressure turbine flowpaths are compared for the two UDF engine configurations in Figure 25. Both of these configurations utilize counterrotating spools to reduce the interaction losses between the two turbines. For the advanced technology engine the discharge swirl out of the second HPT stage has been selected to allow the vane which usually exists between the two turbines to be removed. This vaneless configuration increases the basic efficiency potential of the IP turbine component by 1.3 points. This removal also eliminates the need to cool and purge the hardware which would be associated with the vane assembly.

As was alluded to earlier, the dramatic size reduction indicated by a 4X change in the HPT flow function also requires that the turbine loadings be reduced to enhance turbine efficiency to further improve engine performance. In addition, the elimination of the airfoil cooling flows made possible by the advanced material capabilities has been utilized to redefine the blade Zwiefel levels to minimize the Reynolds number loss sources in these small turbine components. Taking all these items into account, the turbine system performance has been significantly improved compared to the baseline turbine component.

The comparison of the propulsor or power turbines for the UDF fan system is shown in Figure 26. Multistage counterrotating turbine concepts are applied in both configurations. The rotational speeds of these components are directly tied to the tip speed of the UDF at the turbine design point. The tip radius of the turbine is a finite amount below the hub of the fan that it is powering. This leads to blade speeds which are quite low, as indicated in Figure 26. The baseline engine requires a 8x8 stage turbine to achieve the required performance at the desired power extraction. The resulting turbine loading parameter for this configuration was established to be 0.91 to satisfy these requirements.

The advanced technology engine achieves its performance with a high T41 and an ultrahigh cycle pressure ratio. As was indicated in the HP and IP turbine discussion, this has led to very low flow function levels in the turbines. This has had an extreme impact on the propulsor requirements for this engine. The combined impact of flow level, inlet temperature level, and very small annulus height have resulted in a tenuous turbine configuration.

Taking advantage of the advanced aerodynamic performance goals, this turbine is a 12×12 stage counterrotating turbine. This is near the upper bound of what is thought to be practical in a flight type application because of cost and engine weight considerations. The performance demands of this engine system preclude looking at design concepts which would ease the blade height problem in the inlet of this turbine. The transition duct losses are estimated to be 40% greater for this configuration than for the baseline turbine.

The unducted fan baseline configuration is shown in Figure 27. The UDF design aspect ratio was maintained for the advanced engine configuration. In addition, the fan hub diameter was assumed to be the same 4.36 feet between the two engines. Thus, the fan cross-sectional picture only changes by the blade height difference between the two fan configurations.

The acoustics technology and fan weight considerations were the major factors in selecting the fan tip diameter. The acoustics requirement for the engines was selected to be the FAR 36, Stage 3 noise limit compliance with a 1.5 EPNDb margin. It turns out that the fan diameter becomes an inverse function of fan blade number when the aspect ratio is defined for comparable geometries. The weight considerations drive the fan diameter to the smallest possible level. As the number of UDF blades increases, it becomes difficult to achieve reasonable fan efficiencies at the 0.8 M_0, 35,000 ft altitude cruise condition. The total fan blade number was selected with both weight and performance considerations in mind.

For the baseline engine, the results of the NASA-sponsored UDF simulator test series indicated that the F7A7 fan configuration technology was appropriate for a 1984 engine. This is the same technology that has been built into the UDF demonstrator engine which is currently on test.

The weight and acoustics conflict pushed the fan blade number to 18 (10×8). This is two more blades than were actually tested in the F7A7 configuration. The fan diameter which satisfies the acoustics goals is 11.3 feet. As indicated in Figure 27, the resulting disk loading for the baseline configuration is 85.7 hp/ft^2. The fan system net efficiency at the cruise design point is 0.8285.

A similar process was used to select the UDF blade geometries for the advanced engine. Because the fan performance is such a large driver on fuel burn and engine system direct operating cost, the blade count considerations were established to achieve an improvement over the baseline configuration using the General Electric advanced technology UDF performance goals. The total fan blade number was selected to be 20 (11×9). A tip diameter of 10.3 feet satisfies the acoustics requirements. The cruise design disk loading and net efficiency for the advanced fan component are 131.6 hp/ft^2 and 0.841, respectively.

2.11 ADVANCED AST ENGINE CONFIGURATION

The advanced AST engine configuration is also characterized by substantial increases in T41 and OPR. The projected materials allow the evolution of engine cycles having high temperature and pressure at the exhaust nozzle exit for high sea level thrust.

A comparison of the advanced AST engine and the baseline engine cross sections is shown in Figure 2. The cycle parameter changes lead to substantial reductions in the component corrected flow sizes in the engine. For example, the core compressor inlet flow size has been reduced by a factor of 2.4. The turbine inlet flow function has been reduced by a factor of 4.4. These size reductions, coupled with the increased speed limit values, lead to a configuration with very dramatic reductions in component diameters compared with the baseline engine.

In the case of the AST engine mission, the engine volume or weight has a strong influence on the system DOC. Because of this, the component limits were employed in the design studies of this configuration. This can be illustrated in the studies to select the spool to drive the fan stage between the two front bypass ducts. In the initial studies, this stage was driven by the core spool. The problem with this is the core compressor blade speeds were limited to very moderate levels. The larger fan tip speed was limiting the spool rotational speed. This required several more compressor stages than are shown in the proposed advanced configuration. The core turbine energy extraction was also substantially larger which required a much heavier component. By selecting a fan-driven approach, the core speed limits can be

used to minimize the stage count and turbine volume. The resulting engine power turbine has six stages. However, because of the smaller power turbine diameter, the engine volume is still improved relative to a core-driven fan stage approach for this engine.

Direct comparisons of the baseline and advanced AST engine components are shown in Figures 28 through 32. As in the previous discussion, the component details in these figures are shown in the same scale in a size that highlights the salient differences in the two engine concepts.

The takeoff thrust requirements between the baseline and the advanced engine systems were assumed to be essentially the same when the flowpath configurations were being studied for this program. The system flow size has been scaled as the thrust size has changed in the cycle and mission studies. For this discussion these flow sizes were essentially the same as indicated in Figure 28. This figure compares the two AST engine fan components.

The baseline fan is a moderate radius ratio bladed design with modest blade tip speeds. In this configuration the rear block fan is driven off the core spool. The advanced engine configuration maintains the same total stage count in the fan component. The pressure rise of the front block fan has been increased by 1.5 atmospheres by increasing the blade speed and upgrading the fan technology. The radius ratio of the front block has been reduced to 0.33 taking advantage of the advanced material properties. This improves the spool rotational speed characteristics for the turbine design. The front block fan blades utilize the swept airfoil technology that was discussed previously. The fan corrected tip speed for this design was chosen to be 1737 fps using the material property flexibility available for this engine. The front block performance has been improved by 0.8 point in adiabatic efficiency.

Because the advanced configuration has the rear block driven by the low spool instead of the high spool, the performance of the rear block is down 0.5 points in adiabatic efficiency. This results because the pressure rise is up and the stage corrected tip speed is down. In spite of this as was discussed earlier, this engine configuration is improved with this fan driven concept.

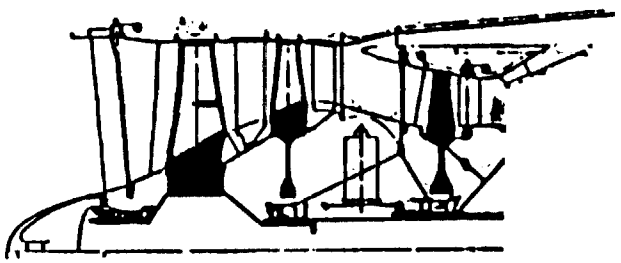

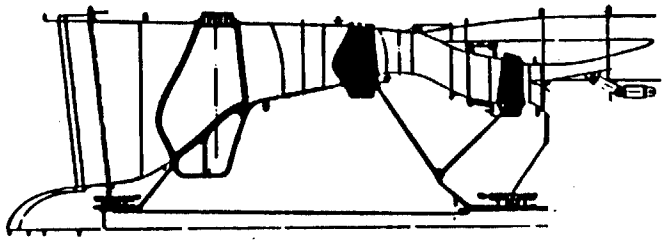

Baseline			Advanced	
Front Block	Rear Block		Front Block	Rear Block
813.9	340.7	Corrected Inlet Flow, $W\sqrt{\theta}/\delta$ ~ lb/sec.	821.3	244.4
42.0	38.5	Inlet Specific Flow, $W\sqrt{\theta}/\delta_A$ ~ lb/sec. ft^2	41.5	35.7
2.804	1.368	Design Pressure Ratio, P/P	4.30	1.53
1436	1309	Corrected Inlet Tip Speed, $N/\sqrt{T}$ ~ rpm	1737	1135
2	1	Number of Stages	2	1
0.400	0.690	Inlet Radius Ratio, r_H/r_T	.330	.738
1546	1612.1	Maximum Tip Speed, U_T ~ fps	1870	1490
0.8840	0.8815	Polytropic Efficiency	0.8980	0.8780
0.8673	0.8769	Adiabatic Efficiency	0.8750	0.8716

Figure 28. AST Engine Component Comparison, Fan.

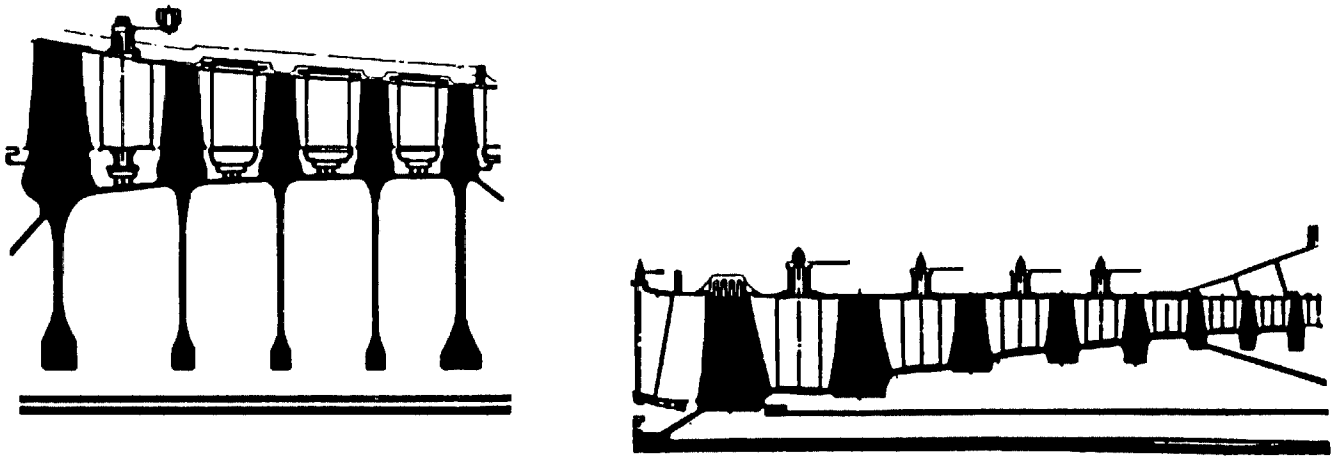

Baseline		Advanced
208.7	Corrected Inlet Flow $W\sqrt{\theta}/\delta$ ~ lb/sec.	85.6
37.0	Inlet Specific Flow, $W\sqrt{\theta}/\delta_A$ ~ lb/sec-ft^2	41.0
4.1	Design Pressure Ratio, P/P	10.0
1123	Corrected Inlet Tip Speed, $U_T/\sqrt{\theta}$ ~ fps	1226
5	Number of Stages	8
0.767	Inlet Radius Ratio, r_H/r_{T1}	0.472
0.859	Exit Radius Ratio, r_H/r_{T_e}	0.874
1612	Maximum Tip Speed, U_T ~ fps	1714
1115	Maximum Rim Speed, U_H ~ fps	1436
0.9010	Polytropic Efficiency	0.9090
0.8811	Adiabatic Efficiency	0.8792

Figure 29. AST High Pressure Compressor.

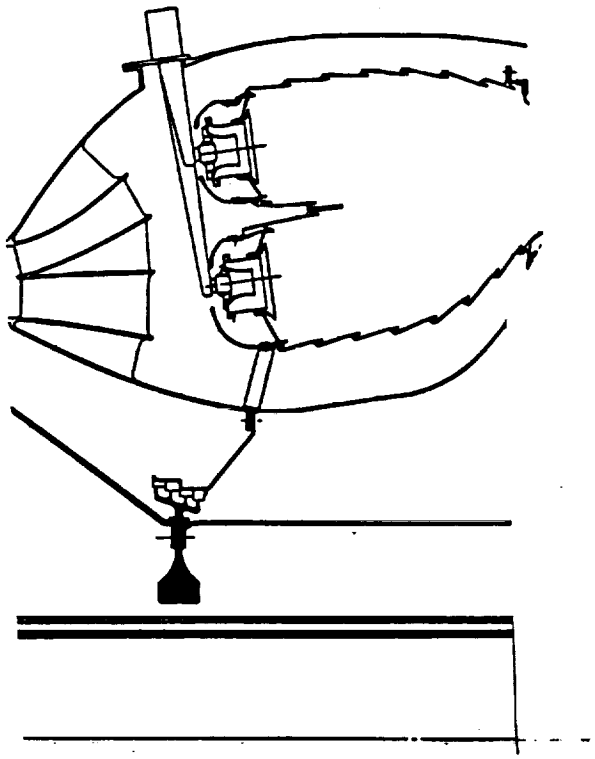

Combustor

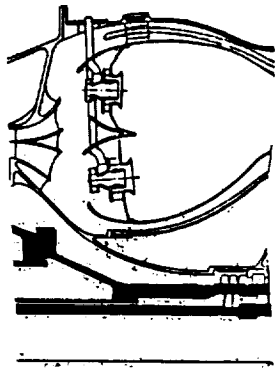

	Baseline	Advanced
Dome Velocity, fps	27.5/55	30/60
Pattern Factor	1.15	1.15
Profile Factor	1.03	1.03
Maximum ΔT, ° F	1565	1912
Length/Dome Height	2.3	2.0
Fuel/Air Ratio	0.0244	0.0357
ΔP/P, %	7	5.6

Figure 30. AST Combustor.

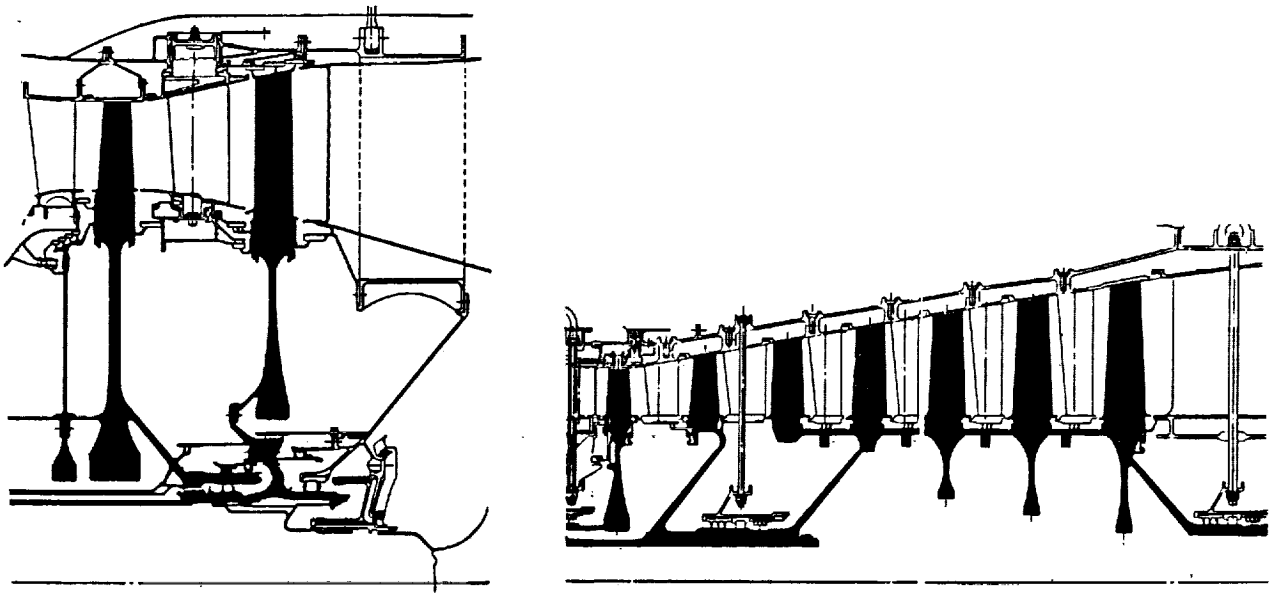

Baseline			Advanced	
HP	LP		HP	LP
126.3	321.0	Inlet Flow Function, $W\sqrt{T}/P$ ~ lb/sec.	28.8	62.0
2.6	2.5	Pressure Ratio, P/P	2.3	3.3
119	116	Corrected Speed, $N/\sqrt{\theta}$ ~ rpm	245	92.0
158	86.0	Energy Extraction, Δh ~ BTU/lb.	170	266
3160	2575	Inlet Temperature, T_{41}, T_{49} ~ ^{o}R	4552	3966
0.90	0.67	Design Pitch Loading, ψ	1.00	1.30
39.0	43.3	Bucket Root Stress Parameter, $AN^2 \times 10^{-9}$	65.0	32.3
0.82	0.71	Radius Ratio, r_H/r_T	0.78	0.56
1	1	Number of Stages	1	6
1680	1465	Maximum Tip Speed, U_T ~ fps	2000	1064
25	7	Exit Swirl, Γ ~ des.	34	31
0.8993	0.8975	Turbine Efficiency	0.9247	0.9122

Figure 31. AST HP and LP Turbines.

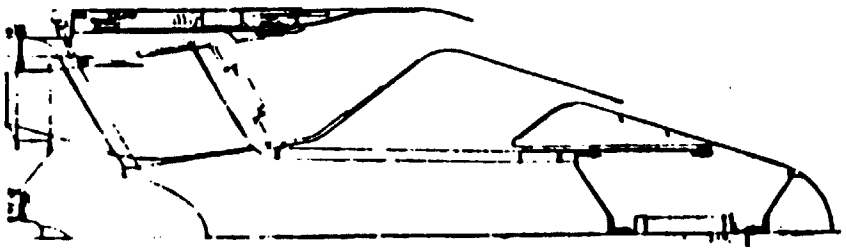

Baseline

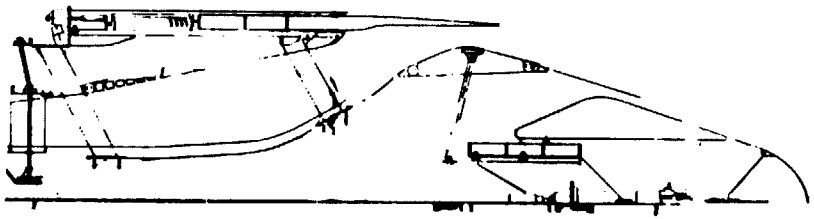

Advanced

	Baseline	Advanced
Rotation Throat Ri/Ro	0.86	0.90
Augmentation	Partial	Dry
Thrust Reverse	50% Maximum Dry	50% Maximum
A8 Maximum	1179	922
A8 Minimum	1125	621
A18 Maximum	416	502
P8/P0 Supersonic Cruise	29	27
P8/P0 Rotation	3	6

Figure 32. AST Exhaust Nozzle.

The core compressor components are compared in Figure 29. This component takes advantage of the new material properties in virtually every aspect. The baseline compressor is a standard product axial machine. It has a relatively high inlet radius ratio and a standard disk drum construction with separate blades with dovetail attachments. The blade speeds are moderate, producing a modest level of pressure rise, 4.1 atmospheres in five stages. This combination of design parameters results in a respectable level of performance as indicated in the figure.

The advanced product compressor has used the mechanical speed allowables of the new materials to define a configuration which has a low inlet radius ratio. This level is typical of product fan components. This radius ratio, combined with the design pressure rise requirement of 10 atmospheres, has produced an eight-stage compressor with an exit hub speed of 1436 fps. This low radius ratio high speed compressor has an aerodynamic performance advantage over the baseline technology of 0.8 points as defined by the compressor polytropic efficiency. The construction of this low radius ratio compressor is likely to require special design techniques such as blisk or bling designs where the airfoils and the disks are manufactured as one piece.

The combustor comparison for the two engines is shown in Figure 30. The technologies used to describe these two components are quite similar. The size of the machine allows the description of a double dome configuration which produces a minimum length combustor design.

The core and fan turbine components of the two AST engines are shown in Figure 31. As was the case in the core compressor, the 16.2 overall cruise cycle pressure ratio has led to dramatic reductions in the turbine flow function parameters. The core turbine size is smaller by a factor of 4 and the fan turbine size is smaller by a factor of 5. In addition, T41 has been pushed to the material allowable limits. In both turbines this temperature increase is just under 1400° F.

The whole engine configuration depends on the ability to increase the core turbine blade root stress parameter, AN^2.

The fan turbine component shows a vary dramatic change in component stage count as indicated in Figure 31. This is a result of several cycle and

configuration changes. The bypass ratio of the improved engine has been increased relative to the base cycle. The core flow is reduced because of this change. In addition, the rear block fan stage has been added to the low pressure spool. The turbine must provide the added power to drive this third fan stage. As indicated in the figure, the specific enthalpy · extraction requirement has increased by 3X for the future engine turbine. If the turbines had the same blade speeds the power turbine stage count would be tripled. However, as indicated in the figure and discussed previously, the turbine system diameter and, therefore, volume has been significantly reduced in this design. For the turbine loading of the baseline component a 12-stage turbine would be required for the turbine. By applying multistage turbine technology and the advanced turbine aerodynamic principles, the design loading can be increased to allow a six-stage configuration. This turbine has a 31° exit swirl which will require a vane frame configuration downstream of the turbine. This is similar to the vane frame in use with current product power turbines.

This advanced component was studied further to attempt to reduce the stage count. The pitch radius was moved out to allow the work extraction to be accomplished in three stages. A transition duct was required to couple the core turbine with this configuration. The result of this examination is interesting. The length of the turbine including the transition duct was virtually the same as the six-stage configuration. Because the diameters are larger and the rotational speed is the same, the volume of the material required in the turbine increases significantly. The blade heights are somewhat smaller. This aggravates the losses which are height related. The component performance is significantly poorer than the six-stage machine. The three-stage machine had an efficiency disadvantage of over 1%. Finally, the number of airfoils required in the three-stage version is 30% more than the total in the six-stage version. The clear choice of this exercise was to stick with the six-stage machine.

The exhaust nozzle flowpaths for these engine configurations are shown in Figure 32. These designs are modeled after the NASA-sponsored "Supersonic Cruise Vehicle Exhaust System Study," contract NAS1-15675. These studies were conducted from 1978 to 1980. This configuration is the coannular ejector

nozzle scheme that yields the required acoustics noise levels for this class engine at takeoff, climb, and approach. The nozzle system reverts to a conventional mixed flow turbofan arrangement for the supersonic cruise engine operation. The details of this configuration are well documented in the reports associated with these studies.

2.12 MATERIAL SELECTION AND MECHANICAL DESIGN

Aerodynamic, thermodynamic, and stress technologies are combined in an aircraft gas turbine design. Materials play an important role in all three technologies. They maintain airfoil and flowpath shapes for aerodynamics, withstand high thermodynamic gas temperature for improved efficiencies and performance, and withstand higher aerodynamic gas and mechanical tensile and bending loads for higher stress capabilities and lighter components.

Aircraft gas turbines are composed of rotating and static components. Each component requires a different design philosophy for their respective materials. Rotating components are generally designed for stress limitations and are generally associated with material allowable stress/material density (σ/ρ) term for lowest weight. Static structural components, with the exception of pressure vessels, are generally designed for deflection or stiffness limitations and are generally associated with material modulus/density (E/ρ) term for lowest weight. Pressure vessels, such as casings, are designed for hoop or tensile stress and biaxial bending loads. Materials whose combinations of σ/ρ and E/ρ yield the best optimum design values are selected for specific components.

2.13 SUBSONIC ENGINE COMPONENT DESCRIPTION AND MATERIAL

Figure 33 is an illustration of the 1984 baseline subsonic engine. Figure 34 is a flowpath comparison of the advanced engine with the baseline. General mechanical design of both engines are similar, specific component detail designs, are different and explained. Figure 34 illustrates the relative engine overall dimensions and weight. Tables XXVI and XXVII list the material and structural changes between the baseline and advanced subsonic engines. Specific material selections and material affecting structural changes are explained in detail.

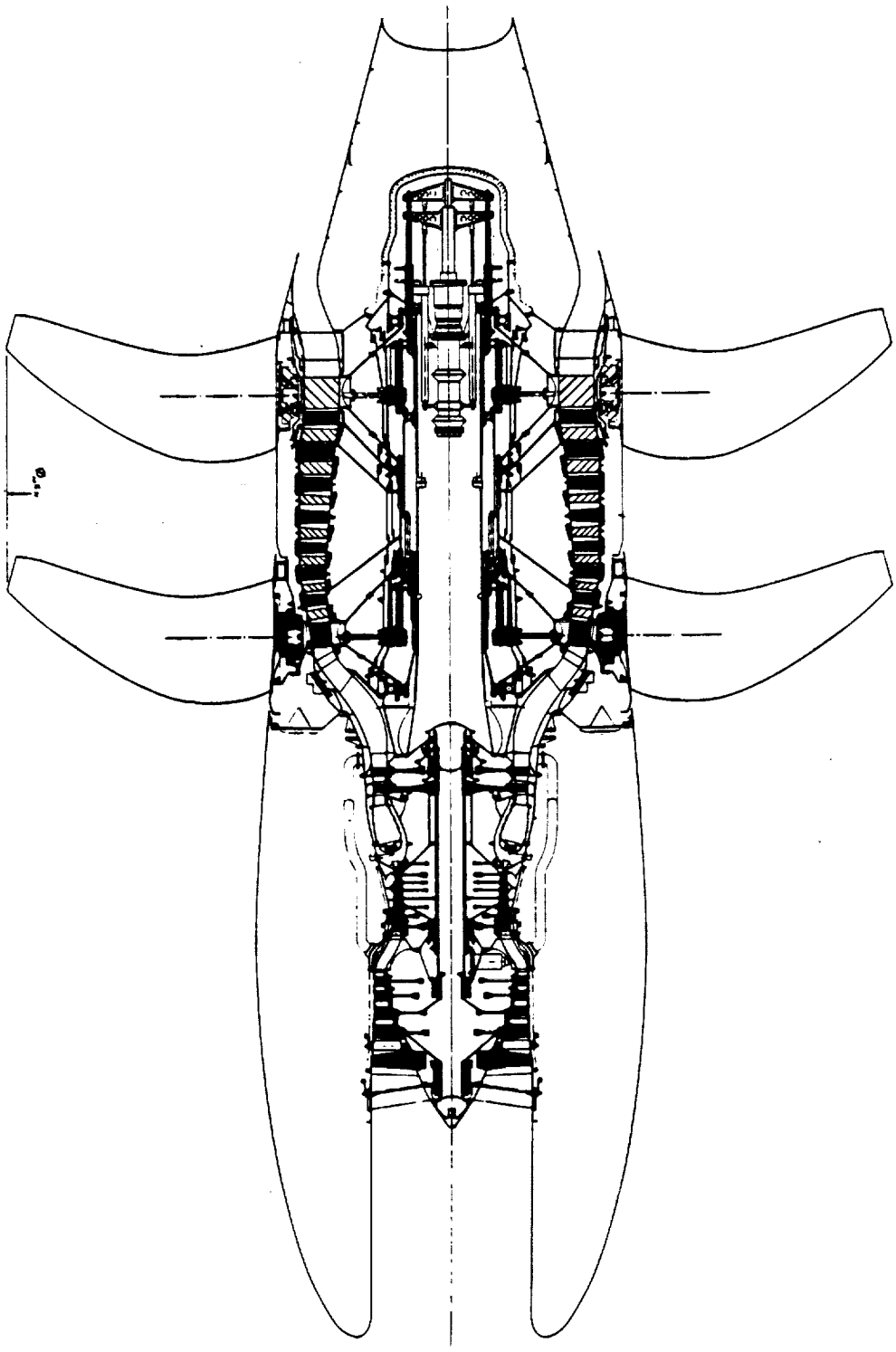

Figure 33. Baseline UDF Engine Cross Section.

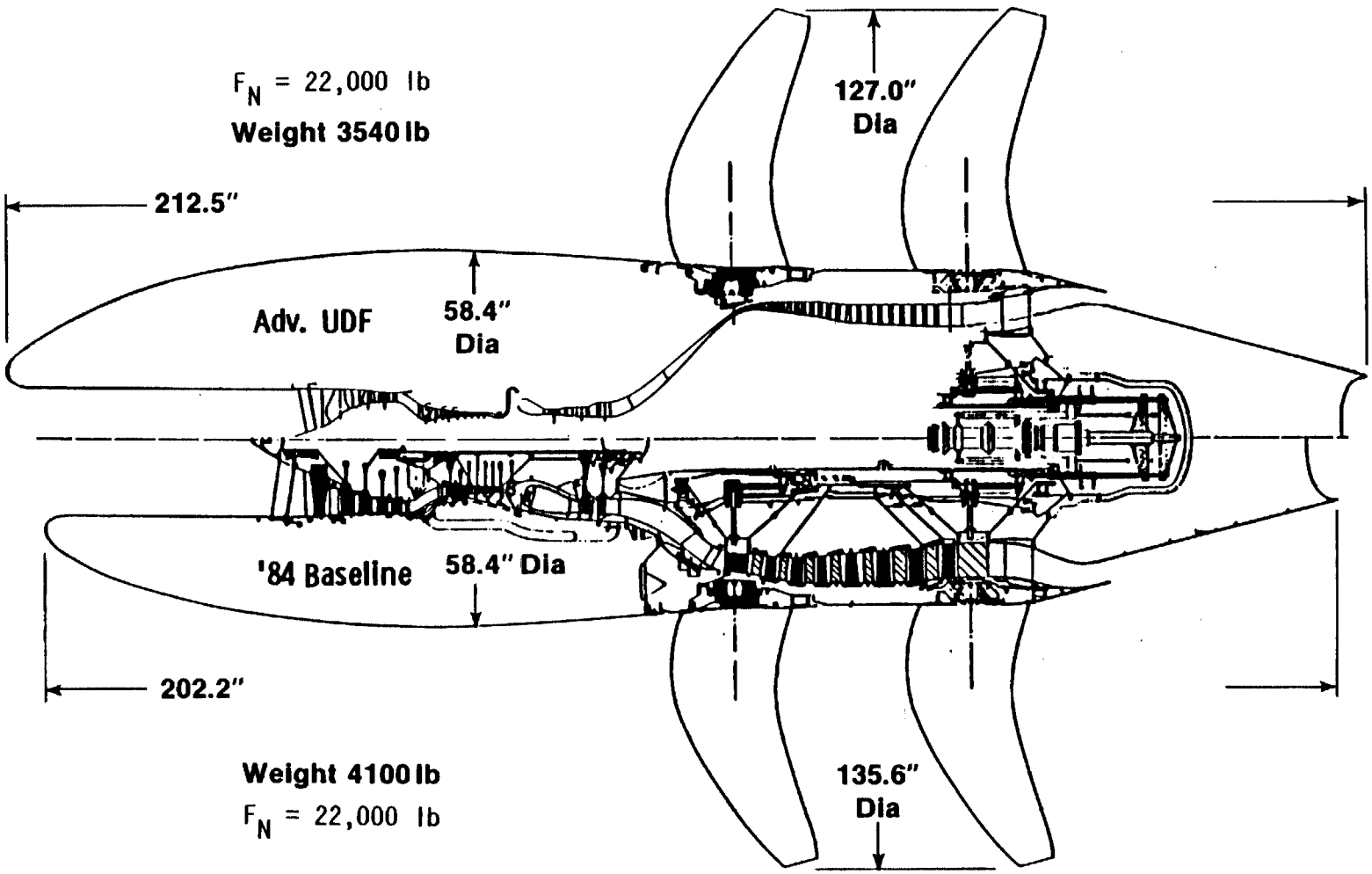

Figure 34. Advanced Versus Baseline Weight and Dimension Comparison.

Table XXVI. Structural Evolutions.

- Structures (Frames, Casings, etc.)
  - Stiffness and Weight (namely, E/ρ Ratio)
  - Spring Constants, Clearances
- Rotating Components
- Strength, Stiffness, Weight, and Blade Vibration
- Overall Engine Size - Smaller Cores, Diameters
- Uncooled Combustor Liners, Turbine Airfoils
- High Turbine Inlet Temperature Capability
- Dry, Solid Film/High Temperature Bearing Lubrication
- Pneumatic/Mechanical, High Temperature Air Turbine Actuators

Table XXVII. Advanced UDF Material Changes.

Component	Material	
	1984	2010
HPC Rotor	Inco 718/René 95	FRM/Inter. and Inco 718
HPC Stator	Inco 718	FRM/Inter. and Inco 718
Diffuser and Case	Inco 718	FRM/Inter.
Combustor	HS188	NMC
HPT Stator	MA754/509	NMC
HPT Rotor	N4/René 95	NMC/Inter.
LPT Stator	N4/Hast X	NMC
LPT Rotor	N4/René 95	NMC/Inter.
LPT Shaft	Inco 718	FRM/Inter.
Configuration	Ti-6-4/Inco 718	Ti-6-4/Inco 718
Front Fan	Composite/Inco 718	Composite Inter.
Aft Fan	Composite/Inco 718	Composite Inter.
Front Turbine	U500/Inco 718	Inter./U500/Inco 718
Aft Turbine	U500/Inco 718	Inter./U500/Inco 718
Front Frame	René 41/HS 188	NMC/Inter.
Bearings and Seals	M50NiL	M50NiL
Turbine Stator	Hast X	Inter.

2.14 GAS GENERATOR STATIC STRUCTURAL COMPONENTS (Figure 1)

Baseline and advanced overall engine static configurations are similar, but advanced engine gas generator high turbine inlet temperatures allow a 30% reduction in advanced engine gas generator size. Both engines have a gas generator front frame, fan frame, and turbine frame which support a cantilevered propulsor.

Overall engine and component stiffness is required to maintain close rotor blade/shrouds operating clearances for maximum engine performance and low specific fuel consumption.

Baseline engine mount planes are the gas generator front frame for vertical loads and the turbine frame for remaining loads. Because of the reduced gas generator diameter, the fan frame and turbine frame are the engine mount points.

Baseline engine gas generator outer casing compressor casings and combustor casings are designed with conventional superalloys having E/ρ stiffness ratio of 90×10^6 in. Similar components for the advanced engine are of fiber-reinforced metal matrix having an E/ρ stiffness ratio of 157×10^6 inch, a 69% increase in stiffness.

2.15 GAS GENERATOR COMPRESSOR, COMBUSTOR, AND TURBINE CASINGS

Casings not only require the same stiffness as frame outer rings, but also require hoop strength capability. Conventional superalloys, used in the baseline engine, have strength to density ratios in the range of 333×10^6 in. Advanced engine fiber reinforced metal matrixes, in contrast, have a range of 870×10^6 in, a 160% increase in strength density. Improved material strength/density and stiffness, modulus/density in vanes and compressor blades are realized with fiber-reinforced metal matrix substitution.

2.16 GAS GENERATOR COMBUSTOR

Table XXVIII lists combustor aerodynamic parameters for the baseline and advanced engines. The baseline engine has a single dome, conventional-machined ring metallic HS-188 convection on film-cooled liner combustor with

multiswirl duplex fuel nozzles. The advanced engine combustor is an ultra-short, nonmetallic composite material, single-dome combustor having uncooled liners and airblast fuel nozzles. Uncooled nonmetallic composite liners, such as carbon-carbon, permit higher temperature rises for more efficient fuel combustion and more uniform combustor temperatures for better turbine engine performance. Unlike conventional combustors, high temperature rise combustors will require radiation barriers between the combustor outer liner and casing and combustor inner liner and inner casing structure to protect these structures from liner thermal radiation.

Table XXVIII. UDF Combustor.

Type	Baseline Single Dome	Advanced Single Dome
Dome Height (Outer/Inner), in	3.5	1.92
Dome Length, in	8.1	3.84
Dome Velocity, (Outer/Inner), fps	25	30
Dome Flow, % of W36	29.7	41.2
Space Rate Btu/(hr-atm-ft^3) $\times 10^{-6}$	4.6	11.8
T4, ° R	2931	3646
(T4-T3), ° R	1304	1686

2.17 LP SHAFT

The baseline engine has a conventional Inconel 718 LP shaft. The advanced engine has a fiber-reinforced metal matrix LP shaft. These shafts are currently under development and some preliminary test results have been obtained. Fiber-reinforced metal matrix LP shafts will have 68% improvement in shaft critical frequencies and will have improved bending stiffness and with proper design, thus eliminating the third bearing on a three-bearing LP shaft.

2.18 ROTATING COMPONENTS

Tables XXVI and XXVII list the structural and material changes and advanced material temperature environments for the baseline and advanced engines. Primary material considerations for these components is the stress/density (σ/ρ) parameter for both blade and disk stress and aeroelastic blade design. The baseline engine is designed with conventional superalloy materials as titanium ($\sigma/\rho \cong 455 \times 10^6$ inch), René 95 ($\sigma/\rho \cong 450 \times 10^6$ inch), and ($\sigma/\rho \cong 123 \times 10^6$ inch) with each material having its temperature limitation.

The baseline HPC rotor is a dovetailed and bolted mechanical design with Inconel 718 Stage 1 and 2 disks bolted to an inertia-welded René 95 rotor drum. Compressor blades are titanium for Stages 1-3 and Inconel 718 for remaining blades.

Baseline engine HP and LP air-cooled turbines are conventional single stage, bladed rotors having René N4 blades and René 95 disks. The blades are thermal barrier coated (TBC) to reduce the hot gas heat flow into the blade walls.

The high pressure rotor for the advanced engine is an axicentrifugal configuration having a one-piece, eight-stage, fiber-reinforced metal matrix axial compressor in line with a one-stage, fiber-reinfirced metal matrix centrifugal compressor. The rotor mechanical design used 1500° F fiber-reinforced metal matrix material design data.

Advanced engine turbine rotors have intermetallic disks and nonmetallic composite (carbon-carbon) turbine blades. Blade centrifugal loads produce a 17 to 18 ksi compressive stress on the blade dovetails and nonmetallic composite (carbon-carbon) coatings. Current carbon-carbon coatings have a maximum coating compression strength in the range of 4 to 5 ksi. Therefore, the coating compressive strength problem is a definite design roadblock.

2.19 PROPULSOR

Table XXVII lists the materials and structural changes of the baseline and advanced propulsors. Overall configurations of both baseline and advanced propulsors are similar. Bladed forward and aft counterrotating fans attached to eight-stage turbine rotors are supported and cantilevered from a common

tube bolted to the turbine frame inner ring. Both configurations are low stressed and have a turbine rotor tip speed of about 260 ft/sec compared with 1300 ft/sec for conventional low pressure turbines. However, both designs require rotor stiffness (E/ρ) for rotating seal and turbine blade tip clearances. Therefore, the advanced subsonic engine will be designed with 2300° F intermetallic in the turbine rotor drum sections. Turbine blades are shrouded 2300° F intermetallic sectors for low turbine blade-shroud clearances.

Attached to and being driven by each rotor is a fan blade rotor assembly consisting of fan blades and a rotating fan blade mount ring. The blade mount ring withstands all fan blade radial and bending forces. The mount ring for the baseline engine is Inco 718, and for the advanced subsonic engine the mount ring is fiber-reinforced metal matrix. The added stiffness/density parameter reduces the mount ring weight. Supporting both rotors is a fiber-reinforced metal matrix stiff tube rigidly bolted at one end to the turbine frame. The baseline engine has the fan blade pitch change hydraulic/mechanical mechanism located at, and supported at, the opposite end of this tube. The fan blade mechanism is an hydraulically actuated mechanical system. A duplex hydraulic cylinder internally located inside the support tube, actuates the mechanical linkages and rotates fan blades about their own radial axis. Fan blade pitch change mechanism for the advanced engine will be actuated by air turbine driven actuators mounted on the rotating fan blade mount ring and a geared circumferential unison ring which meshes with a gear sector located on the fan blade trunnion.

2.20 ADVANCED VERSUS BASELINE ENGINE COMPONENT WEIGHTS

Table XXIX lists the baseline and advanced subsonic engine component weights and weight changes resulting from direct material improvements and improved thermodynamic cycles resulting from improved materials. The high pressure rotor weight history illustrates the two-step process.

2.21 AST MECHANICAL INTRODUCTION

Figures 35 through 37 are illustrations of the selected 1984 baseline and year 2010 advanced AST supersonic engines and a direct comparison of their lengths, weights, and maximum diameters.

Table XXIX. Advanced UDF Weights.

UDF Gas Generator

Component	Material		Weight	
	1984	2010	1984	2010
Front Frame	17-4PH	17-4PH	45	22
LPC Rotor	Ti-6-4/17	Ti-6-4/17	118	44
LPC Stator	Ti-6-4	Ti-6-4	61	31
Mid Frame	Ti-6-2-4-2	Ti-6-2-4-2	77	58
HPC Rotor	IN718/René 95	Fiber Reinf. Metal Matrix/ Intermetallic and IN718	72	103
HPC Stator	IN718	Fiber Reinf. Metal Matrix/ Intermetallic and IN718	70	99
Diffuser and Case	IN718	Fiber Reinf. Metal Matrix/ Intermetallic	68	40
Combustor	HS188	Nonmetallic Composite	47	26
HPT Stator	MA754/509	Nonmetallic Composite	29	19
HPT Rotor	N4/René 95	Nonmetallic Composite/ Intermetallic	78	34
LPT Stator	N4/Hast X	Nonmetallic Composite	63	57
LPT Rotor	N4/René 95	Nonmetallic Composite/	75	68
LPT Shaft	IN718	Fiber Reinf. Metal Matrix/ Intermetallic	48	12
Configuration	Ti-6-4/IN718	Ti-6-4/IN718	69	69
Acces./Remote APU	---	---	51	51
Bearings and Seals	M50NiL	M50NiL	42	42
C&A	---	---	126	126
		Sub Total	1139	901
		Margin	111	90
			1250	991

C-2

Table XXIX. Advanced UDF Weights (Concluded).

UDF Propulsor

Component	Material		Weight	
	1984	2010	1984	2010
Front Fan	Composite/IN718	Composite/Intermetallic	400	350
Aft Fan	Composite/IN718	Composite/Intermetallic	326	260
Front Turbine	U500/IN718	Intermetallic/U500/IN718	456	459
Aft Turbine	U500/IN718	Intermetallic/U500/IN718	586	568
Front Frame	René 41/HS 188	Nonmetallic Composite/ Intermetallic	313	240
Turbine Frame	IN718	---	233	179
Bearings and Seals	M50NiL	M50NiL	166	166
Turbine Stator	Hast X	Intermetallic	52	37
C&A	---	---	57	57
		Propulsor Totals	2589	2316
		Margin 10%	261	233
		Gas Generator	1250	991
		Total UDF	4100	3540

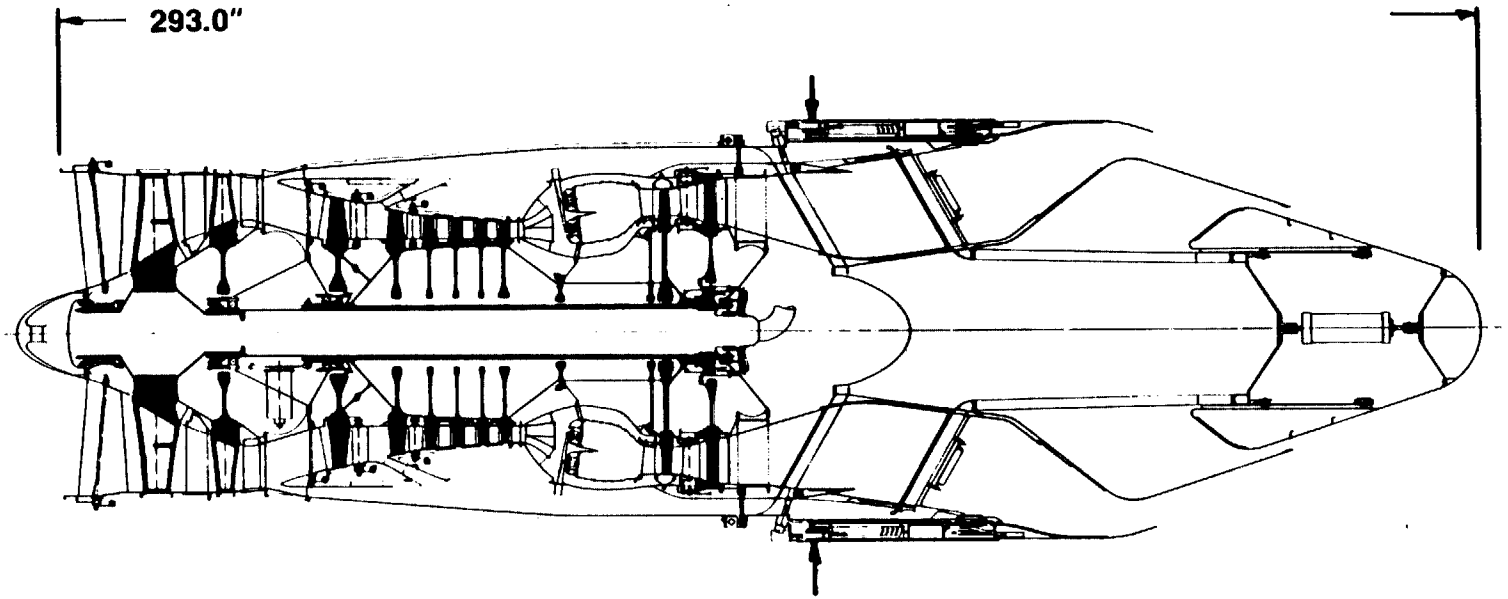

Figure 35. 1984 AST Baseline.

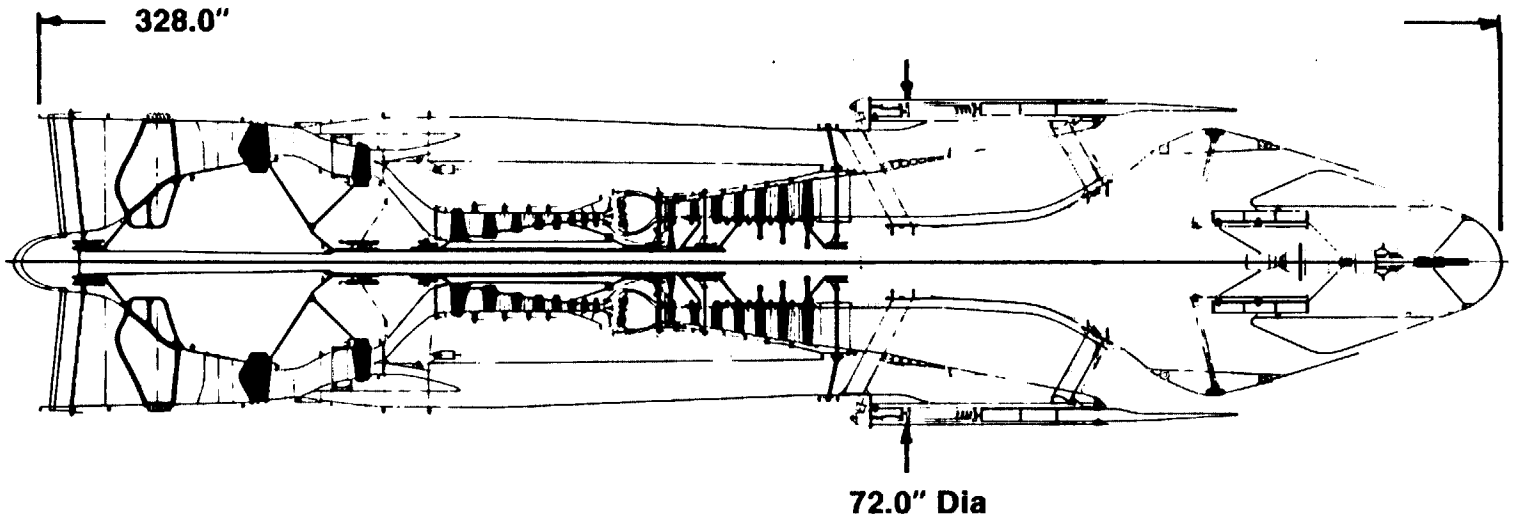

F_N = 47,500 lb

Weight 7830 lb

Figure 36. Advanced AST.

ADVANCED

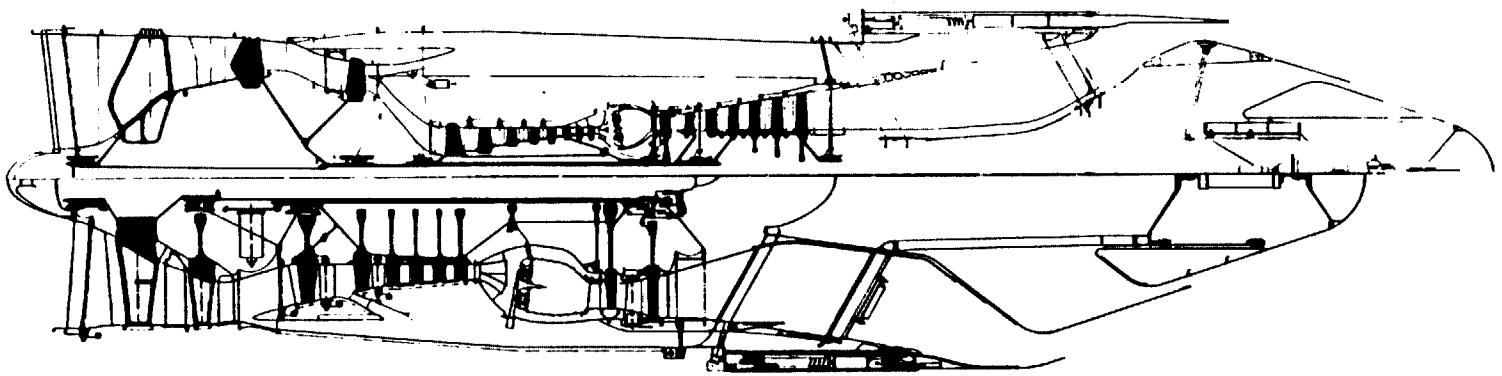

1984 BASELINE

Δ Length - 35.0"

Δ Max Dia - 14.01"

Δ Weight - 6090 lb

Figure 37. Advanced Versus Baseline AST Comparison.

2.22 AST STATIC STRUCTURAL COMPONENTS

Compression system static structural components are similar for both engines, each having conventional front and fan frame configurations. The baseline engine has a 17-strut front frame, with inlet guide vanes similar in design and configuration to the conventional metallic subsonic engine front frame. The advanced AST engine front frame is of stiff, lightweight fiber-reinforced metal matrix. Both frame designs have 1×10^6 lb/in radial spring constants and are deflection and not stress limited.

The fan frames for the baseline and advanced AST engines are similar in design philosophy. Both frames provided a major engine mount station, support low and high pressure rotor bearings, and provide a smooth flowpath transition between the low and high pressure compression systems.

Static structural components, with the exception of pressure vessels, are generally designed for deflection or stiffness limitations and are generally associated with material modulus/density (E/ρ) term for lowest weight. Pressure vessels, such as casings, are designed for hoop or tensile stress and biaxial bending loads. Materials whose combinations of σ/ρ and E/ρ yield the best optimum design values are selected for specific components.

The baseline engine turbine frame supporting the turbine differential bearing is a conventional metallic design having a René 41 eight-strut bearing support structure and HS188 flowpath heat shields. On the advanced AST engine, the conventional bearing support structure is replaced with 16 slender rods supporting the LP bearing, and the HS188 flowpath heat shields are replaced by a carbon-carbon aerodynamic flowpath transition. The intermetallic rods are rigidly attached to the outer casing, and the No. 6 ball bearing housing and turbine frame withstand flowpath transition axial aerodynamic loads.

A similar rod structure provides radial support to the high pressure rotor No. 4 and No. 5 ball bearings located forward of the high and low pressure turbine rotor assemblies. Thirty-two rods rigidly attached to the turbine casing, and passing radially through the HP turbine vanes, are bolted to the bearing housing and withstand bearing radial loads. Bearing axial loads are resisted by the combustor diffuser structure which is connected to

the bearing housing by the combustor inner casing. Rod frames have radial spring constants equivalent to heavy conventional frame structures, but only about 1/10th the weight.

2.23 AST COMBUSTOR

Table XXX lists the combustor aerodynamic parameters for AST baseline and advanced engines. The baseline engine has a double-dome combustor similar in aerodynamic design to the baseline subsonic combustor. The advanced AST engine is a short double-dome combustor having an airblast type fuel system with uncooled nonmetallic (carbon-carbon) liner and swirl cups. This design will have the same design limitations as those for advanced subsonic engine combustors.

Table XXX. AST Combustor Aerodynamic Parameters.

Type	Baseline Double Dome	Advanced Double Dome
Dome Height (outer/inner), inches	5.5/5.5	4.0/4.0
Dome Length, inches	12.8	8.0
Dome Velocity (outer/inner), fps	27/55	28/56
Dome Flow, % of W_{36}	33.3	60.8
Space Rate, Btu/(hr-Atm-ft^3) x 10^{-6}	4.21	9.6
T4, ° F	2793	4166
(T4 - T3), ° F	1502	2427

2.24 AST BEARINGS, SUMPS, SEALS, AND LP SHAFTS

Table XXXI lists parameters related to the baseline and advanced AST engine sump and LP shaft systems. Baseline and advanced AST engine sump and LP shaft systems are similar in design to the subsonic engine sump system.

Table XXXI. AST Bearings, Seals, and LP Shaft.

Bearing	Baseline			Advanced		
	N, rpm	DN x 10^{-6}	Type	N, rpm	DN x 10^{-6}	Type
1	5060	1.20	Roller	6237	1.08	Roller
2	5060	1.21	Ball	6237	0.95	Ball
3	6372	1.81	Ball	17020	3.0	Ball
4	6372	0.014 (Corotation)	Roller	17020	3.0	Roller
5	5060	1.36	Roller	6237	0.95	Roller
6	---	---		6237	1.05	Ball

	Baseline LP Shaft	Advanced LP Shaft
Length, in.	100.2	76.4
Diameter, in.	9.25	4.56
σ/σ Allow	0.64	0.89
N/N_{Cr}	1.80	2.30

2.25 AST ROTATING COMPONENTS

Table XXXII lists the structural and material changes and advanced material temperature environments for the baseline and advanced engines. Tables XXXIII and XXXIV list the material operating stress parameters for these components.

The baseline AST engine illustrated in Figure 36 has a conventional two-stage, dovetailed LP compressor rotor having Stage 1 blade midspan dampers to control blade aeroelastic vibrations, a conventional six-stage dovetailed HP compressor rotor and an air-cooled, conventional, single-stage HP and LP bladed turbine. Rotor design philosophies, as described in "Subsonic Engine Rotating Components," apply to AST baseline and advanced rotors, respectively.

Figure 36 illustrates the rotor system for the advanced AST engine. LP rotor, supported by four bearings, has a three-stage fiber-reinforced metal matrix blisk fan attached to a six-stage nonmetallic blade and intermetallic

Table XXXII. AST Structural Component Changes.

Baseline Component	Advanced Component (Temperature)
Front Frame	(500° F)
No Configuration Change	
17-4PH	Fiber Reinforced Metal Matrix
Fan Rotor	(830° F)
Bladed Rotors	Swept Blade Blisks
Ti-6-2-4-2	Fiber Reinforced Metal Matrix
Core Drive	Fan Drive
Fan Stator	(830° F)
Material Change	
Ti-6-2-4-2	Fiber Reinforced Metal Matrix
Fan Frame	(830° F)
Integral Vane/Frame Structure	
IN718	Fiber Reinforced Metal Matrix
HPC Rotor	(1680° F)
IN718/René 95	Fiber Reinforced Metal Matrix/Intermetallic
Dovetailed Rotors vs. Blisks, Curvics and Tiebolts	
HPC Stator	(1680° F)
IN718	Fiber Reinforced Metal Matrix/Intermetallic
Diffuser and Casing	(1700° F)
IN718	Fiber Reinforced Metal Matrix/Intermetallic
Combustor	(4100° F)
HS188	Nonmetallic Composite
HPT Stator	(4100° F)
MA754/509	Nonmetallic Composite
Vaned	Vanes Integral with Combustor Bearing Support Rods in Vanes
HPT Rotor	(4100° F)
N4/René 95	Nonmetallic Composite/Intermetallic

Table XXXII. AST Structural Component Changes (Concluded).

Baseline Component	Advanced Component (Temperature)
LPT Stator	(3500° F)
N4/IN718	Nonmetallic Composite/Intermetallic
Single Stage	6 Stage
LPT Rotor	(3500° F)
N4/René 95	Nonmetallic Composite/Intermetallic
LPT Shaft	(1300° F)
IN718	Fiber-Reinforced Metal Matrix
Turbine Frame	(2800° F)
Conventional	Rod Frame
René 41/HS188	Nonmetallic Composite/Intermetallic
8 Struts	16 Rods
Duct	(800° F)
Ti-6-2-4-2	Fiber-Reinforced Metal Matrix/Advanced Titanium
Configuration	(500°-1000° F)
Ti/IN718	Adv. Titanium/Nonmetallic Composite
Bearings and Seals	(1500° F)
M50NiL	Ceramic
Wet Lube	Dry Lube, High Temperature
Accessories	(500° F)
G/B and PTO Shaft	Remote APU/Electrical Generator
Hydraulic Actuators	Air Turbine/Dry Geared
Augmentor and Exhaust Nozzle	(1800° F)
René 41/HS188	Nonmetallic Composite/Intermetallic
Augmentor	No Augmentor
Shorter, Large Diameter Nozzle	Longer, Smaller Diameter Nozzle
C&A	(500° F - 1000° F)
Conventional (Oil Pumps, FADEC Hydraulics)	Integrated Components Lightweight, Nonhydrocarbon Lube & Actuator Systems

Table XXXIII. AST LP Compressor Rotor Stresses.

Disk	Baseline σ/σ Allow Blades	No. Blades	Stage	Disk	Advanced σ/σ Allow Blades	No. Blades
1.0	0.86	26	1	1.0	0.83	18
0.86	0.68	54	2	1.0	0.40	40
---	---	---	3	1.0	0.3	62

Table XXXIV. AST HP Compressor Rotor Stresses.

Disk	Baseline σ/σ Allow Blades	No. Blades	Stage	Disk	Advanced σ/σ Allow Blades	No. Blades
1.0	0.89	40	1	1.0	0.64	20
1.0	0.58	38	2	1.0	0.59	20
1.0	0.57	52	3	1.0	0.53	28
1.0	0.52	58	4	1.0	0.52	36
1.0	0.59	62	5	1.0	0.65	44
1.0	0.56	60	6	1.0	0.68	52
---	---	---	7	1.0	0.98	52
---	---	---	8	1.0	0.96	54

rotor LP turbine by a fiber-reinforced metal matrix LP shaft. Strutted fiber-reinforced metal matrix front and fan frames and LP turbine front and rear intermetallic rod frames provide support for the LP rotor system. The HP rotor system is an eight-stage, fiber-reinforced metal matrix intermetallic blisk rotor attached to a single-stage, bladed turbine rotor having uncooled nonmetallic composite blades (carbon-carbon) and an intermetallic disk. The strutted fan frame and HP turbine rod frame support the HP turbine rotor.

The materials and mechanical design of the advanced AST engine rotors are similar in design principles and temperature to the subsonic engine gas generator rotor.

2.26 AST ENGINE COMPONENT WEIGHTS

Table XXXV lists the baseline and advanced AST engine component weights and weight changes resulting from direct material improvements, and improved thermodynamic cycles resulting from improved materials.

2.27 AST EXHAUST SYSTEM

The AST exhaust system consists of a translating shroud thrust reverser and a nozzle configuration that provides coannular flow at takeoff to yield a moderate amount of noise suppression. The coannular flow is effected by ducting most of the cooler bypass air through struts to the inside of the plug and exhausting it through a variable area slot about halfway down the plug while the hotter core flow is ducted between struts and exhausted near the plug crown. At other flight conditions where noise suppression is not required, most of the bypass air is mixed with the core flow through mixer doors located between struts, and the mixed flow is discharged near the plug crown.

This engine does not use an augmentor in the exhaust system, so that compared to augmented exhaust systems, the temperatures in this exhaust system are much lower and the performance documents associated with unburned cooling air are not encountered. Therefore, the major advantages of advanced materials over current materials involve the higher stiffness-to-density and strength-to-density properties of the advanced materials, and use of the low density advanced materials in areas where minimum thickness requirements for manufacturing or for avoidance of high panel type vibration stresses precludes the maximum utilization of the stiffness-to-density or strength-to-density properties of current materials.

The materials employed to effect these advantages are nonmetallic composites for liners in the core stream and for the mixer doors, advanced titanium in the cooler portions of the aft plug, and intermetallics for the

Table XXXV. AST Component Materials and Weights.

	Material		Weight	
	1984	2010	1984	2010
Front Frame	17-4PH	Fiber Reinf. Metal Matrix	425	220
Fan Rotor	Ti6-2-4-2	Fiber Reinf. Metal Matrix	1041	760
Fan Stator	Ti6-2-4-2	Fiber Reinf. Metal Matrix	718	370
Fan Frame	Ti6-2-4-2	Fiber Reinf. Metal Matrix	385	565
HPC Rotor	IN718/René 95	Fiber Reinf. Metal Matrix/ Intermetallic	722	240
HPC Stator	IN718	Intermetallic	633	183
Diffuser & Case	IN718	Fiber Reinf. Metal Matrix/ Intermetallic	481	123
Combustor	HS188	Nonmetallic Composite	356	80
HPT Stator	MA754/509	Nonmetallic Composite	420	50
HPT Rotor	N4/René 95	Nonmetallic Composite/ Intermetallic	531	68
LPT Stator	N4/IN718	Nonmetallic Composite/ Intermetallic	466	273
LPT Rotor	N4/René 95	Nonmetallic Composite/ Intermetallic	570	325
LPT Shaft	IN718	Fiber Reinf. Metal Matrix	195	98
Duct	Ti-6-2-4-2	Fiber Reinf. Metal Matrix	207	164
Configuration	Ti/IN718	Advanced Titanium	170	130
Bearings & Seals	M50NiL	Ceramic	210	156
Access/Remote APU	---	---	195	80
Augmentor and Exhaust Nozzle	René 41/HS188	Nonmetallic Composite/ Intermetallic	3495	2615
C&A	---	---	1016	515
Subtotal			12656	7117
~10% Margin			1264	713
Totals			13920	7830

major structures which include the struts, plug, outer shroud, and thrust reverser cascades.

2.28 MATERIAL RECOMMENDATIONS

The Revolutionary Opportunities for Materials and Structures study conducted by General Electric clearly shows two materials needed for future advanced engine design and development:

- 4000° F nonmetallic composite
- 1800+° F fiber-reinforced metal matrix composite.

These materials are essential for future engines. The 4000° F nonmetallic composites (such as carbon-carbon) are planned for future high performance engines having near stoichiometric or stoichiometric engine uncooled combustors, turbine vanes, blades, and exhaust nozzles. The 1800° F fiber-reinforced metal matrix will be required for advanced engine, high pressure compressor components; combustor outer and inner casings; and turbine casings.

3.0 TASK III - PROPULSION EVALUATION AND TECHNOLOGY RANKING

3.1 FUEL BURN AND DOC SENSITIVITIES

The ROMS study objectives were to show improvement in fuel burn and DOC between the baseline and 2010 technology readiness engines due primarily to advancements in materials and the use of these materials in unique structures. These fuel burn and DOC improvements expressed as a percentage for both the supersonic and subsonic aircraft were as follows:

	Percent Improvement	
	Fuel Burn	DOC
Supersonic (Maximum Passengers at 5000 nmi)	15	5
Subsonic (Maximum Passengers at 500 nmi)	15	7

The DOC measurements were based on a 0% and a 3% interest rate, and fuel cost of $1.00 to $2.50 per U.S. gallon in $0.50 increments.

To screen and assess propulsion technology and material ranking versus these fuel burn and DOC objectives, supersonic and subsonic fuel burn and DOC rubber sensitivities were calculated for the approved baseline configurations. The calculated sensitivities covered changes in propulsion system weight, nacelle drag due to changes in engine diameter, and improvements in sfc.

3.1.1 Subsonic Sensitivities

The weight, drag, and sfc sensitivities for the subsonic aircraft were calculated using General Electric's Commercial Aircraft Mission Analysis software program "CAMAL". CAMAL has the capability to rubberize a weight and aerodynamic aircraft model to specific requirements. CAMAL's rubber mode takes the baseline engine/airframe configuration, resizes the engine/aircraft (except fuselage),and evaluates the fuel burn for perturbations in sfc (climb, cruise, and overall mission), engine weight, and nacelle drag. The fuselage dimensions, wing loading, thrust-to-weight, and tail volume coefficients were held constant while dimensions and weights associated with the engine, wing, horizontal tail, and vertical tail were scaled to meet mission requirements such as TOFL or top of climb ROC.

The flowchart in Figure 38 shows the process used in rubberizing the 1984 baseline subsonic aircraft and calculating the fuel burn sensitivities for the referee 500 nmi mission. Tables XXXVI though XXXVIII show the fuel burn sensitivities for perturbations in the baseline sfc, engine weight, and nacelle drag. Figure 39 shows a pie chart representation of the baseline DOC, Tables XXXIX through XLI show the corresponding DOC sensitivities, and Figures 40 and 41 show carpet plots for the sfc and engine weight sensitivities.

3.1.2 Supersonic Sensitivities

The supersonic model as described in Task I was based on NASA LaRC's model of AST 205-1. For expedience, the AST 205-1 model and NASA LaRC's aircraft analysis software Aircraft Synthesis Program (ASP) were used to incorporate the OEW weight reductions, the increase in range to 5000 nmi, and to calculate the rubber fuel burn sensitivities. The flowchart of this process is shown in Figure 42. The rubber fuel burn sensitivities for -5%, -10%, -15%, and -20% climb, cruise, and overall delta sfc; and +10%, -10%, -15%, and -20% variations on propulsion weight and engine diameter were calculated. The results are shown in Tables XLII through XLIV.

The DOC sensitivities for the supersonic aircraft were calculated in the same manner as those for the subsonic application. The resultant values are shown in Tables XLV through XLVII. Carpet plots of the sfc and engine weight sensitivities are shown in Figures 43 and 44. A pie chart showing the contribution of each element of DOC for the baseline 5000 nmi supersonic mission is shown in Figure 45 for 0% interest.

3.2 PAYOFFS

Both subsonic and supersonic payoffs were measured against fuel burn and DOC goals. These goals were defined as shown on Table XLVIII. The DOC analysis was based on $1.00, $1.50, and $2.00 per gallon fuel prices. The DOC analysis was also performed for 0% and 3% interest. Performance against goals was determined by $1.50 per gallon fuel price and 0% interest.

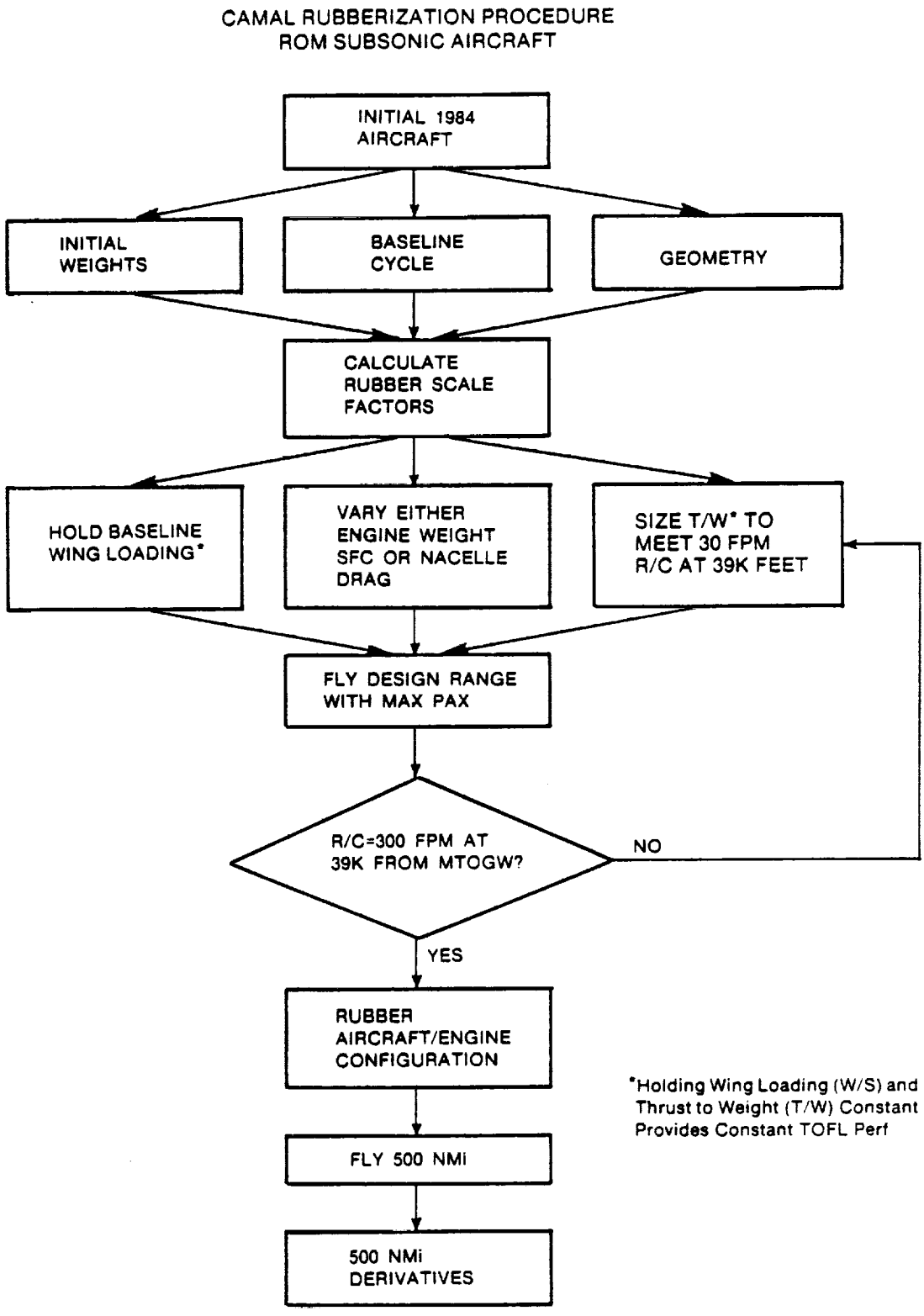

Figure 38. Subsonic Rubberization Flow Chart.

Table XXXVI. Subsonic Fuel Burn Sensitivities - Δ SFC.

ENGINE: NASA ROMS STUDY, 1984 UDF BASELINE

RUBBER FUEL BURN DERIVATIVES (PERCENTAGE) FOR 500 NM RANGE

OVERALL SFC IMPROVEMENTS

A/C AND ENGINE BASELINE SCALED DOWN FROM INITIAL INPUT BARE ENGINE WT OF 4100 LBS, SLS THRUST=22980 LBS USING DESIGN RANGE=1700 NM, WING LOADING=105.33 LB/SQ.FT. AND A T/W TO OBTAIN R/C OF APPROX 300 FPM @ 35K' ALT.

ITEM	BASELINE FUEL BURN (LBS)	-5% SFC	-10% SFC	-15% SFC	-20% SFC
CLIMB	2363	-5.29	-10.50	-15.70	-20.86
CRUISE	1758	-5.67	-11.27	-16.79	-22.24
DESCENT	294	-5.44	-10.88	-16.33	-21.77
BLOCK FUEL	4808	-5.43	-10.82	-16.18	-21.44
ENGINE SCALE FACTOR	.881	.876	.871	.866	.862
T/W	.311608	.312750	.313940	.315100	.316300
BARE ENGINE WEIGHT (LBS)	3552.6	3530.3	3508.7	3486.2	3465.8

NOTE: WS=105.33 LB/SQ.FT. WAS HELD CONSTANT DURING RUBBERIZATION PROCESS. T/W WAS VARIED TO OBTAIN R/C OF APPROX 300 FPM @ 35K' ALT FOR DESIGN RANGE OF 1700 NM FOR EACH CASE.

Table XXXVII. Subsonic Fuel Burn Sensitivities - Δ Propulsion Weight.

ENGINE: NASA ROMS STUDY, 1984 UDF BASELINE

RUBBER FUEL BURN DERIVATIVES (PERCENTAGE) FOR 500 NM RANGE

BARE ENGINE WEIGHT VARIATION (INITIAL INPUT WT=4100 LBS, SLS THRUST=22980 LBS)

A/C AND ENGINE BASELINE SIZED AT DESIGN RANGE OF 1700 NM, WING LOADING OF 105.33 LB/SQ.FT. AND A T/W TO OBTAIN R/C OF APPROX 300 FPM @ 39K' ALT.

ITEM	BASELINE FUEL BURN (LBS)	INPUT WEIGHT VARIATION +10% WT	-10% WT	-15% WT	-20% WT
CLIMB	2363	1.06	-0.93	-1.40	-1.86
CRUISE	1358	0.22	-0.37	-0.52	-0.74
DESCENT	294	1.36	-1.02	-1.70	-2.04
BLOCK FUEL	4808	0.79	-0.77	-1.14	-1.50
ENGINE SCALE FACTOR	.881	.887	.874	.871	.868
T/W	.311603	.310500	.312500	.312950	.313400
BARE ENGINE WEIGHT (LBS)	3552.6	3940.7	3169.2	2980.4	2793.5

NOTE: WS=105.33 LB/SQ.FT. WAS HELD CONSTANT DURING RUBBERIZATION PROCESS. T/W WAS VARIED TO OBTAIN R/C OF APPROX 300 FPM @ 39K' ALT FOR DESIGN RANGE OF 1700 NM FOR EACH CASE.

Table XXXVIII. Subsonic Fuel Burn Sensitivities - Δ Engine Diameter.

Engine: NASA ROMS Study, 1984 UDF Baseline

Rubber Fuel Burn Derivatives (Percentage) for 500 nmi Range

Nacelle Drag Variation

A/C and engine baseline scaled down from initial input bare engine weight of 4100 lb, SLS Thrust = 22980 lb using design range + 1700 nmi, Wing Loading = 105.33 lb/ft^2 T/W to obtain R/O of approximately 300 fpm at 39,000 ft Alt.

Item	Baseline Fuel Burn (lb)	Input Weight Variation				
		+10% Drag	-5% Drag	-10% Drag	-15% Drag	-20% Drag
Climb	2363	0.21	-0.04	-0.17	-0.25	-0.34
Cruise	1358	0.52	-0.37	-0.59	-0.88	-1.18
Descent	94	0.00	0.00	0.00	0.00	0.00
Block Fuel	4808	0.29	-0.17	-0.31	-0.46	-0.60
Engine Scale Factor	0.881	0.883	0.879	0.878	0.877	0.876
T/W	0.311608	0.312150	0.311200	0.310900	0.310600	0.310280
Bare Engine Weight (lb)	3552.6	3563.0	3545.4	3539.8	3534.2	3528.3

Note: W/S - 105.33 lb/ft^2 was held constant during rubberization process. T/W was varied to obtain R/C of approximately 300 fpm at 39,000 ft Alt for Design Range of 1700 nmi for each case.

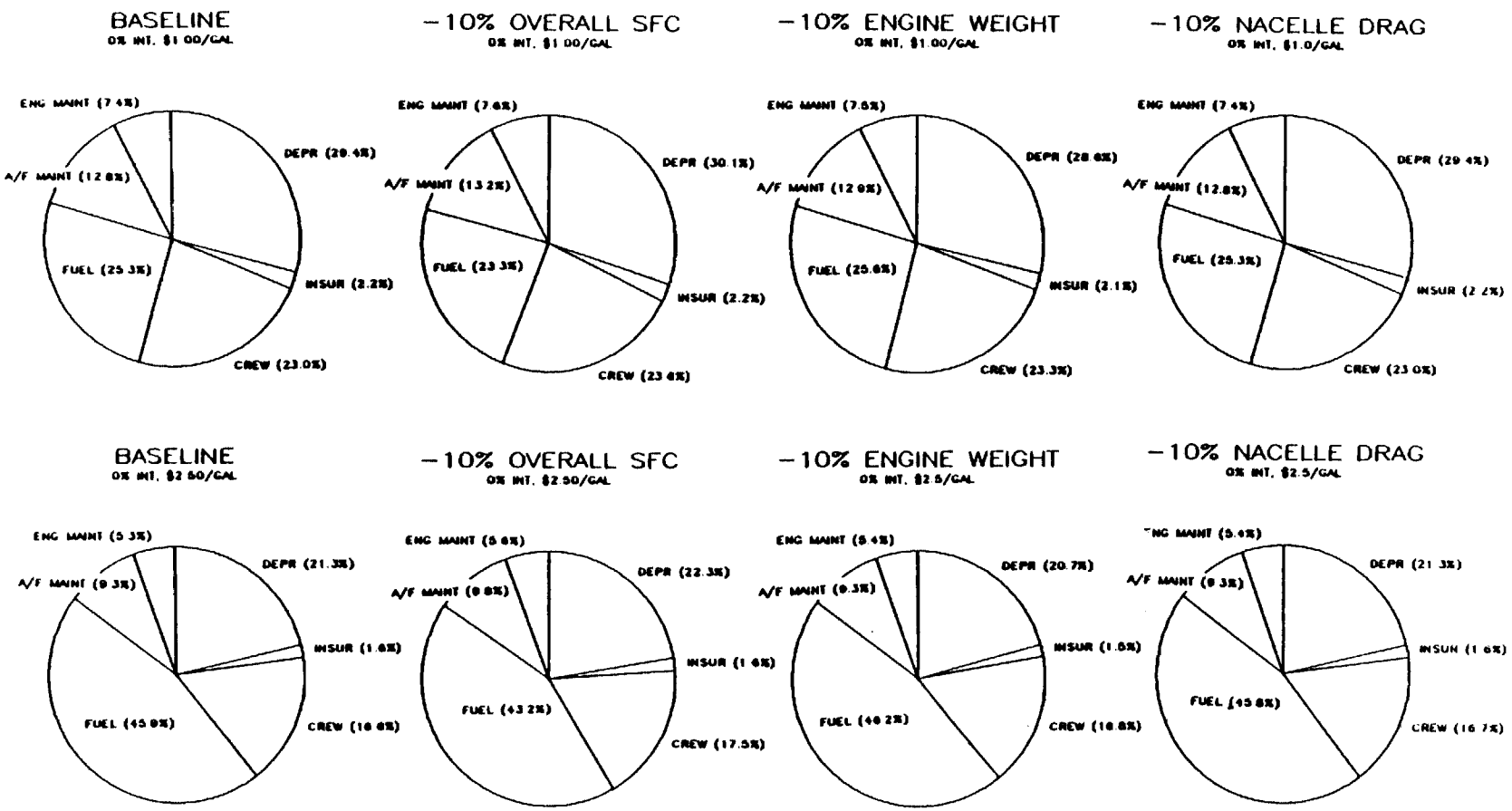

Figure 39. Subsonic DOC Pie Charts.

Table XXXIX. Subsonic DOC Sensitivities - Δ SFC.

0% Interest DOC/DOC-Baseline for Δ Overall SFC

	Fuel Price $/Gal			
Δ% Overall SFC	$1.00	$1.50	$2.00	$2.50
-5%	0.984	0.980	0.976	0.973
-10%	0.968	0.960	0.953	0.947
-15%	0.952	0.939	0.929	0.921
-20%	0.936	0.919	0.906	0.895

3% Interest DOC/DOC-Baseline for Δ Overall SFC

	Fuel Price $/Gal			
Δ% Overall SFC	$1.00	$1.50	$2.00	$2.50
-5%	0.985	0.981	0.977	0.975
-10%	0.970	0.961	0.955	0.949
-15%	0.955	0.942	0.932	0.924
-20%	0.940	0.924	0.910	0.900

Table XL. Subsonic DOC Sensitivities - Δ Propulsion Weight.

0% Interest DOC/DOC-Baseline for Δ Engine Weights

	Fuel Price $/Gal			
Δ% Overall Wt	$1.00	$1.50	$2.00	$2.50
+10%	1.018	1.017	1.016	0.105
-10%	0.983	0.984	0.985	0.986
-15%	0.975	0.976	0.977	0.978
-20%	0.967	0.969	0.970	0.972

3% Interest DOC/DOC-Baseline for Δ Engine Weights

	Fuel Price $/Gal			
Δ% Overall Wt	$1.00	$1.50	$2.00	$2.50
+10%	1.019	1.018	1.017	1.016
-10%	0.981	0.982	0.983	0.984
-15%	0.972	0.974	0.975	0.976
-20%	0.963	0.966	0.967	0.969

Table XLI. Subsonic DOC sensitivities - Δ Engine Diameter.

0% Interest DOC/DOC-Baseline for Δ Nacelle Drag

Δ% Nacelle Drag	Fuel Price $/Gal			
	$1.00	$1.50	$2.00	$2.50
+10%	1.001	1.001	1.002	1.002
-10%	0.999	0.998	0.998	0.998
-15%	0.998	0.998	0.997	0.997

3% Interest DOC/DOC-Baseline for Δ Nacelle Drag

Δ% Nacelle Drag	Fuel Price $/Gal			
	$1.00	$1.50	$2.00	$2.50
+10%	1.001	1.001	1.002	1.002
-10%	0.999	0.998	0.998	0.998
-15%	0.998	0.998	0.997	0.997

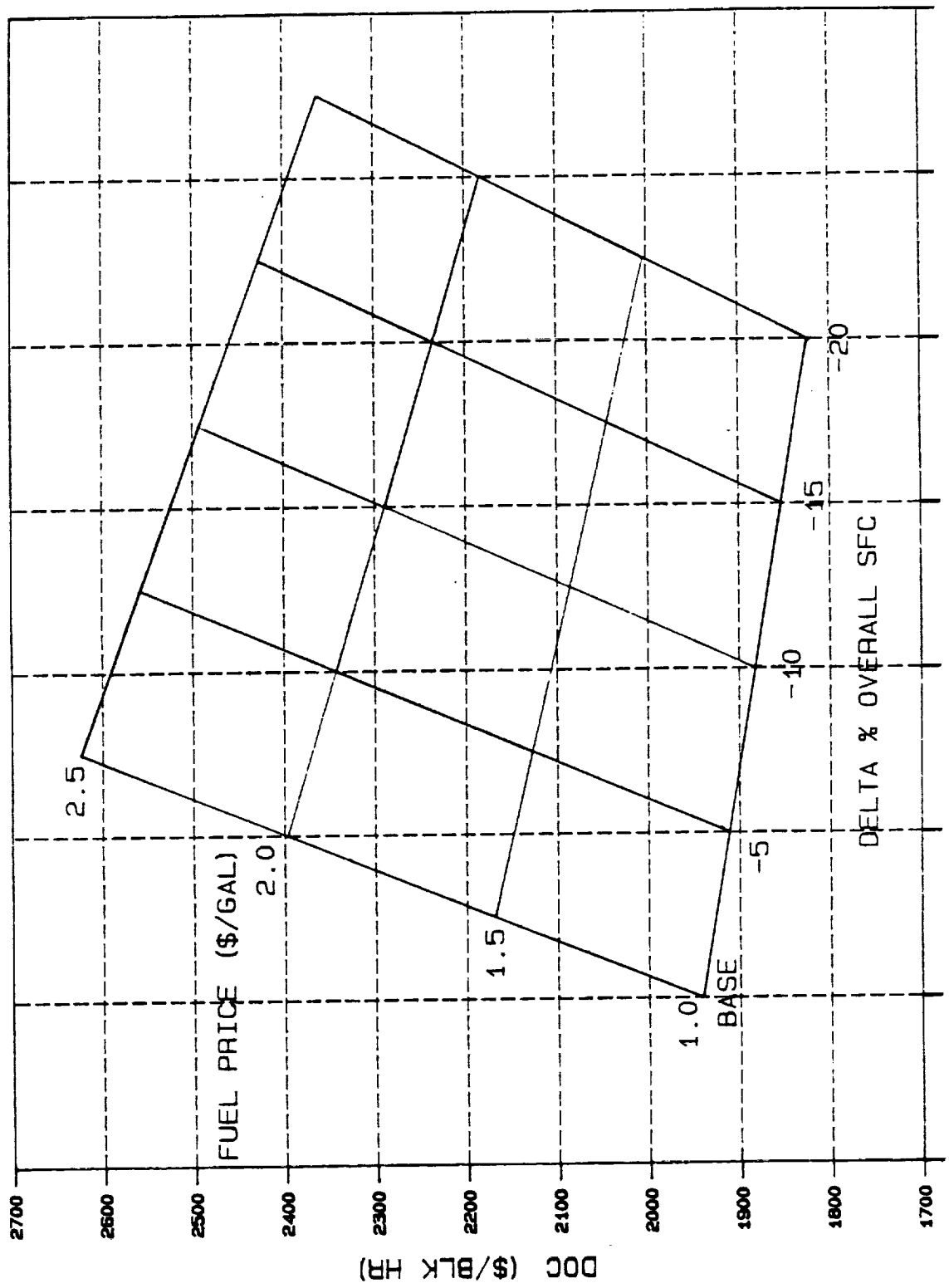

Figure 40. Subsonic Aircraft DOC Sensitivity to SFC.

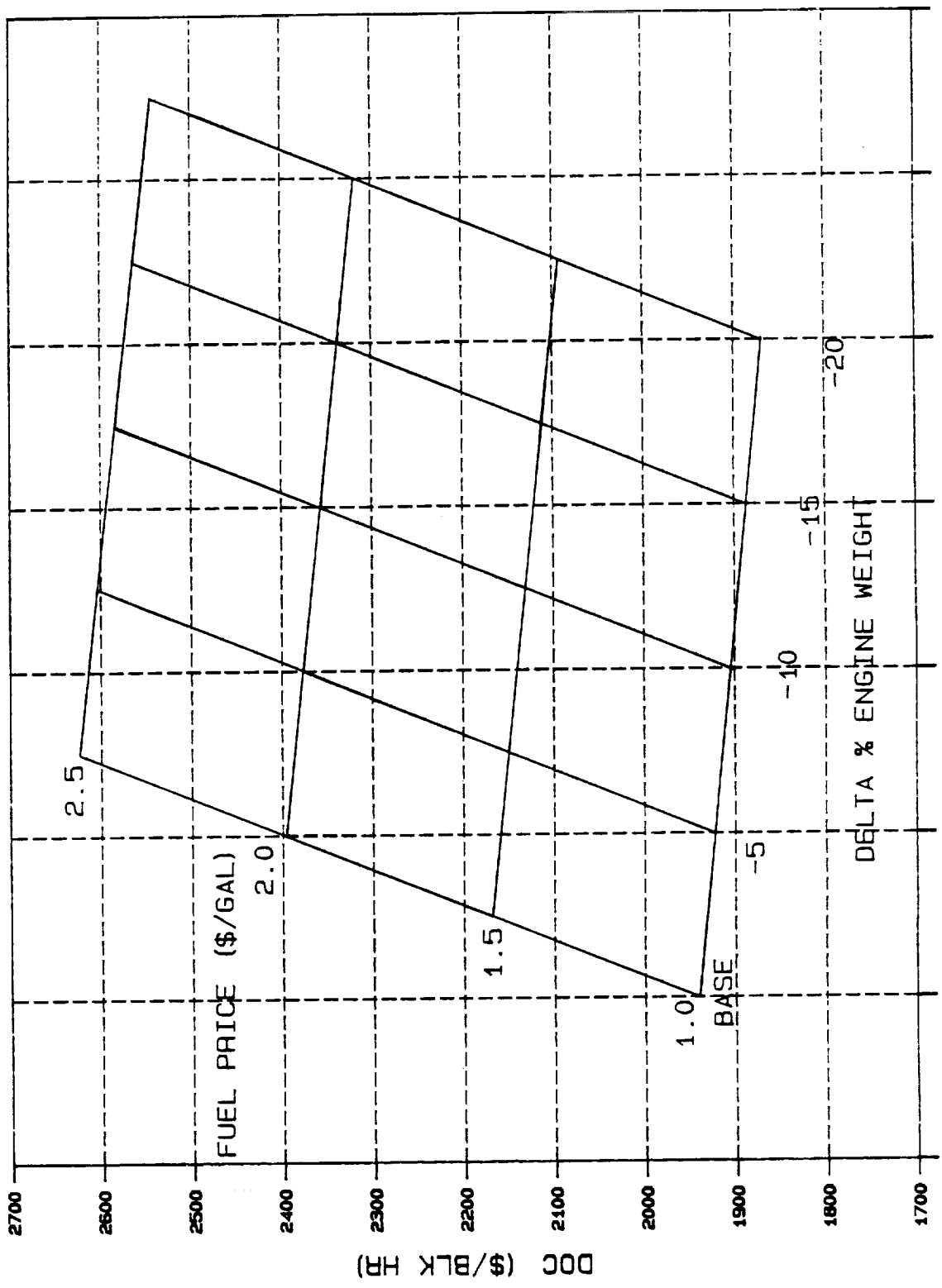

Figure 41. Subsonic Aircraft DOC Sensitivity to Engine Weight.

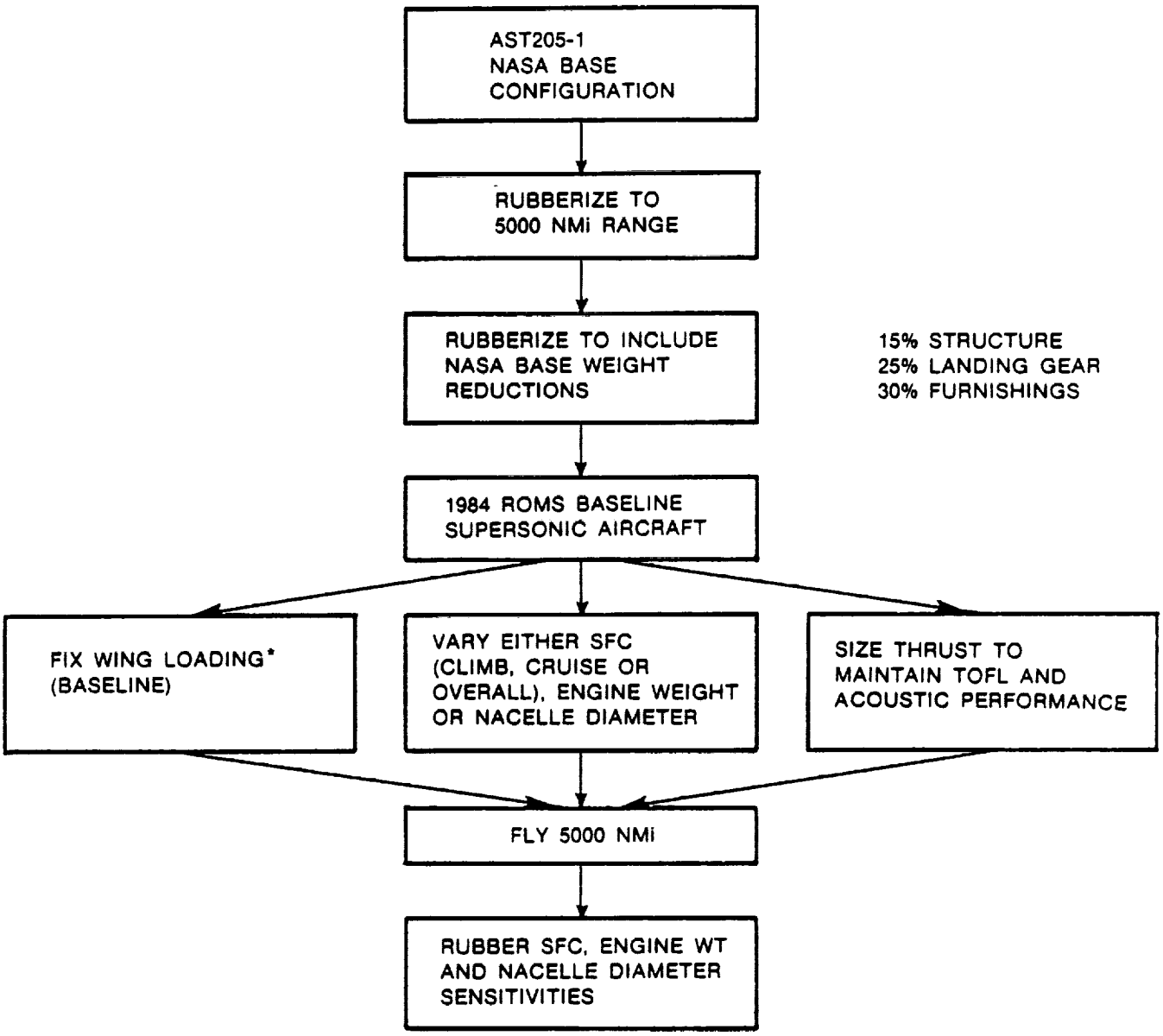

*Maintaining the Baseline Wing Loading (W/S) and Thrust to Weight (T/W) Maintains the Same Approximate TOFL and Acoustic Performance for Rubber Aircraft.

Figure 42. Supersonic Rubberization Flow Chart.

Table XLII. Supersonic Fuel Burn Sensitivities - Δ SFC.

AST - 205 - 1 (ROMS Baseline Model)
Engine: GE21/J11-B14a (Scaled to 45,107 lb Thrust SLS)
Rubber Fuel Burn Derivatives (Percentage)
Overall SFC Improvements
Baseline Scaled to 5000 nmi Range with Fixed Weight Reductions

Item	Baseline Fuel Burn (lb)	-5% SFC	-10% SFC	-15% SFC	-20% SFC
Climb	58646.755	-9.2	-17.7	-25.7	-32.5
Cruise	196999.325	-8.8	-16.7	-24.1	-31.0
Descent	3647.562	-11.9	-22.4	-32	-40.5
Block Fuel	264616.76	-9	-17.1	-24.7	-31.6
Engine Size Scale Factor		0.935	0.876	0.821	0.77

Table XLIII. Supersonic Fuel Burn Sensitivities - Δ Propulsion Weight.

AST - 205 - 1 (ROMS Baseline Model)
Engine: GE21/J11-B14a (Scaled to 45107 lb Thrust SLS)
Rubber Fuel Burn Derivatives (Percentage)
Engine Weight Variation (Baseline Wt = 10192.8 lb)
Baseline Scaled to 5000 nmi Range with Fixed Weight Reductions

Item	Baseline Fuel Burn (lb)	+10% SFC	-10% SFC	-15% SFC	-20% SFC
Climb	58646.755	1.8	-1.6	-2.4	-3.0
Cruise	196999.325	1.7	-1.7	-2.5	-3.4
Descent	3647.562	2.7	-2.6	-3.7	-4.9
Block Fuel	264616.76	1.7	-1.7	-2.5	-3.3
Engine Size Scale Factor		1.022	0.984	0.968	0.951

Table XLIV. Supersonic Fuel Burn Sensitivities - Δ Engine Diameter.

AST - 205 - 1 (ROMS Baseline Model)
Engine: GE21/J11-B14a (Scaled to 45107 lb Thrust SLS)
Rubber Fuel Burn Derivatives (Percentage)
Nacelle Diameter Variation (Baseline Average Inlet Dia. = 5.307 ft)
Baseline Scaled to 5000 nmi Range with Fixed Weight Reductions

Item	Baseline Fuel Burn (lb)	+10% Dia	-10% Dia	-15% Dia
Climb	58646.755	1.7	-1.2	-1.8
Cruise	196999.325	1.2	-1.2	-1.8
Descent	3647.562	0.8	-0.7	-1.1
Block Fuel	264616.76	1.2	-1.2	-1.8
Engine Size Scale Factor		1.01	0.99	0.985

Table XLV. Supersonic DOC Sensitivities - Δ SFC.

0% Interest DOC/DOC-Baseline for Δ Overall SFC

Δ% Overall SFC	Fuel Price $/Gal			
	$1.00	$1.50	$2.00	$2.50
-5%	0.923	0.921	0.919	0.916
-10%	0.853	0.849	0.845	0.840
-15%	0.787	0.780	0.774	0.769
-20%	0.727	0.719	0.712	0.704

3% Interest DOC/DOC-Baseline for Δ Overall SFC

Δ% Overall SFC	Fuel Price $/Gal			
	$1.00	$1.50	$2.00	$2.50
-5%	0.923	0.923	0.921	0.917
-10%	0.854	0.849	0.846	0.841
-15%	0.789	0.783	0.778	0.770
-20%	0.729	0.720	0.711	0.705

Table XLVI. Supersonic DOC Sensitivities - Δ Propulsion Weight.

0% Interest DOC/DOC-Baseline for Δ Engine Weights

Δ% Overall Wt	Fuel Price $/Gal			
	$1.00	$1.50	$2.00	$2.50
+10%	1.019	1.019	1.019	0.018
-10%	0.981	0.981	0.982	0.982
-15%	0.972	0.973	0.973	0.973
-20%	0.963	0.963	0.964	0.965

3% Interest DOC/DOC-Baseline for Δ Engine Weights

Δ% Overall Wt	Fuel Price $/Gal			
	$1.00	$1.50	$2.00	$2.50
+10%	1.020	1.019	1.019	1.019
-10%	0.981	0.981	0.981	0.982
-15%	0.971	0.972	0.972	0.973
-20%	0.962	0.963	0.964	0.964

Table XLVII. Supersonic DOC Sensitivities - Δ Engine Diameter.

0% Interest DOC/DOC-Baseline for Δ Nacelle Drag

Δ% Nacelle Drag	Fuel Price $/Gal			
	$1.00	$1.50	$2.00	$2.50
+10%	1.011	1.011	1.011	1.012
-10%	0.989	0.989	0.989	0.988
-15%	0.984	0.983	0.983	0.983

3% Interest DOC/DOC-Baseline for Δ Nacelle Drag

Δ% Nacelle Drag	Fuel Price $/Gal			
	$1.00	$1.50	$2.00	$2.50
+10%	1.011	1.011	1.012	1.012
-10%	0.989	0.989	0.989	0.988
-15%	0.984	0.983	0.983	0.983

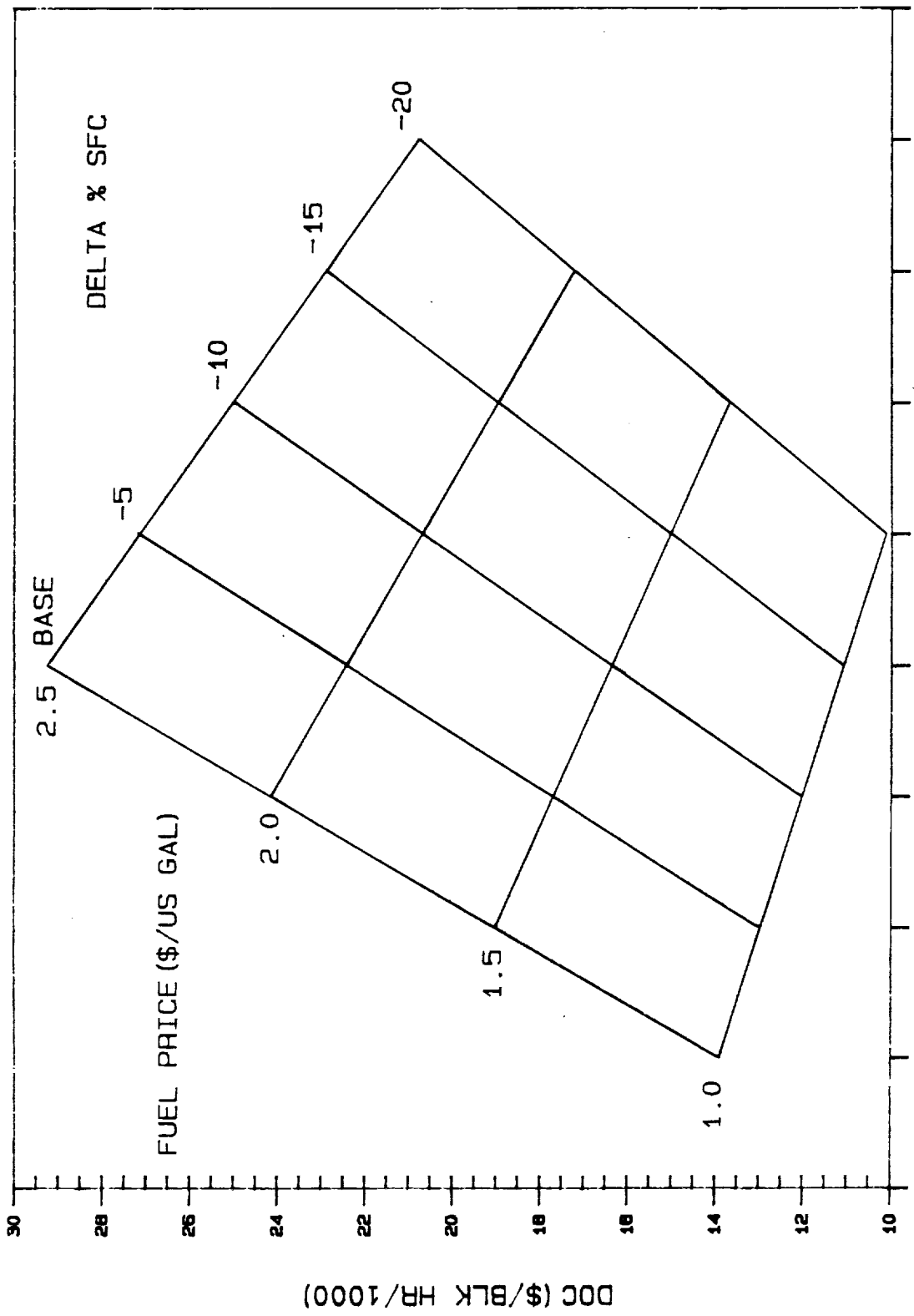

Figure 43. Supersonic Aircraft DOC Sensitivity to SFC.

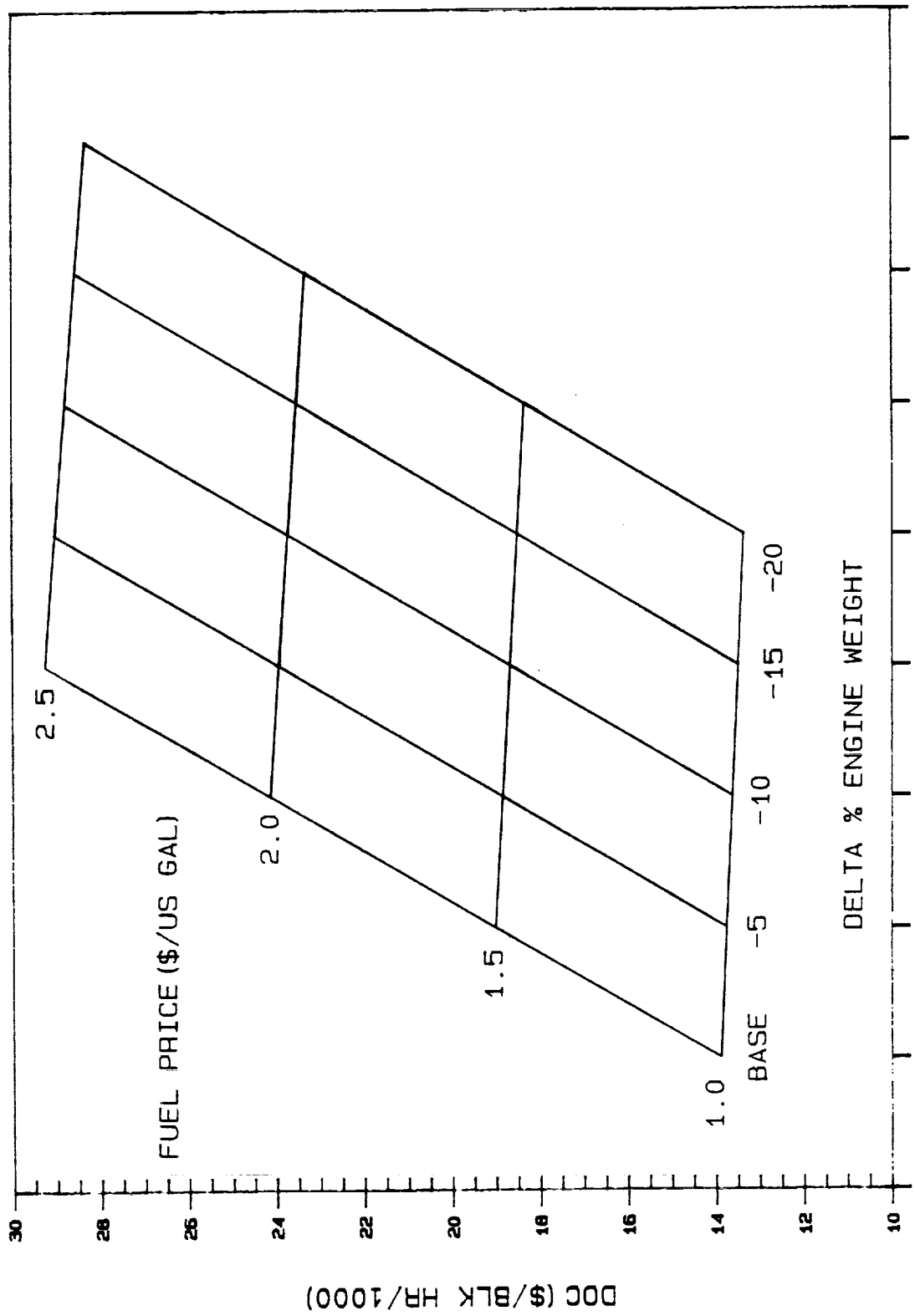

Figure 44. Supersonic Aircraft DOC Sensitivity to Engine Weight.

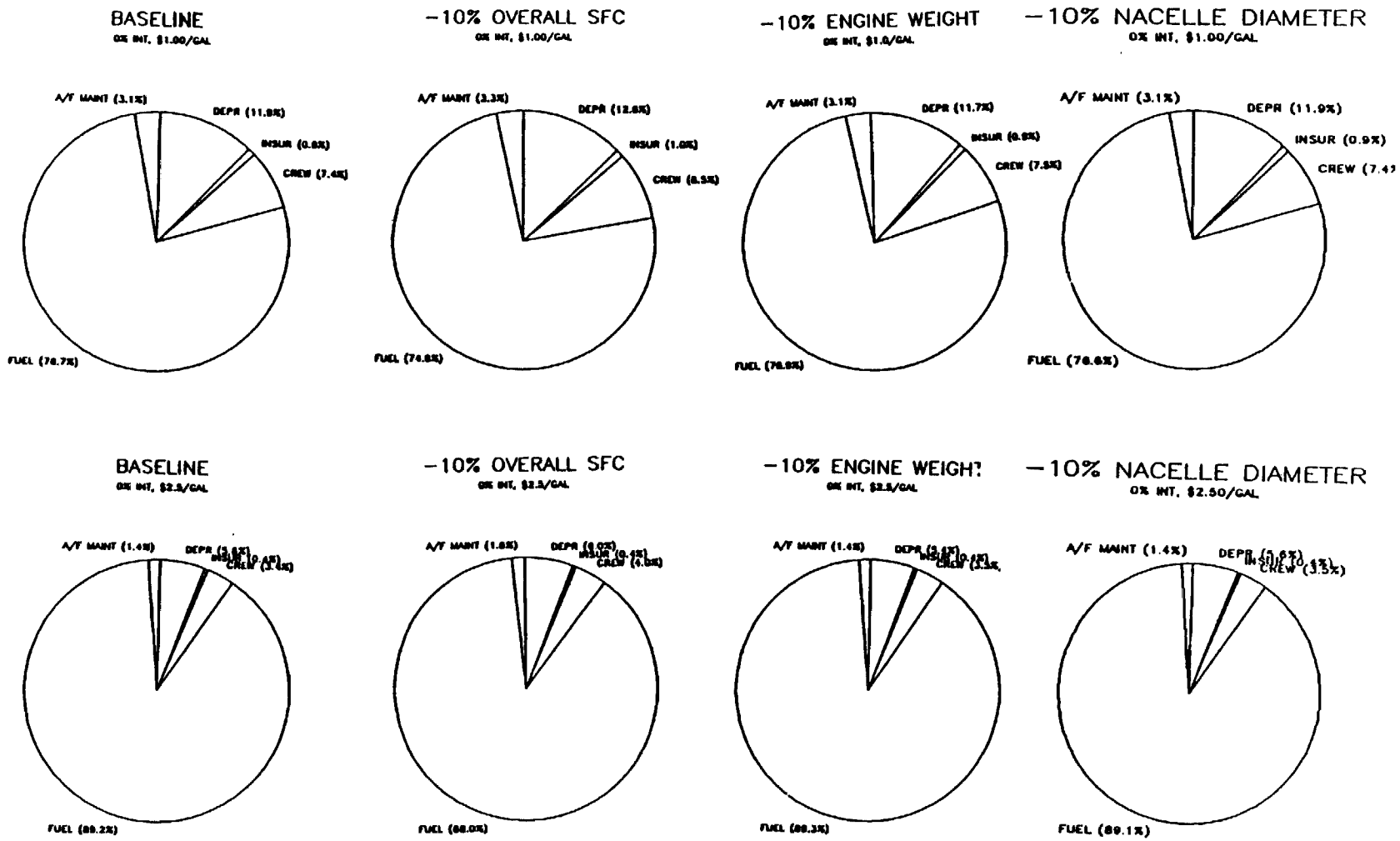

Figure 45. Supersonic DOC Pie Charts.

Table XLVIII. Engine Technology Improvement Targets.

• Year 1984	-	Technology Readiness Base
• Year 2010	-	Technology Improvements to Provide:
- Subsonic	-	15% Fuel Burn, -5% DOC[1]
- Supersonic	-	15% Fuel Burn, -5% DOC

[1] Revised downward by NASA from -7% to -5%.

Table XLIX is a summary of the subsonic DOC analysis for 0% interest rate, and Table L is a summary of the subsonic DOC analysis for 3% interest rate. The 0% interest rate DOC with fuel cost of $1.50 per gallon will be used to determine DOC payoffs and will also be used in the material rankings. The goal was to achieve 5% subsonic DOC payoff with advanced materials and improved aerodynamics. The bottom line on Table XLIX shows that the goal was achieved by setting Δ engine acquisition cost and Δ maintenance cost to zero. To achieve this zero Δ cost, we must supply additional compression and turbine stages and significantly more airfoils at a slightly smaller size (0.8600 scale factor versus 0.8810 scale factor) for no increase in manufacturing cost.

Table LI is a summary of the supersonic DOC analysis for 0% interest rate, and Table LII is a summary of the supersonic DOC analysis for 3% interest rate. The 0% interest rate DOC with fuel cost of $1.50 per gallon will be used to determine DOC payoffs and will also be used in the material rankings. All supersonic DOC's reflect manufacturing estimates of advanced engine acquisition costs and manufacturing estimates of the advanced material portion of the engine maintenance costs.

The DOC analysis was used to generate the following DOC derivatives for engine Δ acquisition cost and Δ maintenance cost:

Table LIII - ROMS Subsonic DOC Derivatives

Table LIV - ROMS Supersonic DOC Derivatives.

Table XLIX. ROMS Subsonic DOC Payoffs (0% Interest Rate).

Configuration Definition	Scale Factor	Delta SFC, %	Delta Acquisition Cost, $/Eng	Delta Eng Maint Cost/AC $/AC Hour	Delta % Block Fuel Burn	Delta % DOC		
						$1.0/Gal	$1.5/Gal	$2.0/Gal
84 Baseline	0.8810	Base	0	0	0	---	---	---
84 Baseline	0.8810	Base	500,000	0	0	+2.56	+2.27	+2.04
84 Baseline	0.8810	Base	0	20	0	+0.94	+0.84	+0.75
Improved Installed SFC (-5.5%)	0.8755	-5.5	-4170	-0.16	-6	-1.66	-2.15	-2.54
Reduced Engine Weight (13.7%)	0.8660	-5.5	-11,380	-0.43	-7.1	-2.13	-2.69	-3.13
Increased[(1)] Acquisition Cost	0.8660	-5.5	5130	-0.43	-7.1	-2.05	-2.62	-3.06
Increased[(2)] Maint Cost	0.8660	-5.5	5130	0.19	-7.1	-2.02	-2.59	-3.04
Improved Aero	0.8600	-11.6	0	0	-13.4	-3.86	-4.97	-5.85

(1) Engine Acquisition Cost Increased by $16,510 to Reflect Zero Δ Cost Between Baseline and Advanced Engine

(2) Engine Maintenance Cost Increased by 62¢ to Reflect Zero Δ Cost Between Baseline and Advanced Engine

Table L. ROMS Subsonic DOC Payoffs (3% Interest Rate).

Configuration Definition	Scale Factor	Delta SFC, %	Delta Acquisition Cost, $/Eng	Delta Eng Maint Cost/AC $/AC Hour	Delta % Block Fuel Burn	Delta % DOC		
						$1.0/Gal	$1.5/Gal	$2.0/Gal
84 Baseline	0.8810	Base	0	0	0	---	---	---
84 Baseline	0.8810	Base	500,000	0	0	+2.93	+2.62	+2.37
84 Baseline	0.8810	Base	0	20	0	+0.88	+0.79	+0.71
Improved Installed SFC (-5.5%)	0.8755	-5.5	-4170	-0.16	-6	-1.58	-2.04	-2.42
Reduced Engine Weight (13.7%)	0.8660	-5.5	-11,380	-0.43	-7.1	-2.02	-2.56	-2.99
Increased(1) Acquisition Cost	0.8660	-5.5	5130	-0.43	-7.1	-1.92	-2.47	-2.91
Increased(2) Maint Cost	0.8660	-5.5	5130	0.19	-7.1	-1.89	-2.45	-2.89
Improved Aero	0.8600	-11.6	0	0	-13.7	-3.65	-4.71	-5.56

(1) Engine Acquisition Cost Increased by $16,510 to Reflect Zero Δ Cost Between Baseline and Advanced Engine

(2) Engine Maintenance Cost Increased by 62¢ to Reflect Zero Δ Cost Between Baseline and Advanced Engine

Table LI. ROMS Supersonic Payoff Study (0% Interest Rate).

Configuration Definition	Engine Corrected Flow Size, lb/sec	Delta SFC, %	Delta Acquisition Cost, $/Eng	Delta Eng Maint Cost/AC $/AC Hour	Delta % Block Fuel Burn	Delta % DOC		
						$1.0/Gal	$1.5/Gal	$2.0/Gal
NASA LT WT Size	599.16	Base	0	0	0	---	---	---
NASA LT WT Size	599.16	Base	1,000,000	0	0	+0.96	+0.69	+0.54
NASA LT WT Size	599.16	Base	0	40	0	+0.29	+0.21	+0.16
Improved Installed SFC (-7.7%)	541.13	-7.7	-170,650	-6.06	-13.4	-11.37	-11.93	-12.25
Reduced Engine Weight (-44.3%)	467.50	-7.7	-398,090	-13.04	-20.1	-16.92	-17.80	-18.30
Increased Acquisition Cost	467.50	-7.7	809,210	-13.04	-20.1	-15.76	-16.96	-17.65
Increased Maint Cost	467.50	-7.7	809,210	24	-20.1	-15.50	-16.78	-17.50
Improved Aero	461.10	-8.5	778,810	23.1	-21.5	-16.68	-18.03	-18.78

Table LII. ROMS Supersonic Payoff Study (3% Interest Rate.)

Configuration Definition	Engine Corrected Flow Size, lb/sec	Delta SFC, %	Delta Acquisition Cost, $/Eng	Delta Eng Maint Cost/AC $/AC Hour	Delta % Block Fuel Burn	Delta % DOC $1.0/Gal	$1.5/Gal	$2.0/Gal
NASA LT WT Size	599.16	Base	0	0	0	---	---	---
NASA LT WT Size	599.16	Base	1,000,000	0	0	+1.14	+0.83	+0.65
NASA LT WT Size	599.16	Base	0	40	0	+0.28	+0.20	+0.16
Improved Installed SFC (-7.7%)	541.13	-7.7	-170,650	-6.06	-13.4	-11.23	-11.82	-12.16
Reduced Engine Weight (-44.3%)	467.50	-7.7	-398,090	-13.04	-20.1	-16.67	-17.60	-18.14
Increased Acquisition Cost	467.50	-7.7	809,210	-13.04	-20.1	-15.29	-16.60	-17.35
Increased Maint Cost	467.50	-7.7	809,210	24	-20.1	-15.04	-16.41	-17.20
Improved Aero	461.10	-8.5	778,810	23.1	-21.5	-16.22	-17.65	-18.46

Table LIII. ROMS Subsonic DOC Derivatives.

	Fuel Costs		
	$1.00/Gal	$1.50/Gal	$2.00/Gal
Delta Engine Acquisition Cost ($/Engine M.C.) Equivalent to Δ DOC = 1% with 0% Interest Rate	195,313	220,264	245,098
Delta Engine Acquisition Cost ($/Engine M.C.) Equivalent to Δ DOC = 1% with 3% Interest Rate	170,648	190,840	210,970
Delta Engine Maintenance Cost ($/Engine Hour) Equivalent to Δ DOC = 1% with 0% Interest Rate	21.28	23.81	26.67
Delta Engine Maintenance Cost ($/Engine Hour) Equivalent to Δ DOC = 1% with 3% Interest Rate	22.73	25.32	28.17

Note: All derivatives are based on mature engine cost in the 1984 baseline aircraft size.

Table LIV. ROMS Supersonic DOC Derivatives.

	Fuel Costs		
	$1.00/Gal	$1.50/Gal	$2.00/Gal
Delta Engine Acquisition Cost ($/Engine M.C.) Equivalent to Δ DOC = 1% with 0% Interest Rate	1,041,667	1,449,275	1,851,852
Delta Engine Acquisition Cost ($/Engine M.C.) Equivalent to Δ DOC = 1% with 3% Interest Rate	877,193	1,204,819	1,538,462
Delta Engine Maintenance Cost ($/Engine Hour) Equivalent to Δ DOC = 1% with 0% Interest Rate	137.93	190.48	250.00
Delta Engine Maintenance Cost ($/Engine Hour) Equivalent to Δ DOC = 1% with 3% Interest Rate	142.86	200.00	250.00

Note: All derivatives are based on mature engine cost in the 1984 baseline aircraft size.

3.3 SUBSONIC AND SUPERSONIC MATERIAL RANKINGS

Advanced material and aero rankings were determined by combining the DOC results with the previous fuel burn, weights, sizing, and cost inputs. The rankings were grouped in the following categories:

- Advanced materials related to increase in overall cycle pressure ratio
- Advanced materials related to increase in turbine inlet temperature and elimination of turbine cooling flow
- Advanced materials related to weight reductions
- Advanced component aero.

Table LV ranks the advanced material or advanced aero improvements for the subsonic study. Table LVI ranks the advanced material or advanced aero improvements for the supersonic study.

3.4 MEASUREMENT AGAINST GOALS

Table LVII is an up-to-date measurement of subsonic and supersonic DOC and fuel burn payoffs versus goals.

Table LV. ROMS Subsonic Study.

Advanced Material and Aero Rankings.

	DOC Payoff, %	Material or Aero	Fuel Burn Payoff, %
	-2.34	Adv Aero	-6.5
	-1.55	Carbon-Carbon	-3.9
	-1.08	Intermetallics	-3.0
Totals	-4.97		-13.4

Notes:
- 0% interest
- $1.50/gal fuel cost
- No increase in advanced material costs
- No increase in engine maintenance cost

Table LVI. ROMS Supersonic Study.

Advanced Material and Aero Rankings.

	DOC Payoff, %	Material or Aero	Fuel Burn Payoff, %
	-10.79	Intermetallics	-11.40
	-5.57	Carbon-Carbon	-6.70
	-1.25	Advanced Aero	-1.50
	-0.48	Fiber Reinforced Metal Matrix	-1.10
	+0.03	Advanced Titanium	-0.05
	+0.03	Ceramic Composites	-0.05
Totals	-18.03		-21.50

Notes:
- 0% Interest Rate
- $1.50/gal fuel cost
- 100% of estimated advanced materials costs
- Material content of maintenance costs proportional to acquisition costs.

Table LVII. Comparison of DOC and Fuel Burn Payoffs with DOC and Fuel Burn Goals.

	Fuel Burn, %	DOC, %
Subsonic		
• 1984 Baseline UDF	Base	Base
• Initial Goal	-15	-7
• Revised Goal	-15	-5
• Advanced UDF (w/o Aero)	-6.9	-2.63
• Advanced UDF (w/Aero)	-13.4	-4.97
Supersonic		
• 1984 Baseline AST	Base	Base
• Goal	-15	-5
• Advanced AST (w/o Aero)	-20	-16.8
• Advanced AST (w/Aero)	-21.5	-18

Notes:
- 0% Interest Rate
- $1.50 per gallon fuel cost
- Subsonic Δ maintenance and acquisition cost = 0, Supersonic Δ maintenance and acquisition cost as estimated by manufacturing engineering

3.5 TASK IV - RECOMMENDED TECHNOLOGY PROGRAMS

3.5.1 Nonmetallic Composites

The overall objective of this effort is to develop high temperature nonmetallic composites suitable for applications identified for advanced subsonic and supersonic transports. The various applications and associated temperature requirements are listed in Table LVIII. The two material technologies with potential to meet these requirements are carbon-carbon (C-C) and ceramic-matrix composites.

Table LVIII. ROMS High Temperature Nonmetallic Composite Applications.

ROMS Material Applications/Temperatures

	Maximum Temperature, ° F	
	AST	UDF
Carbon-Carbon or Ceramic Composites		
Combustor	4100	3200
HPT Blades/Vanes	4100	3200
LPT Blades/Vanes	3500	2300
Exhaust Nozzle	2700	---
Turbine Frame Fairings	2600	2100

Roadmaps for recommended programs, their timing, and estimated cost are shown in Tables LIX and LX for carbon-carbon and ceramic-matrix composites, respectively. (The tables appear in the Addendum to this volume.) The objective, scope, and approach to each program are described below.

3.5.1.1 Carbon-Carbon

<3000° F Carbon-Carbon Coating System Development

Objective - The objective of this program is to develop an oxidation protective coating system for carbon-carbon composites suitable for temperatures to 3000° F and life up to 4000 hours. The coating must be suitable for rotating and static airfoils and static panels.

Scope - This program will develop the capabilities of coatings that are based on or derived from the current SiC system. This includes work on outer coatings, bond coatings, sealants, and pore coatings. Improvements in temperature capability, life, and reliability are required. In addition, moisture absorption and the effects of a centrifugal field on the glass sealants will be investigated. An oxidation test technique will be selected and/or established to test the coatings in both the stressed and unstressed conditions. The program will also have to evaluate the coatings as applied to several substrate systems.

Approach - Existing coating systems will be evaluated to determine their chemical and microstructural characteristics and to assess their oxidation performance under a variety of conditions. The oxidation degradation mechanisms for various test conditions will be determined based on analysis of tested coatings. Work would proceed to negate or minimize these degradation mechanisms through material and process innovations. Examples of mechanisms which are anticipated to require action are oxygen transport through internal pores, moisture absorption, and coating/substrate thermal mismatch. Work to address these issues will begin early with development of a pore coating, refinement of the sealant chemistry, and better thermal matching of the outer layer to the substrate. Examples of processes which will be brought to bear on the development of the coating are chemical vapor deposition (CVD), chemical vapor infiltration (CVI), sol-gel, and melt infiltrations.

<3000° F Carbon-Carbon Fiber Development

Objective - The objective of this program is to develop and/or select fibers that will enable C-C composite systems to meet the strength and life goals of applications at 3000° F or less. The goals for 2D laminates at 3000° F are as follows:

- In-plane tensile strength - 40 ksi
- In-plane elastic modulus - 10 ksi.

In addition to meeting these strength goals, the fibers must be compatible with processing and may play a role in the oxidation protection system.

Scope - The program will evaluate fibers over a range of moduli to compare their strength and stability at temperature. The effect of fiber inhibitor on strength and oxidation resistance will be evaluated. Fiber coatings will also be evaluated for their effect on strength, oxidation resistance, and matrix/coating interactions.

Approach - Fiber temperature capability will be established with temperature stabilized fibers. This will establish the relative importance of so called high versus low modulus fiber for 3000° F applications. Various fiber inhibitor approaches will be evaluated for their effect on fiber oxidation resistance and fiber strength. Boron nitride, silicide, and oxide fiber coatings will be evaluated for their effect on fiber oxidation, strength, and reaction with the matrix or coating.

<3000° F Carbon-Carbon Substrate Development

Objective - The objective of this program is to develop a 3000° F composite C-C substrate that can meet the laminate property goals outlined in the fiber development, plus have a interlaminar shear strength of 2.5 ksi and density of 0.065 lb/in^3. The substrate materials and processing will play a key role in the success of carbon-carbon both from a property and oxidation standpoint.

Scope - This program will bring together various fiber, matrix, and inhibitor approaches to define suitable panel and airfoil structures and properties. Variables to evaluate include the matrix, consolidation process, inhibitor, fiber system, and 3D composite architecture. Both properties and oxidation resistance will be evaluated, with particularly close attention to the effect of processing on interlaminar shear, the effect of inhibitors on interlaminar shear and oxidation resistance, the effect of 3D architecture on properties, and the effect of fiber/matrix interaction on properties.

Approach - Candidate substrates will be developed through the characterization of substrates with variations in the weaving and densification processes, fiber and matrix materials, and the size and type of inhibitors. The characterization will include both in-plane and cross-ply properties. The evaluations will investigate the effects of exposure to the operating environment in order to determine the degradation due to moisture, oxidation, coating

or sealant interactions, and fiber/matrix interactions. The effect of these variations in the substrates will be evaluated in an iterative fashion, thus allowing trends in the variables to lead one to the correct balance in properties. After several iterations have increased the understanding of the variable involved in 2D layups, a similar approach will be followed to develop the materials, processing, and architecture of 3D substrate material.

<3000° F Carbon-Carbon Materials Characterization

Objective - The objective of this task is to characterize the mechanical capability of <3000° F carbon-carbon material systems. It will establish a micromechanical model and tests will be conducted under the proper environment to validate the model and determine the environmental effects on properties.

Scope - This program will cover the development of micromechanical models for carbon-carbon composites, the development of test techniques for both 2D and 3D carbon-carbon, and the characterization of the candidate and final material systems. The program will involve both monotonic and cyclic tests.

Approach - The micromechanical models will attempt to predict properties based on the matrix and fiber properties and matrix/fiber interaction. The test development will concentrate on the design and trial of heating systems, gripping arrangements which will handle the coating systems without damage, and extensometry technology to measure strain at these types of temperatures. The test techniques will evolve through the material development phase and will be used in material development process. The final test techniques will be used to characterize the final materials, validate the models, determine the effects of environment on properties, and supply the design engineers with data for development of the design methodology.

<3000° F Carbon-Carbon Attachment Methods

Objective - The objective of this task is to define the methods by which carbon-carbon structures can be attached to structures of carbon-carbon and other materials.

Scope - The program will concern itself with both the mechanical and material problems associated with attaching carbon-carbon. This includes reactions between the carbon-carbon coating and the mating surfaces, the durability of the coating under the attachment loads, and the thermal expansion differences between carbon-carbon and other materials. The situations to be considered include flanges, hooks and hangers, dovetails, and pinned joints.

Approach - The carbon-carbon substrate and coatings will be characterized for their reactions with other materials as a function of temperature. The results will be used to identify materials that can be used as reaction barriers. Carbon-carbon substrate and coating wear resistance will be evaluated against these barrier materials as a function of bearing stress and temperature. Finally, the crush stress and thermal expansion characteristics of the system will be evaluated or collected from other sources. These data will be supplied to the design engineer for use in designing attachment methods that address the needed situations. Those designs will be evaluated and iterated upon in a series of component tests.

Design Methodology for Carbon-Carbon

Objective - The objective of this program is to develop the design methodology or guidelines to be used to determine that a carbon-carbon component will perform its required mission.

Scope - The program will include the development of a design methodology for both static and rotating components. It will involve setting limits as to allowable static, cyclic, and dynamic stresses in relation to the material properties obtained in the materials characterization efforts. Work will be undertaken for both 2D and 3D woven components.

Approach - The design methodology will be based initially on current polymeric composite guidelines. However, it is anticipated that it will need to quickly advance beyond this point due to the much more aggressive environmental degradations associated with carbon-carbon and the higher thermal stresses involved. The static, cyclic, and dynamic guidelines or limits will be evaluated and iterated upon using a series of component or component feature tests which simulate typical engine conditions.

Component Process Development

Objective - The objective of this program is to develop and demonstrate the process to produce a 2D and 3D weave carbon-carbon composite component capable of operating in a 3000° F environment. The parts produced are to meet the properties outlined in the preceding programs and be worthy, from a quality standpoint, of a demonstration engine test.

Scope - The program will develop and produce a 2D laminated flat panel carbon-carbon component and 3D woven airfoil component. It will encompass the critical elements of the programs discussed above, that is, the fiber, substrate, coating, attachment, and design methodology. In addition, it will develop the NDE and process control technology needed to assure a quality component.

Approach - This program will integrate the processes developed in the coating, fiber, and substrate programs to produce the components. In addition, this program will develop the process models and sensors needed to define and monitor the process for consistent quality. X-ray, infrared, and ultrasonic NDE procedures will also be developed to ensure the needed part integrity. Components will be produced and inspected to the point where they are ready for engine test. Extra components or similar shapes will also be produced for destructive property evaluation.

Cost Effective Industrial Capability

Objective - The objective of this program is to develop the industrial capability to produce carbon-carbon components capable of service in a 3000° F environment at a cost which is affordable for commercial as well as military applications. The property goals remain as stated above unless the intervening work has shown that the life cycle cost and performance requirements dictate a change.

Scope - The program will need to include all aspects of component manufacture. The critical functions that will be addressed include component design, fiber manufacture, the matrix materials, ply prepregging and/or fiber weaving, densification, and all the coating steps. Process modeling,

monitoring, and control will be key to the successful development of a cost effective component capability.

Approach - All aspects of the component from design through manufacture will have to be rethought keeping in mind the problems and benefits of a production volume environment. Each of the processes will be modeled to provide both an aid to designing the process and to enable the component designer to evaluate producibility as part of his design study. The emphasis will be on automated processing with process sensors linked with the control functions to provide real time monitoring and control wherever possible. The process control objective being to control quality to the point where final part NDE requirements are minimized.

The process modeling, development, scale-up, and automation will be conducted at the suppliers to ensure that the process does work in the real manufacturing world. The program will end with component demonstrations and a life cycle cost study to document the cost effectiveness of the components.

>3000° F Carbon-Carbon Coating Thermochemical/Kinetic Analysis

Objective - The objective of this program is to analyze and evaluate the thermochemical reactions and kinetics involved in providing oxidation protection for carbon-carbon components at temperatures above 3000° F and to select coating materials which have promise for providing protection at these temperatures.

Scope - The program will evaluate the properties of materials in the oxide, carbide, nitride, and high temperature metal classes. Properties to be evaluated and considered include melting point, vapor pressure, oxygen permeability, carbon permeability, coefficient of thermal expansion, thermal conductivity, density, modulus, and chemical stability with carbon and oxygen.

Approach - The initial data for this program will be collected in large part from other sources. The holes in this data base will be filled in by experimentation. Additional experiments would then be run to confirm the data and, more important, to see how the various materials react with one another, since this coating is anticipated to be a multilayered system.

>3000° F Carbon-Carbon Coating Development

Objective - The objective of this program is to develop and demonstrate a coating to protect a carbon-carbon composite at temperatures of 4000° F for 2500 hours.

Scope - The program will include selection of the coating candidates, application of the experimental coatings, and evaluation for stability, properties, and oxidation resistance.

Approach - It is anticipated that the coating will use a multilayered approach, with the inner layers resistant to carbon reaction and diffusion and the outer layers resistant to oxygen reaction and diffusion. The layered approach will also be utilized to minimize strain due to thermal expansion mismatches by grading the thermal expansion coefficients. Results from the previous program will aid in selecting the coating constituents which will be layered in a manner outlined in Table LXI. The coatings could be applied by a variety of techniques ranging from sputtering to CVD to plasma spray to pack diffusion. Each coating will be exposed at temperatures from 3000° to 4000° F and evaluated for stability and oxidation resistance. The final coating candidates will be evaluated in thermal cycle oxidation tests for oxidation resistance under stress and for its effect on properties of the substrate.

Additional >3000° F Carbon-Carbon Programs

The other carbon-carbon programs aimed at developing the system for applications at temperatures greater than 3000° F are listed in Table LIX and deal with fiber development, substrate development, materials characterization, attachment methods, design methodology, component process demonstration, and developing a cost effective industrial capability. The objectives, scope, and approach for each of these efforts directly parallel those stated for the <3000° F carbon-carbon programs discussed previously, except the property goals for in-plane tensile strength and modulus at 4000° F are 48 ksi and 12 Msi, respectively. Further discussion of these programs would not be worthwhile at this time, since in general it would just be a reiteration of the <3000° F carbon-carbon programs.

Table LXI. Selection Criteria for External Coating Material Subsystems.

Location Function	Outer Layer Primary Oxygen Barrier	Intermediate O Diffusion Barrier	Inner Layer C Diffusion Barrier	C-C Surface CTE Match Adherence
Property				
Melting Point	2210° C (4000° F)	>Outer	>Outer	No Melt Phases
Vapor Pressure	Very Low	Low	Low-Moderate	Low
O Permeability	Low-Moderate	Very Low	Low-Moderate	---
C Permeability		Low-Moderate	Very Low	Low
CTE	Match ± 20% Intermediate	Match or ± 20% Inner-Outer	Match or ± 20% C-C Surf.	Match or ± 20% Inner Layer
Chemical Stability	No Reaction to Fuel Add. Stability to Intermediate Layer	Stable to Outer, Inner Layer Low Vol.O. Prod.	Stable to Interm. Layer, C Modified Surface	No Active Diffusers No Reaction to Inner Layer
O Resistance	No Reaction O_2,H_2O,Co,Co_2	Stable to O Diffusion through Outer Layer	Moderate	---
Thermal Conductivity	Moderate to Good	Moderate to Good	Good	High

3.5.1.2 Advanced Ceramic Matrix Composite Development

Evaluate Ceramic Fibers and Matrices

Objectives - The objective of this task is to select ceramic fibers and matrices as potential constituents in ceramic matrix composites (CMC). Their thermomechanical and thermochemical stability to temperatures of 3000° F will be determined in oxidizing environments.

Scope - This task will evaluate state-of-the-art ceramic fibers and matrices, both oxide and non-oxide, for strength and environmental stability up to 3000° F. Candidate fibers should have high tensile strength, modulus, be creep resistant, and thermally stable to the maximum use temperature, while matrices should have low elastic modulus, good thermal stability to 3000° F, and have a lower thermal expansion than the candidate reinforcement.

Approach - Available ceramic fibers will be evaluated to determine their physical characteristics such as composition, diameter and thermal stability, also extensive characterization thermomechanical properties such as tensile strength, stress rupture and creep to temperatures up to 3000° F in oxidizing environments will be carried out. Candidate matrices will be evaluated to determine their physical characteristics such as composition, thermal expansion, elastic modulus and thermal expansion to temperatures up to 3000° F. The data obtained will be reviewed to select the candidate ceramic fibers and matrices capable of being used in a CMC to 3000° F in oxidizing environments or give direction for developing a reinforcing material or matrix with sufficient high temperature properties for turbine engine applications.

Barrier Coating Development and Compatibility

Objective - The objective of this task is to identify and characterize coatings capable of being applied to ceramic fibers which can inhibit fiber/matrix interfacial reactions and also produce a weak interface. Selected barrier coatings should be stable with both fiber and matrix to temperatures up to 3000° F in oxidizing environments. The process by which the fiber coating is applied will also be defined.

Scope - Ceramic fibers will be coated by a number of state-of-the-art processes. The coating will be assessed for uniformity, thickness, adherence, and purity, and the most efficient coating process identified. The coatings on the ceramic fibers will be evaluated for oxidation protection, thermal stability, and reactivity up to 3000° F in oxidizing environments. The chemical reactivity of the barrier coating with both fiber and matrix will also be investigated.

Approach - Ceramic fibers will be barrier coated using processes such as sputtering, CVD, sol-gel, and prepregging, and then evaluated for coating uniformity, thickness, purity, adherence, process scaleability, and continuous coating capability. Thermochemical reactivity of the barrier coatings with candidate fibers and matrices will be investigated using electron microscopy and chemical analysis.

Simple composite systems consisting of fiber/coating/matrix will be fabricated and evaluated for oxidation protection, thermal stability, and interfacial thermomechanical properties up to 3000° F in oxidizing environments. Chemical analysis of the fiber/coating and coating/matrix interfaces will be carried out on samples thermally treated to 3000° F in oxidizing environments to evaluate the extent of reaction.

Composite Fabrication Process Development

Objective - The objective of this task is to develop a process of incorporating barrier-coated ceramic fibers into a ceramic matrix without damaging the fibers. The selected process must be amenable to the fabrication of large nonsymmetric shapes.

Scope - This task will evaluate CMC consolidation processes such as chemical vapor infiltration, hot pressing, pressureless sintering, organometallic/polymer precursor infiltration processes, tape casting, and sol-gel techniques. CMC's will be fabricated and evaluated for maximum density, processing temperature, and fiber damage. The CMC consolidation process must also be capable of forming large complex fiber-reinforced composite shapes.

Approach - Barrier-coated ceramic fibers will be oriented either unidirectionally or woven into 2D or 3D architectural forms. These structures

will then be consolidated into simple shapes using processes such as chemical vapor infiltration, hot pressing, pressureless sintering, organometallic/ polymer precursor infiltration processes, tape casting, and sol-gel techniques. Some of these processes will require the matrix to be incorporated into the fiber form before consolidation, while others, such as the infiltration processes, can be carried out after the fiber form has been produced. The efficiency of the consolidation process will be evaluated by measuring density and shrinkage of the composite; degree of fiber damage as a consequence of maximum processing temperature; extent of chemical interaction between fiber, coating, and matrix; and near-net shape forming capability.

Mechanical Property Characterization and Micromechanical Model Validation

Objective - The objective of this task is to identify and implement test methodologies that will accurately evaluate the thermomechanical properties of ceramic matrix composites to their ultimate use temperature in oxidizing environments. Micromechanical models of the CMC systems will then be validated using these test data.

Scope - Structural use of CMC's is currently limited due to the lack of meaningful material property data and understanding of the basic failure criteria. This task will therefore investigate testing methods for CMC's both at room temperature and up to 3000° F. A number of specimen gripping arrangements and testing fixtures will be designed and then evaluated for use at elevated temperatures. The mechanical properties obtained will then be compared with those obtained through micromechanical modeling of the CMC system by computer.

Approach - The capability of measuring the mechanical properties of CMC's from room temperature to 3000° F in oxidizing environments will be developed. In order for these tests to be carried out, it is required that test specimen gripping methods be evaluated and testing fixtures be designed for elevated temperature use. The following mechanical properties will be determined at room temperature and up to 3000° F:

- Tensile strength
- Compression strength

- In-plane shear
- Interlaminar shear
- Cross-ply tension
- Fatigue
- Toughness.

The fracture morphology of the tested specimens will be characterized using electron optic techniques and the mode of failure will be identified identified. Mechanical property data obtained will then be compared with that obtained by micromechanical modeling of the CMC system by computer.

NDE Methods Development

Objective - The objective of this task is to define the nondestructive evaluation techniques that reliably identify flaws within ceramic matrix composites materials.

Scope - This task will assess the capability of state-of-the-art NDE techniques as applied to CMC materials. The techniques will be characterized for their ability to consistently detect flaws within a CMC and to determine its surface and thickness sensitivity. The techniques will also be evaluated for ease of operation and ability to detect flaws in complex nonsymmetrical shapes.

Approach - State-of-the-art NDE techniques, such as ultrasonics and X-ray computer tomography (CT), will be used to study defects in CMC materials. These techniques will be evaluated for their ability to detect the most common flaws found in CMC's, such as delaminations, porosity, fiber damage, and variation in density. Composites will be analyzed for defects by these NDE techniques and the findings correlated with the actual defects found in the test specimen. The NDE techniques will also be evaluated for their ability to detect flaws reliably in large nonsymmetric CMC components.

Scale-Up Fiber Manufacturing

Objective - The objective of this task is to scale up the process of manufacturing the ceramic fiber which has been identified as a candidate

reinforcement for a CMC having structural integrity at temperatures up to 3000° F in oxidizing environments.

Scope - This task will identify all the process parameters necessary to enable a candidate reinforcement to be manufactured in the quantity and quality required for CMC production. The cost of process scale-up will be assessed including equipment and technical training. Fibers produced by the scale-up process will be evaluated to ensure that thermomechanical properties are consistent with the originally produced fibers.

Approach - The process by which the candidate reinforcing fiber is made will assessed for its adaptability to scale up to the production of large quantities of continuous fiber. The process will also be evaluated for cost effectiveness, ease of operation and reproducibility. Process parameters such as raw material cost, uniformity of fiber diameter, fiber production rates, and ease of handling will all be determined. The fibers produced will be evaluated for tensile strength, elastic modulus, high temperature creep, and stress rupture behavior and these data compared with the original fiber data. Scale-up equipment and engineer and technician training costs will be reviewed so that the necessary tooling, equipment, and qualified labor is available for production manufacturing.

Cost Effective Industrial Capability

Objective - The objective of this task is to develop a cost effective capability for manufacturing specific components from an advanced ceramic matrix composite.

Scope - This task will address the problems related to the transfer of CMC fabrication technology from the laboratory scale to an advanced manufacturing process.

Approach - A review of all the process parameters involved in transferring the laboratory scale fabrication process to an advanced component production capability will be undertaken. Important areas such as process shape limitations, cost effective methods of production, component reproducibility, quality control methodologies, and product evaluation will be assessed and implemented.

3.6.1.3 Intermetallics

The overall objective of this effort is to develop intermetallic materials suitable for applications identified for advanced subsonic and supersonic transports. The various applications and associated temperature requirements are listed in Table LXII. The intent is to meet these application needs with a monolithic material rather than a continuously reinforced metal matrix composite. The temperature requirements are all at least 1500° F, which is judged to be beyond the limits of Ti_3Al based alloys, thus this program will concentrate on the development of alloys based on the higher temperature TiAl and Ti_5Si_3 systems. The property goals for the material are listed in Table LXIII.

Roadmaps for recommended programs, their timing and estimated cost are shown in Table LXIV (found in the Addendum). The objective, scope, and approach to each program are described below.

Alloy/Process Screening

Objective - The objective of this program is to investigate candidate intermetallic systems with the goal of identifying an alloy system and process that has the potential to meet the goals stated in Table LXIII. These candidate alloys will also be used and evaluated in the subsequent programs. How they process and perform in these development and demonstration programs will provide much of the data and experience needed to develop a successful material.

Scope - The program will initially include a broad range of intermetallic systems such as titanium aluminide (TiAl), and Ti_5Si_3 NiAl, and Ni_3Al (all intermetallic class). Rapid solidification technology (RST) processing is expected to be the baseline alloying process but mechanical alloying will also be evaluated. The program will evaluate the materials for their mechanical, physical, and microstructural characteristics.

Approach - Alloy development will proceed through an iteration of a series of alloy trials in each of the candidate systems. The lightweight Ti based systems will receive the higher level of effort, at least initially, due to their larger weight reduction potential. This iterative approach will be

Table LXII. ROMS Intermetallic Alloy Applications.

	Maximum Temperature, ° F	
	AST	UDF
HPC Rotor/Stator	1700	1500
Turbine Casings	1800	1600
HPT/LPT Disk	1800	1600
Turbine Frame	1700	---
Propulsor Airfoils		2100

Table LXIII. Intermetallic Materials Goals (1700° F).

Tensile Strength	66 ksi
Yield Strength	40 ksi
Elongation	12%
Elastic Modulus	18 Msi
1000 hr Rupture	15 ksi
Density	0.14

accompanied and supported by efforts to model the effects of the alloying variations on the crystal structure of the material and how this affects properties. A breakthrough in improving the ductility of these materials is required for this program to be successful. Rather than try to schedule this breakthrough in a typical 3-year program, a 6-year effort is shown.

Alloy Refinement

Objective - The objective of this program is to define the alloy which meets the goals of Table LXIII and will be scaled up to production reality.

Scope - The scope of this program will largely depend on the outcome of the preceding program efforts, but it is anticipated that it will be much narrower in scope, concentrating on a single alloy/process system and several compositions which will be refined and evaluated to select the final alloy.

Approach - This program will build upon the results of the previous alloy and process development programs. Based on these programs, a very limited set of compositions will be selected for refinement. Each composition would be fine tuned by adjusting the limits of the major alloying elements and the maximum limits of the minor and trace elements. Before freezing the selection, the final alloy would be characterized for its full range of properties, defect distribution, and environmental sensitivities.

RST Process Development

Objective - The objective of this program is to develop a pilot plant capability to produce clean, rapidly solidified powder for reactive alloys of titanium and/or titanium aluminide.

Scope - The program will begin with the design and building of new equipment or equipment modifications to atomize titanium and titanium aluminide type alloys. That will be followed by melting and atomization process development and powder characterization to demonstrate the acceptability of the product. Also included in the program will be an effort to model the heat transfer, fluid flow, and surface behavior of the melting and atomization processes. Real time process monitoring and control of the melting and

atomization process will also be a key consideration in the equipment design and process development.

Approach - General Electric has shown that gas atomization can produce reactive Ti-based powder with the required solidification rates. The approach in this program will be to scale up a gas atomization process to produce 50 to 100 pounds of powder per run. Two melting processes are being considered: the first involves induction melting; the second, plasma arc hearth melting. In both instances the melt is isolated from the crucible by its own shell and thus remains uncontaminated by the crucible materials. The atomization nozzle materials to be evaluated include both refractory metals and ceramics. Recent work has demonstrated that a refractory metal nozzle can control the flow of at least 40 pounds of titanium without nozzle degradation. Design of the atomization nozzle will be based on General Electric's close coupled nozzle, which produces an excellent yield of fine powder.

The powder produced by the process will be evaluated for typical loose powder characteristics such as chemistry, size distribution, solidification morphology, flow, and tap density. It will also be consolidated and evaluated to judge its acceptability from a property and cleanliness standpoint.

Consolidation Development

Objective - The objective of this program is to develop the consolidation techniques for producing intermetallic materials on a laboratory scale; culminating with a demonstration of the process by producing a shape for a small component.

Scope - At this time, it is anticipated that the intermetallic alloy will be available as a gas atomized powder; however, another powder product (namely, mechanically alloyed powder) is also a possibility. HIP, HIP plus forge, extrude, extrude plus forge, and explosive compaction will be evaluated as a means of consolidating and shaping the material. The selected process will be used to produce a small component shape for evaluation.

Approach - A developmental titanium intermetallic alloy from the alloy development program will be selected for consolidation development. Powder will be initially consolidated by extrusion, HIP'ing and explosive compaction

over a preselected temperature range. The consolidated material will be characterized microstructurally and evaluated for density, properties, and hot workability. Based on these results, material from selected consolidation techniques will be characterized to determine its stress/strain characteristics under the range of temperatures and strain rates anticipated in isothermal forging. Using CAE techniques, a forge process would be modeled and then validated for selected conditions. The forging made to validate the model would be evaluated for properties. Based on that evaluation, a consolidation technique would be selected and a forging process designed and demonstrated by forging and evaluating a small component.

Metalworking Development

Objective - The objective of this program is to develop the capability to produce full size components from an intermetallic alloy developed in the Alloy/Process Screening program. This would culminate in the demonstration of the process by producing and evaluating at least one, but more likely two, of the full size components listed in Table XVII.

Scope - The alloy will be available as powder produced by the pilot plant process developed earlier, but blended into a large master powder blend. This program will model, develop, and demonstrate the consolidation, forging, heat treatment, and machining processes needed for producing full size components.

Approach - The consolidation technique established earlier will be modeled and scaled up to produce a billet of an appropriate size. The billet will be evaluated for microstructure and uniformity of structure and properties. It will be fully characterized as to its deformation behavior over the appropriate temperature, stress, strain, and strain rate range. Based on these data, a forging process will be modeled and designed for a selected part or parts. Using the designed process, the part or parts will be forged, most likely using an isothermal process. The heat treat process will be developed through the use of heat transfer models which predict the temperature profile as a function of time and incorporate the material's mechanical response to predict residual stress and sensitivity to cracking. These models would first be validated on a subscale basis and then applied to the full size components. Following heat treatment, the component would be evaluated for

its critical properties, and section size effects will be established. Machining techniques will be developed, and a full size component will be machined and made available for test. Once again, the heat treatment model will be used and further modeled to develop a machining pattern designed to minimize distortion due to residual stress induced during processing.

Understand Mechanical Behavior

Objective - The objective of this program is to understand how limited ductility and high temperature environment will affect the mechanical behavior of Ti-based intermetallic alloys. Initially, this understanding is needed to set more definitive goals for the development efforts, and later these data will be needed to correctly design engine components.

Scope - Ti-based intermetallic alloys will be characterized for smooth and notch tensile, rupture, and fatigue properties. Cyclic crack growth tests will also be conducted with and without hold times. The influence of environment will also be evaluated by conducting some tests in vacuum or inert atmospheres and/or with protective coatings.

Approach - The initial alloys to be evaluated will include materials from both the Ti_3Al and TiAl families. The Ti_3Al alloys will be used because it is anticipated that a variation in ductility will not be available in the TiAl materials at that time. Ti_3Al family materials will be tested to establish development goals for the higher temperature intermetallic system. Testing will include tensile, rupture, and fatigue in both a smooth and notched condition over the temperature range of RT to 1500° F. Cyclic and static crack growth tests will also be conducted. The microstructure and fracture surface will be characterized at appropriate test points for the purpose of correlating with the property data. This experience will be used to better define the goals and give clues as to what appropriate paths might be followed in developing the higher temperature systems.

A later follow-on program will be conducted to yield much the same data, except that it will concentrate on the higher temperature intermetallic system and extend the temperature range to 1700° or 1800° F. The program will also more heavily evaluate the environmental effects by testing in inert

atmospheres and atmospheres containing typical gas turbine combustion products. The program will also evaluate the effects of protective coatings.

NDE Needs/Methodology

Objective - The objective of this program is to identify the NDE needs and to demonstrate the ability to inspect the hardware or in-process materials to those requirements. One of the goals of this effort will be to improve in-process NDE and controls and thus minimize the need for final part NDE.

Scope - The program will involve definition of defect limits, development of techniques to detect those defects, and demonstration of that capability on hardware and in-process material.

Approach - The initial work will define the defect limits by coordination of the expected stresses obtained from our engine design organization with the results from the mechanical behavior program. This information will also be fed into the materials and process development programs to ensure that the material defect distribution is in agreement with the defect limits. Once the limits are established, NDE and in-process control techniques will be developed to control or inspect the material to those limits. It is expected that these defect limits will be very challenging, and significant innovations in the current NDE and process control techniques will be required. This includes work in melting and atomization controls, consolidation and billet inspection, forging design, control and inspection, and final machined surface inspections.

Coating Development

Objective - The objective of this program is to define whether a coating is needed or not and if so, to develop one to the point of demonstrating it on a component.

Scope - This program is to include environmental tests of candidate alloys with the intent of defining the need for a coating and giving direction to the alloy development activity on the influence of the alloy variables on environmental resistance. The environment is to include typical oxidation and corrosion conditions appropriate to gas turbine operation and hardware

manufacture. The coating development activity will include the identification of effective coating materials and a process to apply the coating. The coating will be evaluated for environmental effectiveness and its effect on mechanical properties.

Approach - The materials to be environmentally tested will be selected from the material development activity. The alloy will be tested in combustion flame tunnels with salt and combustion products added to the fuel or gas stream to simulate the range of environments expected in operation. They will also be exposed to the expected manufacturing environment to ensure its behavior is understood from that standpoint. The program will also consider input from the mechanical behavior program to ensure that it addresses the mechanical aspects of environmental effects. It is not known at this time if a coating will be required. Based on work to this point on lower Al content Ti alloys and intermetallics, it is anticipated that aluminides and/or silicides are the appropriate coating choices for Ti-based substrates at high temperatures. Coatings of those types can be applied a variety of ways, ranging from pack diffusion to CVD to sputtering. The coatings will be applied initially to specimens for environmental and mechanical testing. Following selection of a coating based on these evaluations, hardware would be coated for evaluation.

Fabrication Development

Objective - The objective of this program is to define the manufacturing processes required to produce intermetallic components and to develop those processes to the point where hardware can be produced for evaluation.

Scope - The processes involved in manufacturing a component after the initial shape is produced include conventional and nonconventional metal removal, cleaning, joining, thermal spray, shot peening, and others. This program will evaluate, develop, or modify these processes to the point where a component can be produced.

Approach - The program will select a component or two components which together require all the foreseen processes. The process requirements will therefore be set by the component needs, and the component design will

evolve around the developed process capability. Metal removal capability will be established in the conventional arena through a machining study which addresses turning, drilling, milling, etc. with various cutting tools to establish good machining parameters. The nonconventional machining arena will require the development of electrolytes for chemical and electrochemical milling. Nonconventional drilling will require evaluation of EDM and laser drilling and machining operations. Because of an anticipated high degree of surface sensitivity in these materials, the effect of these metal removal practices on fatigue properties will be carefully evaluated and will be tied to surface enhancement techniques, such as shot peening, which will likely be required in these components. The initial joining development will evaluate solid state welding, diffusion bonding, brazing, and fusion welding and will result in the selection of those techniques with the most promise. The hardware will be designed with these techniques in mind. Process development will then continue in those techniques with the aim of producing the hardware design by the end of the program. Nonaggressive cleaning techniques will need to be developed and evaluated as will finish part heat treat processes and thermal spray processes.

Cost Effective Industrial Capability

Objective - The objective of this program is to develop the industrial capability to produce a high temperature intermetallic component at an affordable cost for commercial as well as military applications.

Scope - This program is intended to cover the entire manufacturing sequence from the beginning to the finished component. The list of technologies which will be addressed includes raw materials, melting and atomization, powder handling, consolidation, forging, heat treatment inspection, metal removal, coating, joining, and surface enhancement. A key to making the technology affordable will be process modeling and real-time process monitoring and control. As such, the processes will be designed with this incorporated whenever possible.

Approach - The program will involve an integrated effort of the powder supplier, forging house, finishing house, and hardware engineering team. It is anticipated that the cost of the raw materials involved in these alloys will

not lead to an unaffordable component unless the product quality and process yields cause it to be so. Thus, the key to making this material affordable is a high quality product made by a high yield process. The process that is anticipated to carry the most weight in this regard is melting, atomization, and powder handling. This program will attack this problem with an adequate capacity, steady-state process which is amenable to process control and has a powder handling system designed to automatically collect the in-size powder and recycle out-size powder. The melt residence time, skull control, nozzle durability, and atmosphere control will be developed to provide consistent high cleanliness powder which negates the need for extensive internal inspection. The forging process will be designed using CAE and deformation modelling to ensure no flaws are introduced and that an effective near-net shape is obtained. A large portion of the program will be concerned with confirming that the cleanliness and internal flaw goals are met in order to minimize further inspection costs, scrap rates, and yield problems. The second area with a high cost sensitivity is component finishing. Efficient metal removal will be obtained through optimization of machining parameters and through the use of models to design a metal removal sequence which adjusts for the residual stress in the component. The joining processes will be scaled up, automated, and process controlled in order to improve cycle time and minimize joint inspection. The finishing or coating process will likewise need to be scaled up and process controlled to produce a consistent high quality surface condition. Finally, the part needs to be designed with the limitations and cost effectiveness of the processes in mind.

VI. CONCLUSIONS

The conclusions of the ROMS Program are as follows:

- Year 2010 technology materials provided good advanced subsonic and advanced supersonic study engine fuel burn improvement
- Year 2010 technology materials provided significant advanced supersonic study engine DOC improvement
- Nonmetallic composites and intermetallics provided a majority of the fuel burn and DOC improvements and were selected for the material program writeups
- Carbon-carbon will require improved life at elevated temperatures if it is to provide the supersonic improvements.

The Year 2010 technology materials allowed higher T41 and higher overall engine pressure ratio to produce good fuel burned improvements. The advanced subsonic fuel burn improvement was 13.4% with advanced materials and improved aero and the advanced supersonic improvement was 21.5% with advanced materials and improved aerodynamics.

The Year 2010 technology materials allowed significant DOC improvement for the advanced supersonic study engine. The DOC improvement was 18%, which was more than three times the goal. Advanced materials costs had a large influence on subsonic DOC payoff but a lesser effect on supersonic DOC payoff.

The two classes of advanced materials which gave the greatest payoff were nonmetallic composites and intermetallics. Eighty percent of the subsonic DOC improvement and 90% of the supersonic DOC improvement was due to these two classes of materials; therefore, it is logical that they receive priority in consideration for development funds.

Carbon-carbon was responsible for 30% of the supersonic DOC improvement and the high temperature capability contributed to this improvement; therefore, carbon-carbon will require improved life at elevated temperature if this payoff is to be realized.

REFERENCES

1. Walkey, B.K.; Espil, J.G.; Lovell, A.W.; Martin, L.G.; and Swanson, E.E.; "Concept Development of a Mach 2.7 Advanced Technology Transport Employing Wing - Fuselage Blending," NASA Contractor Report 165739.

2. Molloy, K.J.; Grantham, D.W.; and Neubauer, Jr., J.M.; "Noise and Economic Characteristics of an Advanced Blended Supersonic Transport Concept," NASA Technical Paper 2073.

ROMS DISTRIBUTION LIST

Naval Air Propulsion Center
P.O. Box 7176
Trenton, NJ 08628-0176
Attn: PE 34/Mr. R. Valori
PE 34/Mr. S. L. Fowler

Naval Air Development Center
Attn: 6052/Mr. John Cyrus
Warminster, PA 18974-5000

Wright Patterson AFB
Attn: AFWAL/POT/Tom Sims
Wright Patterson AFB, OH 45433

McDonnell Douglas Corporation
Douglas Aircraft Company
Advanced Engineering
3855 Lakewood Blvd.
Long Beach, CA 90846
Attn: Mr. D. A. Graf
Mr. Louis Harrington

Lockheed Georgia Company
Dept 72-47, Zone 418
86 South Cobb Drive
Marietta, GA 30637
Attn: Mr. W. Arndt
Mr. R. H. Lange

Northwest Airlines, Inc.
Attn: Mr. B. H. Lightfoot
Minneapolis/St. Paul Int'l
St. Paul, MN 55111

TRW Aircraft Components Group
Attn: Dr. C. S. Kortovich
Mail Stop 37
23555 Euclid Avenue
Cleveland, OH 44117

Allison Gas Turbine Division
Attn: Mr. W. L. McIntire
General Motors Corp.
P.O. Box 420
Indianapolis, IN 46206-0420

United Technologies Corp.
Pratt and Whitney Aircraft Group
Commercial Products Division
400 Main Street
East Hartford, CT 06108
Attn: Mr. J. Godston
Mr. W. L. Webb

American Airlines, Inc.
Tulsa Maintenance and Engineering Center
Attn: Mr. K. Grayson
3800 N. Mingo Road
Tulsa, OK 74151

Delta Airlines, Inc.
Hartsfield Atlanta Int'l Airport
Atlanta, GA 30320
Attn: Mr. C. Daves
Mr. W. J. Overend

United Airlines, Inc.
San Francisco Int'l Airport
San Francisco, CA 94128
Attn: Mr. R. E. Coykendal
Mr. R. D. Tabery

NASA Scientific and Technical (20 copies)
Information Facility
Attn: Accessioning Dept.
P.O. Box 8757
Baltimore/Washington Int'l Airport, MD 21240

NASA Headquarters
Washington, DC 20546
Attn: RP/J. Facey
RJ/J. McCarthy
RM/M. Greenfield
RJ/L. Williams

NASA Langley Research Center
Hampton, VA 23665-5225
Attn: 406/R. Koenig
406/C. Morris
412/J. Morris
410/C. Jackson
412/S. Dollyhigh

NASA Ames Research Center
Moffett Field, CA 94035
Attn: 237-11/T. Galloway

General Electric Company
Attn: Mr. Thomas F. Donohue
Cincinnati, OH 45215

Boeing Commercial Airplane Company
P.O. Box 3707
Seattle, WA 98124-2207
Attn: Mr. Malcom McKinnon
Mr. Mark E. Kirchner
Mr. Albertus D. Welliver
Mr. F. H. Brame

Rockwell International Corp.
Attn: Leslie M. Lackman
Bethany, OK 73008

NASA Lewis Research Center
21000 Brookpark Road
Cleveland, OH 44135
Attn: 0300/J. Acurio
0133/H. Grimes
0133/L. Shaw
0133/R. Graham
1950/Library (10 copies)
2000/D. Poferl
2000/N. Saunders
2400/D. Mikkelson
2400/W. Strack
2430/A. Glassman
2430/G. Knip (10 copies)
2700/F. Kutina
2740/K. Sievers
5100/S. Grisaffe
5110/H. Gray
5110/R. Dreshfield
5120/D. McDaniels
5120/J. Stephens
5130/J. DiCarlo
5170/R. Davies
5200/L. Nichols
5210/C. Ginty
5210/D. Gauntner
5210/R. Johns
5210/R. Thompson
5240/D. Sokolowski